Shear Strength of Timber Beams with End Splits

By

Shanta Das

A thesis submitted to
the Faculty of Graduate Studies of The University of Manitoba
in partial fulfilment of
the requirements of the degree of
Master of Science

Department of Civil Engineering
University of Manitoba
Winnipeg

Abstract

Timber beams with end splits were investigated in this study to determine their shear strength. Two conditions were considered: a) Group 1 had supports located near the ends with the portion of the beam extending beyond the support, and b) Group 2 had supports located right at the end of the beam subjected to a horizontal split at approximately mid height. In Group 1, seventeen beams were tested under static loading and four were tested in fatigue. In Group 2, nineteen beams were tested under static loading and four under fatigue. In Group 1, eight beams under static loading failed in shear. In Group 2, all beams under static loading failed in shear. Group 1 and Group 2 beams under static load produced average shear strength values of 4.93 MPa and 4.49 MPa, respectively. During fatigue tests, Group 1 sustained more cycles than beams in Group 2.

Acknowledgments

The author would like to express her sincere appreciation and deepest gratitude to her supervisor Dr. Dagmar Svecova, for her constant guidance, generous help, invaluable suggestions and remarkable patience throughout the progress of this research work.

The author would like to thank Dr. Baidar Bakht, her co-supervisor, for his kind support, encouragement to take challenges, and invaluable suggestions in carrying out this research.

The author would also like to thank Dr. Aftab Mufti and Dr. Leslie G. Jaeger for their invaluable suggestions and keen interest in this research. The author is grateful to her committee members, Dr. D. Polyzois and Dr. C. Wu, for their valuable time and interest to this research.

The author would like to acknowledge the support from the Ontario Ministry of Transportation for providing the timber beams that were used in this research. It is noted that Mr. Krisciunas was mainly responsible for making the beams available for the current research. The author also acknowledges the financial support from the ISIS Canada Research Network (Intelligent Sensing for Innovative Structures). The technical support from the staff and graduate students of W.R. McQuade Structures Laboratory at the University of Manitoba is also gratefully acknowledged.

Contents

List of Tables

List of Figures

List of Appendices

Chapter 1

Introduction

1.1 General

Timber is a light weight, durable and easy to construct material which makes it an ideal for bridge construction material. Timber bridge construction does not require any special skill. As a result, timber bridges could be found even from ancient times.

According to the Canadian Encyclopedia (Legget 2010), covered timber bridges were widely used in Quebec during the end of nineteenth century. There were about 1000 covered bridges in Quebec in that period. Timber bridges have also been used for railroad transportation during the nineteenth century. After the nineteenth century the use of new materials like steel and concrete partly replaced the use of timber.

In the United States there are some 71,200 timber bridges which represent, approximately, 12% of the total bridges with span longer than 6 m. About one-third of the total land area is forest land in United States and wood is still used for short and medium span bridges, in these areas (Ritter, 1990).

1.2 Problem Definition

There are 725 timber bridges owned by Manitoba Infrastructure and Transportation (Svecova & Eden, 2004). Among these 725 bridges, 590 were constructed between 1950 and 1980. Therefore these bridges are now 30 to 60 years old. With time, these timbers have developed defects in them such as checks, splits and warp. Splits and checks may occur in timber due to changes in moisture content or due to improper seasoning.

When a timber is supported near its end, the load path crosses the split, as shown in Figure 1. 1 (a), thus reducing the shear strength capacity of timber beams. When the beam is not supported at its end, as shown in Figure 1. 1 (b), checks and splits should have no or little effect on the shear strength of the timber beam. However, the Canadian Highway Bridge Design Code (CAN/CSA S6-06) does not differentiate between varying support conditions when it comes to shear capacity of timber beams.

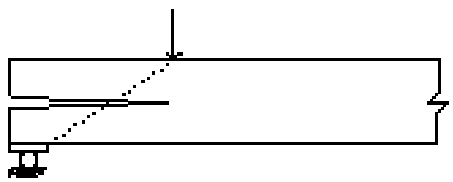

a) Beam supported at its end

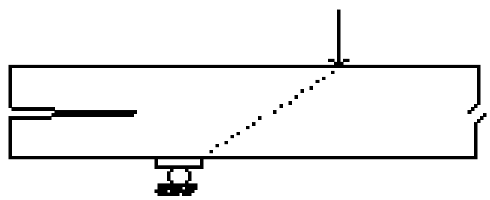

b) Beam not supported at its end

Figure 1. 1 : Load path for different support locations of timber beams.

1.3 Objectives

The purpose of this research was to determine the shear capacity of timber beams with end splits. The research project involved the testing of beams with horizontal splits at their ends under static bending and fatigue. The key objectives of this study are as follows:

a) To determine the shear strength of timber beams with splits at their ends;

b) To investigate the effect of support location on the shear strength of timber beams with end splits;

c) To examine if the crack length propagates further under repeated cycles of loading;

d) To determine the mode of failure of timber beam with end splits under fatigue loading; and

e) To determine the number of cycles that produce failure in timber beams with splits.

The parametric variations in the research study included the location of the supports. The specimens were selected on random basis to perform both static and fatigue tests. There were no control specimens in this study.

1.4 Scope of Work

The timber beams tested were 65 years old, creosote-treated Douglas-fir beams that were obtained from a timber bridge that was taken out of service in Ontario. The beams had artificially induced splits at their ends. As a result, during the splitting of the timber beams, the length of the splits could not be maintained constant. Almost in all the cases, the splits propagated beyond the desired length during the splitting process. Two support locations were investigated for this research; one where the splits were outside the support in a cantilever portion of the beam and one where the splits were between the supports. The beams were subjected to both static and fatigue loads. Eight beams were tested under fatigue, four for each support condition.

The thesis has been divided into six chapters. First chapter gives a brief introduction about the objectives of this research. The second chapter is a summary of literature and the third chapter describes the test setup and instrumentation used in this research. Data collected from the experiments are available in chapter four. Chapter five presents the data analysed in this study and chapter six draws the conclusion of this research.

Chapter 2

Literature Review

2.1 Behaviour of timber

Wood and timber can be treated as two different materials with different failure modes as well (Madsen, 1992). Wood is defined as small, defect-free clear specimen whereas timber is derived from logs of trees which might have defects. Therefore tests on wood do not necessarily reflect the true behaviour of timber. As the timber strength varies along its length, the variation of strength should also be taken care of.

The bending strength of timber can be predicted in two modes of failure depending on the relative compressive and tensile strengths of lumber (Buchanan, 1990). A member having tensile strength less than the compressive strength will fail in brittle tensile failure. Members having moderate tensile strength to compressive strength, with a ratio higher than 1, will also fail in tension but with some compression yielding as well. Members having higher tensile strength than compressive strength will have some compression yielding after which as the member approaches modulus of rupture at the tensile zone the member fails in rupture. Members having much higher tensile strength than compressive strength will fail in compression only.

For the bending strength theory bilinear stress-strain curve is assumed for compression with a descending branch after the maximum compression stress, f_c, is attained. Tension behaviour is related to the size of the member and is assumed to be linear elastic up to f_t, the axial tensile strength, after which brittle tensile fracture occurs. Test results were used to calibrate and verify the model.

The research in this paper will focus on the shear strength behaviour of timber. Most of the previous research on shear strength of split timber was focused on glulam beams. The methods and results should be applicable for this research as well, because artificial split was introduced in this research. Choosing a suitable test method is very important to get shear failures of timber beams. Some experimental work was done to find a suitable test method that will produce higher percentage of shear failure of timber beams.

Yoshihara and Suzuki (2005) used four point bending test method on side tapered speci-men to monitor shear stress/shear strain relationship of wood. Small, clear and defect-free Sitka spruce lumber at 12% moisture content was used for the test. The sample was 15 mm in the radial direction, 10 to 30 mm at 5 mm intervals at the tangential direction and

370 mm in length. The span length was 300 mm. Only the depth of the specimen was varied to get different ratio of shear stress to bending stress.

The load was applied at a rate of 2mm/min for a total testing time of 5 min. The shear strain was recorded using a triaxial strain gage (Tokyo Sokki FRA-2-11, gage length = 2mm) on the longitudinal-tangential (LT) plane.

Iosipescu shear test was also performed to compare the shear properties: shear modulus G, shear stress at the proportional limit τ_p, shear stress at the maximum τ_{max} and principal strain angle φ with those obtained by the asymmetric four point bending test. From the comparison of the two tests it was concluded that the asymmetric four point bending test can be effectively used to find the shear stress/shear strain relationship of wood by minimizing the effect of bending with a proper selection of α that is ratio of shear stress to bending stress.

Bateman et al. (1990) aimed at finding a feasible new test method to find inter-laminar shear stress in structural wood composites as the ASTM D2718 (1976) and ASTM D 1037 (1978) test methods are expensive. Both ASTM D1037 and five-point bending tests were performed on four different oriented strand board (OSB) panel thicknesses. For the five point bending test many span lengths were investigated to study the effect of span to depth ratio. Based on the experimental results the authors concluded that this test had the potential to be used as a method for determining inter-laminar shear strength of structural wood composites.

Comparisons of five different test methods were done to find the parallel to grain shear strength of lumber (Riyanto & Gupta, 1998). Among the five test methods four utilized full size Douglas-fir specimens: three-point bending, four-point bending, five-point bending and torsion. The fifth test was on small, clear shear block specimen according to ASTM D143-94 (1996).

A total of 380 MSR (1800f-1.6E), 2x4 Douglas-fir lumbers were tested for the five tests, with 76 tests for each method. Shear span used for each of the full size specimen test method was 5d. The number of shear failure in three-point bending was 43, four-point bending was 8, five-point bending was 37, torsion was 76 and small, clear specimens had 76 shear failures out of 76 specimens in each group. The authors recommended using torsion test to determine the shear strength of solid wood and three-point bending test to determine shear strength of structural lumber.

Huggins et al. (1966) performed tests on 175 small scale glue-laminated timber bridge members. Static and repeated load tests were performed on the 175 timber beams 82.55 mm by 152.4 mm by2743 mm. Some of the timber beams contained artificially created delaminations. A total of seven patterns of beams were tested having delaminations of full width at different depths. One hundred and twenty seven beams were loaded statically with load applied at the midpoint, 46 were subjected to repeated loading at 200 load cycles per minute and 2 were subjected to repeated loading at 300 cycles per minute.

To find the stresses in the delaminated beams an approximate method was followed by the authors. Average shear stress on a length equal to the depth of the beam from the end of delamination was calculated and compared with beam shear strength (3.45 MPa). Local shear stress at a point 1/12 of the beam depth away from the end of delamination was calculated and compared with shear block strength (7.58 MPa). Computed maximum tensile stresses were compared with the mean modulus of rupture for the Pattern I beams (without delaminations).

Huggins et al. concluded that beam stiffness is not greatly affected by interior delaminations. However, delaminations at or near the end of a beam reduce the strength more than does an equal amount of interior delamination at the mid-span. It was also concluded that the shear strength depends on the ratio of shear span to beam depth and on the type of loading: static or repeated. They recommended for future studies on timber beams having delaminations of partial width and interior delaminations neither at mid-span nor at mid-height.

Presence of high shear stress along the glue lines in a glue-laminated beam causes delamination (Schwaighofer et al., 1968). Shear stress was calculated by the authors along the axis due to a concentrated load of various eccentricities at the end based on the theoretical work of Iyengar (1962). To prove the theoretical shear stress results based on Iyengar’s work, photo elastic method was applied to find shear stresses along the centerline experimentally. The experimental results and the theoretical results matched closely.

Lam et al. (1997) investigated the longitudinal shear strength of three different species group of Canadian softwood select structural lumber. The species tested were Douglas-fir, Hemlock-fir and Spruce-pine-fir using a two-span five-point bending test setup. The two different span ratios used were 6:1 and 5:1.

Almost 100 pieces of nominal 38x185x3000 mm lumber were tested for the three species. Additionally 38x285x4870 mm Hemlock-fir and Spruce-pine-fir were tested to find the effect of size on longitudinal shear. The species were air dried to a moisture content of 12%. Each specimen was tested using the Cook Bolinders AG-SF grading machine to find its modulus of elasticity flat wise. To find the modulus of elasticity edge wise the specimen were tested non-destructively on edge under three-point loading.

After full size shear tests, ASTM shear block test was performed to get the shear strength cutting shear block specimen from the full size specimen near failure zone. The experimental median failure loads were compared with finite element coupled with Weibull (1939) weakest link analyses. Median shear stress values were also compared with an empirical method suggested by Soltis and Rammer (1994)

It was concluded that Weibull (1939) shape parameter, k ($k = cv^{-1.085}$ where cv is the coefficient of variation of shear strength) is species-dependent. A species-dependent 'k' value yields a higher shear strength, τ^* for select structural dimensional lumber. For this study, the authors used different shape parameter values for different species and yielded

5th percentile shear strength values of 15.55 MPa, 14.89 MPa and 12.37 MPa for a unit volume of Douglas-fir, Hemlock-fir and Spruce-pine-fir, respectively.

Soltis and Rammer (1994) investigated the shear strength of glue-laminated timber beams without checks or splits. More than 300 glue-laminated beams were tested to determine their shear strength. The maximum sizes of the beams were 130x610 mm for Douglas fir and 130x560 mm for Southern Pine beams. The beams were tested in a five-point bending test to produce shear failures. After the testing of the beams, shear block specimens were cut from the beams and tested according to ASTM D143 (1987).

From data analysis it was found that the shear strength decreased with the increase in shear area. Based on the data, an empirical equation was proposed by the author to relate τ_{ASTM} to beam shear strength, τ. Here shear area is defined as the beam length under both positive and negative shear multiplied by the width of the beam. The authors concluded that ASTM shear block strength is higher than beam shear strength and beam shear strength decreases with increase in size.

Longworth (1977) investigated the relation between the shear strength of the beam and the volume of the beam subjected to shear. A total of 150 glue-laminated Douglas fir beams were tested in five different groups having different sizes and span lengths to produce different cross-sectional areas and width/depth ratios. Shear block specimen was collected from the failure zone near the beam ends and test was performed to find the shear block shear strength.

The beams were tested in four-point bending and the loading rate was chosen to produce an average failure load at 13 minutes. From the test results the author concluded that the shear block shear strength is not applicable to beams and the timber beam shear strength is related to beam size.

Keenan (1974) investigated the effect of shear span to depth (a/d) ratio to glue-laminated timber beams and developed a model for the calculation of shear strength of glue-laminated Douglas-fir beams.Three different tests were conducted to investigate the effect of compressive stress perpendicular to grain on shear strength parallel to grain: A) ASTM shear block test, B) oblique grain compression test, and C) torsion tubes.

ASTM shear block specimens and oblique grain compression specimens were tested for both tangential and radial direction of loading. Half of the torsion tube specimens were tested for torsion shear only and the other half were tested for both torsion shear and circumferential compression stress perpendicular to grain.

From the three test results it was concluded that application of compressive stress perpendicular to grain does not significantly increase the shear strength parallel to grain when the specimens are free to find their plane of greatest weakness. Finite element studies by the author also proved that transverse compressive stress in a beam is not distributed in such a manner as to increase the shear strength significantly.

From the finite element study it was found that the mid-height shear stresses are greater than the shear stresses elsewhere; therefore, the two beam theory (Newlin et al., 1934) is not applicable for unchecked glue-laminated timber beams.

Keenan et al. (1985) performed experimental work to find the effect of size on longitudinal shear strength of glue-laminated spruce. Various sizes of beams were tested with concentrated load at midspan. The testing covered a large number of spruce glue-laminated beams with different depths, widths and shear spans. For the convenience of testing, the members were divided into three projects. Project A consisted of small clear beams with cross-sections varying from 25x25 mm to 75x75 mm. The shear span to depth (a/d) ratio was kept constant at 2 for the test of 108 specimens in this project. Longitudinal shear failures occurred in 91 out of 108 beams. Project B consisted of glulam beams with cross-sections varying from 20x100 mm to 90x200 mm. A total of 54 tests were done in this project with different shear span to depth (a/d) ratios. Longitudinal shear failures occurred in 42 out of 54 beams. Project C consisted of glulam beams with cross-sections varying from 76x200 mm to 127x400 mm. A total of 30 tests were done in this project with shear span to depth (a/d) ratio of 2. Longitudinal shear failures occurred in 29 out of 30 beams.

Beam width, depth and shear plane had a significant effect on the shear strength of small clear wood beams in project A and small glulam beams in project B. Beam width and depth had very little statistical effect on beam shear strengths for larger glulam beams in project C. This study on spruce clear beams and spruce glulam beams showed no significant effect of sheared volume on shear strength

Shear strength is dependent on the angle between grain and shear force (Liu & Floeter, 1984). Bow-tie shaped specimens were prepared from Sitka spruce with four angles of grain: 0°, 30°, 60°, and 90°. Experimental mean shear strength data for θ=0° and 90° had been used to find the theoretical shear strength data at θ=30° and 60° which matches closely to the experimental data. A decreasing trend in shear strength was found as the angle between the shear strength and grain increases.

The effect of knot location and local grain deviation on stress behaviour of lumber had been investigated by the use of an orthotropic finite element analysis (Cramer & Goodman, 1983). To model the knot grains in finite element analysis, "flow-grain analogy" was used and was found accurate when verified by experiment.

To analyse the effect of knot location, seven knot locations were investigated with uniformly distributed tensile stress along the longitudinal axis. From the analysis it was found that edge knot produces more severe stress concentration than the center knot. To predict the ultimate strength of a section containing knot and cross grain, effective section technique was used with a progressive sequence of failure. The effective section technique was significantly closer to the actual test load than that of ASTM predicted strength.

History of research that led to the design of allowable shear stress in lumber had been reported by Ethington et al. (1979). The report presents a chronological summary of work done to the development of shear factor used in ASTM D245 (1927-1975). It was also pointed out that the two-beam theory developed by Newlin et al. (1934) was not correct and the work done by Foschi and Barrett (1976) holds promise for future research.

Fracture mechanics had been used to measure the strength of a wood beam with end split that resulted in a loss of strength and stiffness (Murphy, 1979). Linear elastic fracture mechanics was used to find the strength of these beams. Boundary value collocation method was used to solve for the unknowns of stress series. One equation was given to find K_{11}, the stress intensity factor (SIF), for end split beam under a concentrated load and under a uniform load. SIF is used in fracture mechanics to predict the correct stress intensity near the tip of a crack. The equation depends on orthotropic parameter for different wood species, grain direction and stress conditions. For a concentrated load on Douglas-fir beam with end split the equation is as follows:

$$K_{II} = [-2.785(\frac{a}{d}) - 0.731]\frac{R}{bd^{1/2}}$$

Where, a is crack length, d is beam depth, b is beam width, and R is reaction at support. Experimental results from (Norris & Erickson, 1951) were compared with the theoretical fracture mechanics equation and showed good agreement.

Fracture mechanics was also used to find a strength prediction formula for dimension lumber with or without end splits subjected to uniform loading (Barrett & Foschi, 1977). Shear strength of clear dimension lumber under uniform loading was developed using the weakest link theory and ASTM block shear strength data.

The shear capacity of timber with an end split under uniform load was calculated using linear elastic fracture mechanics. For a constant span to depth ratio, the shear strength decreases with increase in crack length. For a given survival probability, permissible crack length can be obtained without reduction in shear strength for clear strength values. Strength ratio for end cracked beam was proposed that can be used for different crack length to depth ratio (a/d) and span length to depth ratio (L/d). Expressions were developed to calculate the allowable shear stress from uncracked and cracked beams.

2.2 Fatigue Behaviour of Timber

Kyanka (1980) has confirmed that there is a severe lack in research in the area of wood subjected to fatigue. In 1920's, aircraft designers neglected the need of study into this area, noting that it was difficult. This trend continued till the Second World War. After 1960's, researchers started to look into this matter to get clear ideas. Since a tree withstands a lot of storm and wind during its lifetime than any other materials, researchers considered wood to be fatigue resistant. The use of violin and ships made of wood that normally lasts many years also confirms this idea of fatigue resistance of wood.

According to Kyanka (1980), it is difficult to find the difference in failure between the static and fatigue tests. From various studies, it is found that particle board have a lower level of fatigue endurance capacity than that of solid wood. Design is now based on reliability which requires a clear understanding of fatigue behaviour of wood. The previous use of high safety factors in design made designers to avoid fatigue concerns in their design.

Kyanka (1980) recommends that some standardized test procedures should be developed by researchers for the fatigue test of timber. A proper understanding of wood biology is also necessary to understand the fatigue nature of wood. Kyanka (1980) also emphasizes the development of wood fracture morphology to make wood comparable to other construction materials.

The fatigue strength of wood is not predictable and there is not much difference in fatigue life between solid wood and laminated wood (Tsai & Ansell, 1990). A higher frequency in fatigue test may heat up the specimen and give a longer fatigue life. The other factors that affect the fatigue strength of wood are: moisture content, temperature, density, slope of grain, creosote preservative, notches, holes and grains. Experimental work by Tsai & Ansell (1990) confirms that moisture reduces the fatigue life of wood and a stress reversal has more damaging effect on wood than stress repetitions.

According to Hansen (1991), the fatigue properties of wood and wood laminates are affected by the type of wood, size of wood, moisture content and type of load. Besides these factors, the frequency and total loading time also affects the fatigue resistance. In his study, Hansen (1991) investigated the effect of grain angles of laminated wood beams. The tests were conducted at 10 Hz frequency in four-point bending setup. The test was repeated. For the experimental work four different angles were chosen: 0, 3, 6, and 12°. From the S-N curve, it was found that, there was a remarkable decrease in fatigue properties with the increase in grain angles.

Huggins et al. (1966) found that a fatigue test on laminated Douglas fir beam significantly reduces its shear strengths; they applied a minimum of two million cycles of load to each beam and a load which induced twice the allowable design flexural stress to the beams. The ratio of minimum and maximum load was kept constant at 0.2.

Davids et al. (2005) tested in fatigue nine 6700 mm long Douglas fir glulam beams with different length of glass fibre reinforced polymer on the tension side of the beam. Three beams had reinforcing to the full length of the span and six beams had partial reinforcing along the length. Three of six partially reinforced beams were restrained at the end and the other three partially reinforced beams were not restrained at the end.

A computer program was used to calculate the reinforced glulam and unreinforced glulam flexural stress, F_b. The beams were tested in four-point bending upto $2x10^6$ cycles of loading. The ratio of minimum and maximum loading was chosen to be 0.33 based on the calculation of a 14.6 m long bridge using AASHTO HS-25 loading. The minimum load represented the dead load, and the maximum load represented the total dead and live load. When the beam had reached the $2x10^6$ cycles, it was tested again under static load to find the residual strength.

The beam with full-length reinforcing, survived $2x10^6$ cycles of loading and showed no signs of damage during the fatigue tests. The beams also had no loss in flexural stiffness. Out of the three specimens with unrestrained partial-length reinforcing only one specimen survived $2x10^6$ cycles without any major loss in flexural stiffness.

The rest of the three specimens with restrained partial reinforcing survived $2x10^6$ cycles of loading. Among these three specimens, only one exhibited significant loss of flexural stiffness. The authors concluded that the beams with full length reinforcing can tolerate fatigue loading ($2x10^6$ cycles). Moreover, beams with proper restraint can also be used in fatigue with partial reinforcing. As the number of beams tested in this project was small, the authors recommended more research into this area.

Uppal et al. (2001) studied the fatigue strength of timber railroad bridge stringers. Stringers are the main structural component in a railroad bridge and also undergo heavy axle loads. The purpose of this study was to find the fatigue strength of these stringers for future use of heavy axle loads and to find their remaining strength.

In the research program by Uppal et al., twenty one southern pine and twenty four Douglas fir stringers were tested in a four-point bending setup. All the beams were creosote-treated and solid sawn with high moisture content. Among the 21 southern pine beams, five were tested statically up to failure. Similarly among the 24 Douglas fir beams, six were tested statically up to failure. The remaining beams were tested in fatigue up to failure. The design loads for the fatigue tests were based on the initial static tests and later on the fatigue test data.

All the southern pine specimens in both static and fatigue tests failed in horizontal shear. Among the Douglas fir static tests all failed in horizontal shear, except one. Similarly in fatigue tests of Douglas fir all the beams failed in horizontal shear, except one.

From the fatigue test data, a logarithmic plot was drawn at the mean and at the 95 percent confidence limit to find a relationship between the shear stress and number of cycles. Beams having checks before the test develop into shakes during the test and fail in horizontal shear. According to the author checks at mid depth are of more concern than many small checks at other locations.

For the southern pine species, the smallest mid-depth shear stress for monotonic test was 1.6 MPa and for fatigue test was 1.14 MPa. For the Douglas-fir species the smallest mid depth shear stress for monotonic test was 1.31 MPa and for fatigue test was 1.07 MPa. The smallest shear stress for both monotonic and fatigue test was higher than that of the current specified design values for railroad stringers.

Chapter 3

Experimental Program

3.1 General

The focus of this study was to investigate the shear strength of timber beams with end splits. To determine the shear strength of timber beams with end splits it was necessary to induce splits at the end of the specimens. A setup was fabricated at the University of Manitoba to facilitate creating splits along the length of the timber specimens. The split beams were tested in a three-point bending test setup. Fatigue tests were also carried out to determine the approximate fatigue life of split timber beams. The whole project consisted of two parts: 1) Static bending tests, and 2) Fatigue tests.

3.2 Material

3.2.1 Timber

The Douglas-fir timber beams used for the research were taken from a 65 year old timber bridge in Ontario. All the beams had been treated with creosote. In the "as received" state the specimens had damage and various imperfections such as side checks, holes, knots etc. as shown in Figure 3. 1 and Figure 3. 2. The typical beam size was 130 mm wide, 330 mm deep and 4900 mm long. Split, warp, and checks occur in timber due to improper seasoning or as a result of changes in moisture content. Any kind of defect can have an impact on the structural properties of timber (Aghayere & Vigil, 2007).

Figure 3. 1 Side checks in a timber beam (Beam No. 47) in the "as received" state

Figure 3. 2 Damaged top part of a timber beam(Beam No. 27) in the “as received” state

According to National Lumber Grades Authority (Standard Grading Rules for Canadian Lumber, 2007), split is defined as a complete separation of wood fibres through the piece to the opposite surface or to the adjoining surface. Split is measured as the average penetration in the directions of the fibres. Figure 3. 3 represents a timber beam having a split at its end.

The specimens in this study were originally of select structural grade but in the course of time they developed defects. All the beams were visually inspected for defects according to NLGA guidelines (Standard Grading Rules for Canadian Lumber, 2007). The specimens, falling into the beams and stringer category, were originally used in a timber bridge supporting a deck nailed on the top of the beam. As a result, most of the beams had nail holes on top.

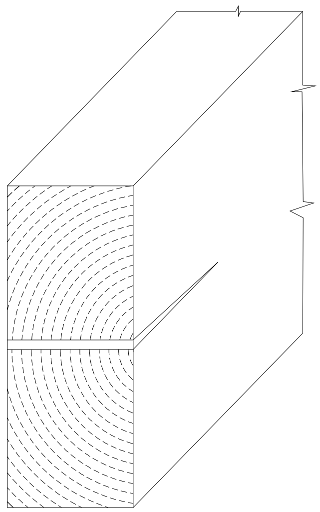

Figure 3. 3 Split at the end of the beam

3.2.2 Moisture Content

The Moisture contents of the specimens were taken before the test. The readings were taken using a resistance type digital moisture meter Delmhorst J-2000 with two 25 mm insulated pins. Readings were taken on both sides of the beam at 1000 mm from both ends and at mid-span at the mid-height for a total of six readings.

3.3 Split Tests

Splits occur at the ends of a beam in a direction parallel to its length due to separation of fibres. In the current study splits were introduced using a mechanical steel wedge. The specimen was supported horizontally in a bulkhead end and on two more supports along its length, as shown in Figure 3. 4. The intermediate two supports were fixed to the strong floor. The height of these two supports was adjustable to accommodate differences in the out-of-straightness of the various specimens. At the free end of each specimen, a steel wedge with a load cell was attached to a hydraulic jack. Load cell was used to find the load needed to induce split at the end of the specimen. The pressure in the hydraulic jack pushed the wedge along with load cell inside the timber. The pressure in the wedge created split along the grain at the end of the timber. Figure 3. 5 shows the attachment of steel wedge to the load cell and the hydraulic jack. To limit the length of the split to 600 mm, two steel angles were clamped together at the top and bottom of the specimen, as shown in Figure 3. 4, at 600 mm from the end of the beam and provided enough pressure to stop the propagation of the split. Splits were induced at both ends of the beams so that the beam can be tested at both ends separately, producing a significant number of tests.

The pressure in the load cell was found using a strain indicator which was calibrated before the start of the splitting process and it could give the pressure reading directly in kilonewtons. The split was thus initiated at the end of the beam and naturally propagated approximately 600 mm into the beam along the grains. Figure 3. 4 shows the test setup that was built in the laboratory to introduce splits at the end of timber specimens.

Although every effort was made to control the length of the splits, their length could not be guaranteed. In average 34 kN load was required to split one end of the beam. The maximum load recorded was 50 kN and the minimum load recorded was 16 kN. The actual length of the splits and the load required to split the beams are shown in Table 3.1 to Table 3.3. As shown in Figure 3. 6 , h_A and h_C is the distance of the split from bottom fibre and l_A and l_C is the length of the split.

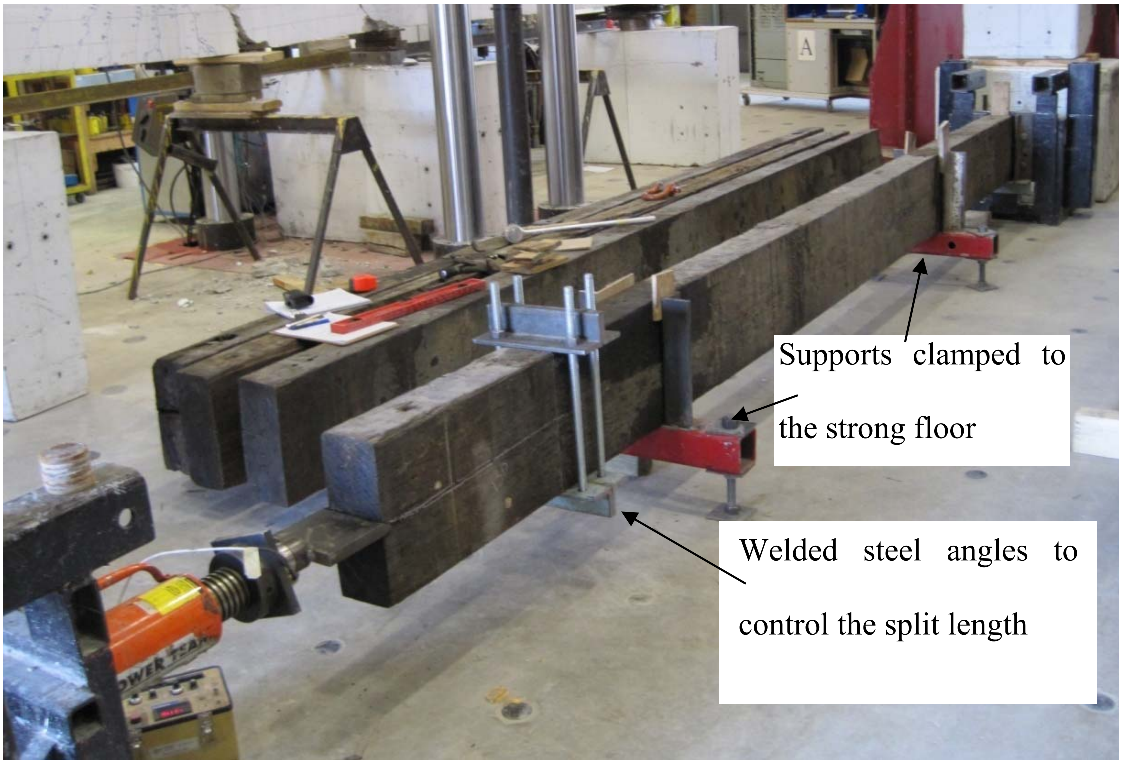

Figure 3. 4 Split setup in the laboratory

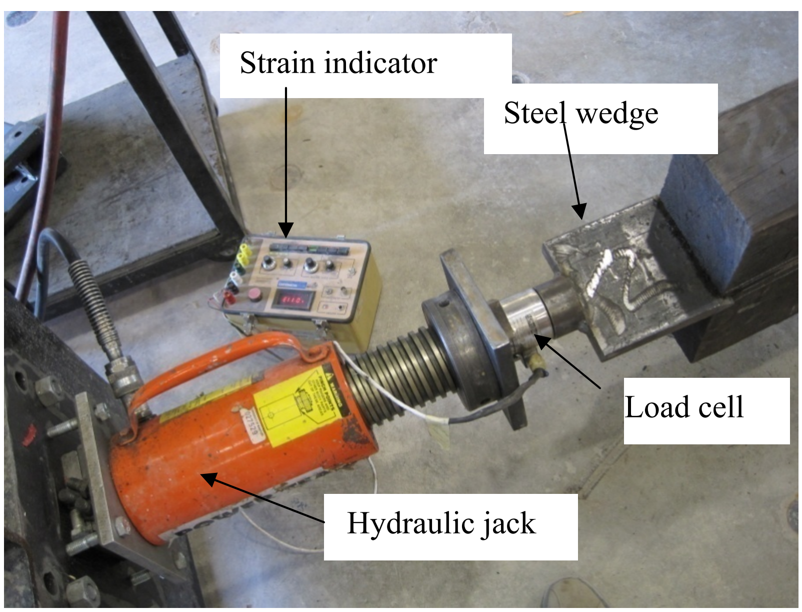

Figure 3. 5 Assembly of hydraulic jack, load cell and steel wedge to split timber

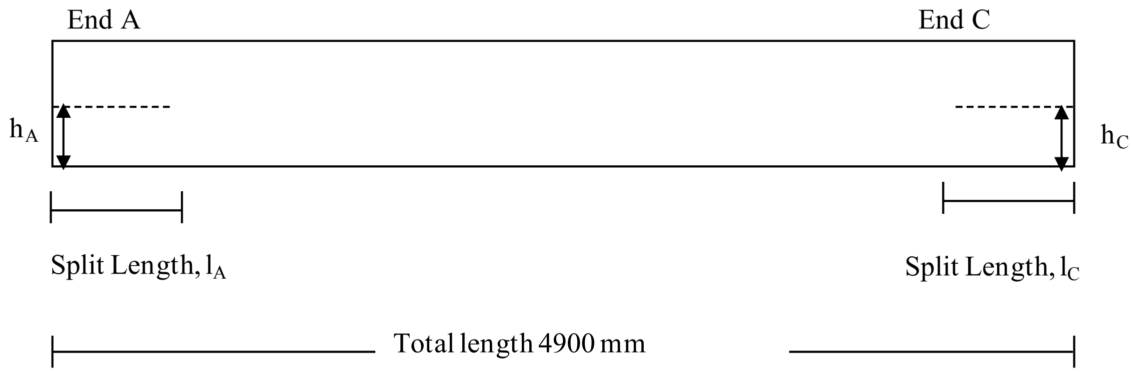

Figure 3. 6 Diagram showing two ends, splits and their heights from bottom fibre of a timber beam

3.4 Five-point static bending test

An attempt was made to test one specimen first under five-point static bending to investigate the potential of this test setup to cause shear failure. The test setup is shown in Figure 3. 7. The beam carried an ultimate load of 283 kN and failed in bearing under load plates. Two load cells were used to measure the reactions located at the middle support and at the outer support. However, from the load cell data it was found that the actual reactions at the supports due to applied loads were non-linear compared to the theoretical support reactions which are linear. Due to the non-linearity of support reactions this test setup was not carried further and three-point static bending test setup was used.

Table 3. 1 Split length and load required to split a specimen in Group 1

Specimen	Splitting Load [kN]	l_A or l_C [mm]	h_A or h_C [mm]	
7A	35.8	722	168	
23A	23	635	167.5	
23C	16	628.5	168.5	
21A	22.2	687	165	
21C	24.2	679.5	165	
17A	31.7	650	180	Presence of side checks
17C	40.5	692.5	165	
16A	30	665	183	Presence of side checks
16C	25.9	817.5	187.5	
28A	35	600	165	
28C	25	617	165	
2A	26	637.5	165	
2C	28	617.5	165	
13A	42	610	165	
13C	48.3	600	165	
4A	24.8	592.5	182.5	Presence of side checks
4C	24	677.5	192.5	

Table 3. 2 Split length and load required to split a specimen in Group 2

Specimen	Splitting Load [kN]	l_A or l_C [mm]	h_A or h_C [mm]	
5A	50	600	155	Twisted shape of beam
5C	44.6	610	171	
10A	29	635	165	Presence of side checks
10C	31	615	165	
22A	40	600	165	
22C	40.5	600	165	
15A	25.2	600	165	
15C	37.8	600	165	
11C	38	632.5	165	
49A	37.8	637.5	160	
49C	33.2	630	160	
50A	33	630	165	
50C	30.7	617.5	165	
44A	34.9	620	165	
44C	31.8	630	167	
41A	31.6	627.5	165	
41C	27.5	630	165	
14A	45.6	652.5	165	Presence of side checks
14C	46.8	610	165	

Table 3. 3 Split length and load required to split a specimen for fatigue test

Specimen	Splitting Load [kN]	l_A or l_C [mm]	h_A or h_C [mm]	
42A	38.5	700	165	
42C	42.8	760	165	
9A	30	665	165	
9C	30	605	165	
6A	42.5	642	165	
6C	42.1	610	165	
3A	38.6	687.5	145	Presence of side checks at 145 mm height
3C	34	615	165	

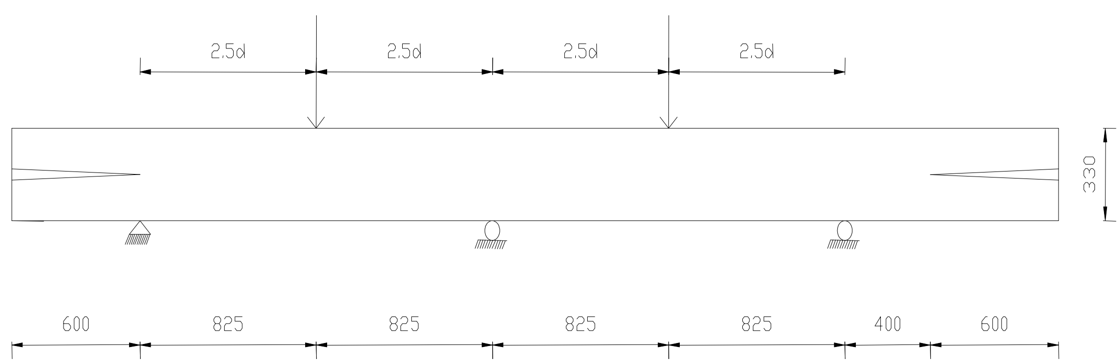

Figure 3. 7 Five-point static bending test setup

3.5 Three-point static bending test

For this study a total of 36 specimens were tested under monotonically increasing static loads in a three-point bending test setup. The beams were divided into two groups. Group 1 specimens were vertically supported 600 mm away from their ends, while Group 2 specimens were vertically supported at their ends as shown in Figure 3. 8 and Figure 3. 9. A total of 17 tests were conducted in Group 1 and 19 tests were conducted in Group 2. An enlarged view of the test setup is shown in Figure 3. 10 and Figure 3. 11. For the rest of the thesis only the enlarged pictures are used.

The rate of loading was chosen to be 3 mm/min to cause failure of the specimens within 6 to 20 minutes and to reach the maximum load within 10 minutes as described in the ASTM D198-05a (2005) standard. To produce shear failure, the three-point bending test was chosen with a point load close to one support. The Canadian Highway Bridge Design Code (2006) ignores any shear effect from the support to a distance equal to the depth of the member. Therefore, the load was applied in such a way that the edge of the loading plate is at a distance equal to the depth of the member away from the edge of the support. To produce a significant number of tests each beam was tested in three-point bending twice, once at each end.

The average length of the beam was 4900 mm and tests on the same beam for both groups did not have any overlapping of span. Therefore, the first test on one beam should not have any effect on the second test on the same beam for any group.

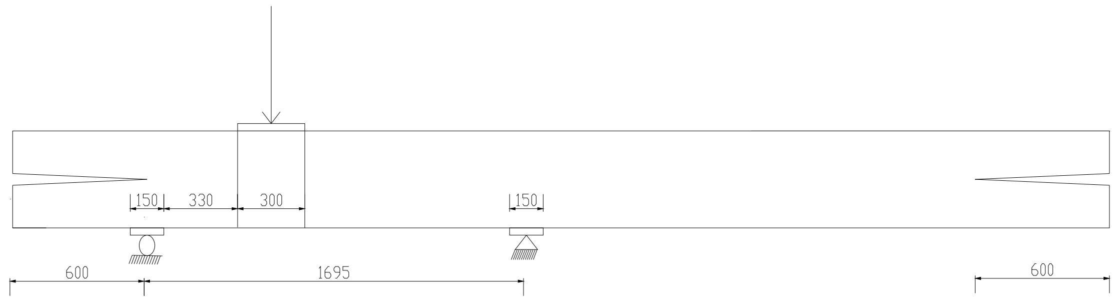

Figure 3. 8 Test setup for Group 1 specimens

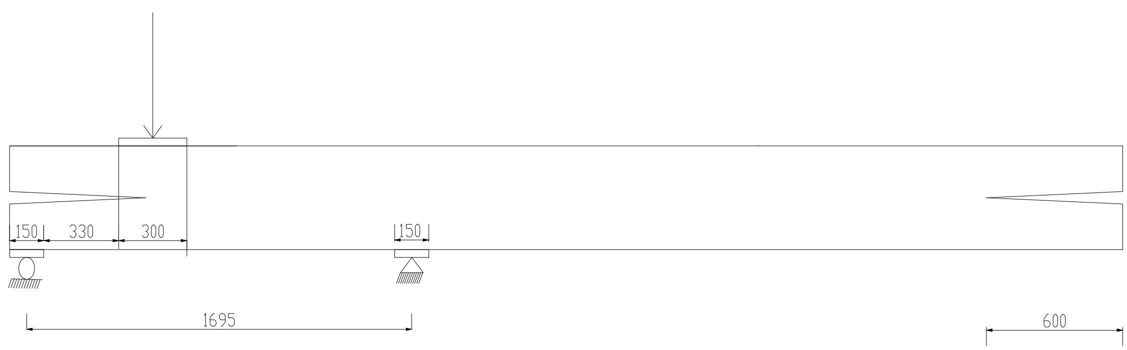

Figure 3. 9 Test setup for Group 2 specimens

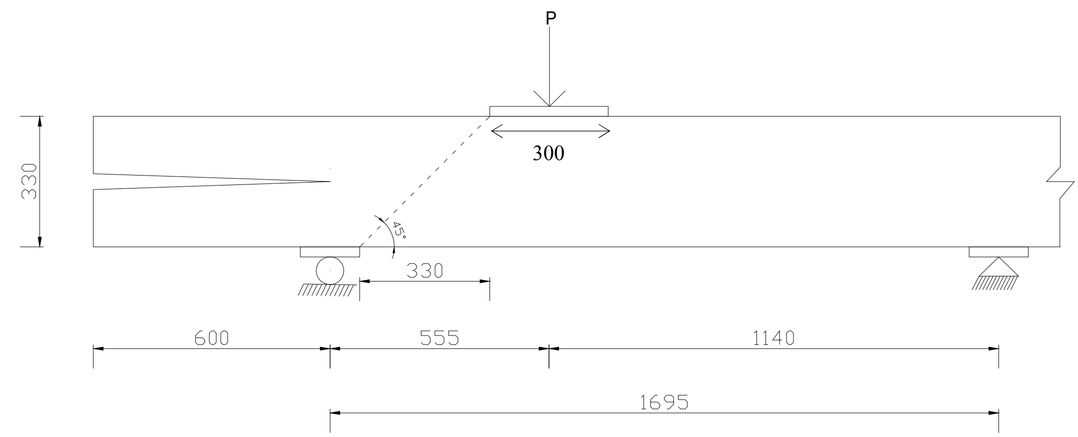

Figure 3. 10 Detail of test setup for Group 1 specimens (all units are in mm)

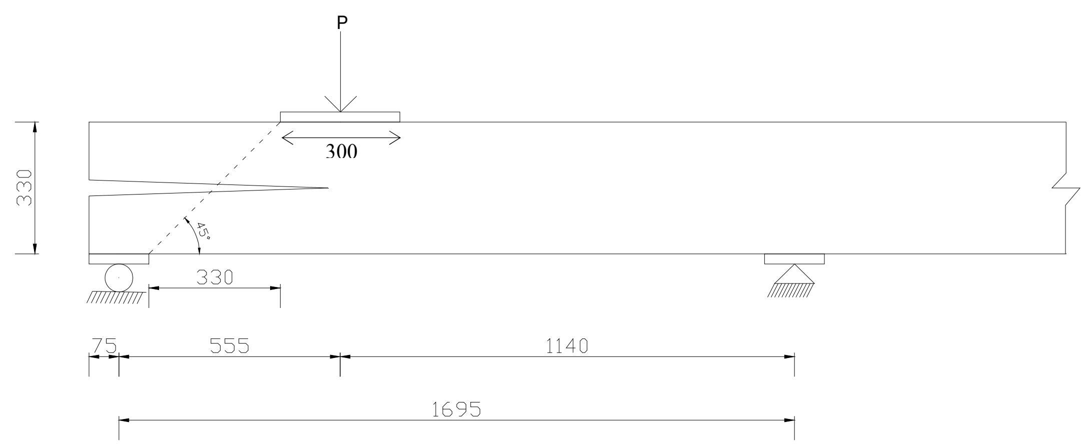

Figure 3. 11 Detail of test setup for Group 2 specimens (all units are in mm)

The beams were supported on 150 mm wide steel plates which were attached to load cells to monitor the reactions at both supports. Two identical load cells were used at the supports. The load cells had capacity of 334 kN. The loading was applied through a 1000 kN MTS Actuator which had a 250 mm stroke. The load was applied to the specimens through a 300 mm long steel bearing plate at the top. To avoid possible bearing failure, both a neoprene pad and plaster were used over the supports and under the load point.

3.6 Instrumentation

A total of five linear variable displacement transducers (LVDTs) and three pi-gages were used for each test. The LVDTs had a working range of 0 to 125 mm and were manufactured by Penny and Giles. The pi-gauges have a gauge length of 100 mm and were manufactured by Tokyo Sokki Kenkyujo Co., Ltd. (TML). All the LVDTs and pi-gauges used in this research program were calibrated at the beginning of the experimental program and were frequently calibrated as well.

Among the five LVDTs, four were used to measure the vertical deflections of the specimen under applied loads as shown in Figure 3. 12 and Figure 3. 13. Two other LVDTs were placed on both sides of each specimen at the load point at mid height. One LVDT was placed at the mid-span and another one at the point of the theoretical maximum deflection which is determined to be 77 mm away from the mid-span. One LVDT was placed horizontally above the split over the support to record the relative slip of the top part of the specimen with respect to the lower part of the specimen. This LVDT was supported using a thin steel plate on the lower half of the beam.

Three 100 mm pi-gages were used to measure strain in the maximum shear force region. The pi-gages were placed at three different angles: 0°, 45° and 90° at mid height of the beams as shown in Figure 3. 14. The instrumentation was similar for all specimens. Figure 3. 12 and Figure 3. 13 represent the typical instrumentation that was adopted for Group 1 and Group 2 beams for both static and fatigue tests.

A data acquisition system (DAQ) was used to record the applied load, displacement, and strain.

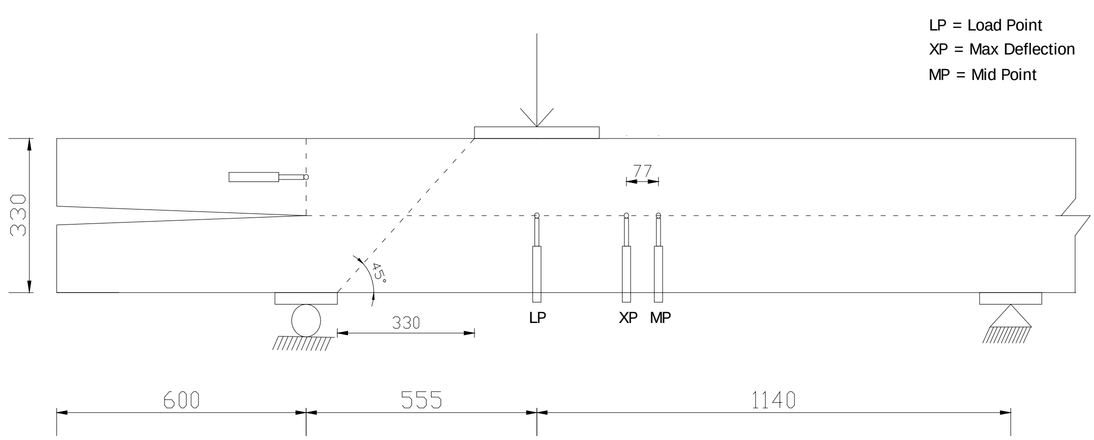

Figure 3. 12 Instrumentation details for Group 1 beams

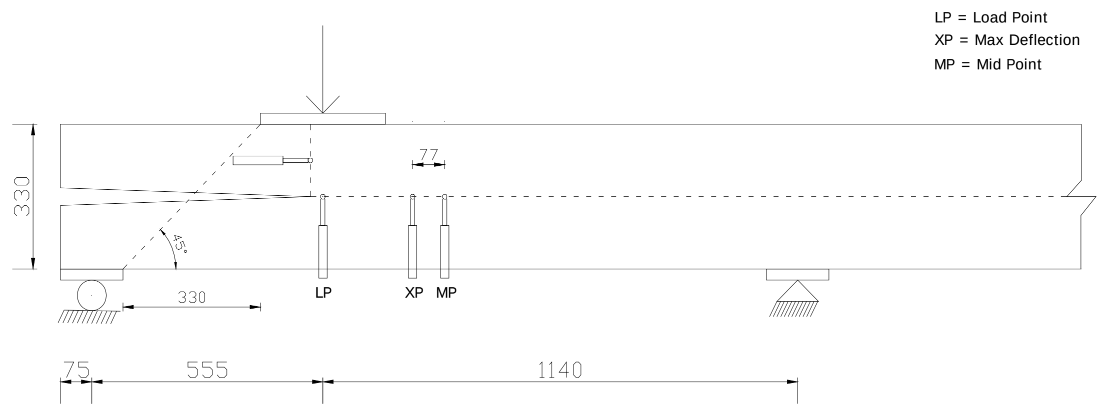

Figure 3. 13 Instrumentation details for Group 2 beams

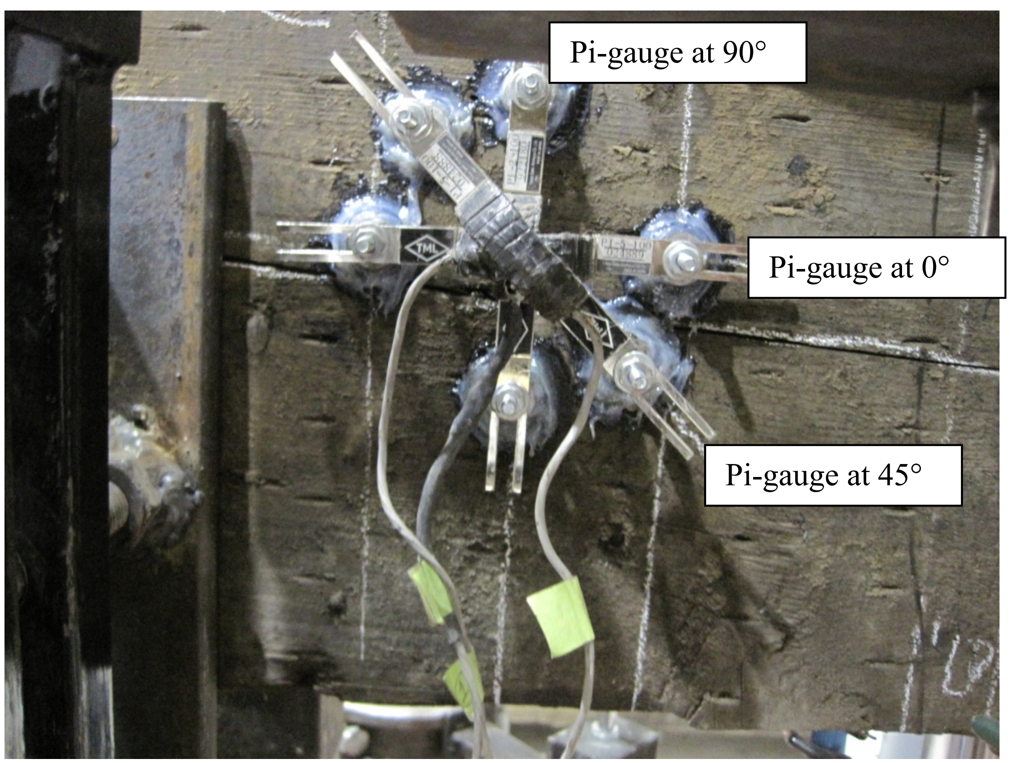

Figure 3. 14 Placement of pi-gauges in three different angles

3.7 Fatigue tests

The fatigue tests were conducted using MTS hydraulic testing machine in a load-control setup. The MTS actuator has a load capacity of 1000 kN and a displacement capacity of 250 mm. The maximum frequency that the 1000 kN MTS machine was able to achieve was 0.75 Hz. The test setup was similar to that of the static test setup for both Group 1 and Group 2 specimens (Figure 3. 10 and Figure 3. 11). Two support locations were investigated for the fatigue test setup: a) Group 1 had support at 600 mm away from the edge of the beam and b) Group 2 had support near the end of the beam. A total of eight fatigue tests were conducted, which included four tests in each group.

After four fatigue tests were performed, the 1000 kN MTS test machine was not working properly and the test setup had to be moved to another MTS machine. For the remaining tests, a 5000 kN load capacity MTS machine with a displacement capacity of 360 mm was used. The highest frequency that could be achieved using this machine was 0.5 Hz.

Chapter 4

Experimental Results and Discussion

4.1 General

In this chapter the results from the experimental program are presented and the effect of splits on the structural behaviour of timber beams is discussed. The discussion focuses on the mode of failure, the beam stiffness, the load-deflection behaviour and the ultimate load, shear stress and bearing stress.

4.2 Mode of Failure

The beams under static tests exhibited three types of failure mode: (a) compression failure perpendicular to grain, (b) flexural failure, and (c) shear failure. Although the static test was designed to produce shear failure, shear failure was not dominant in Group 1, in which a total of eight (8) shear failures were observed out of seventeen (17) tests producing a 47% shear failure rate.

All the beams in Group 2 failed in shear. Shear failure was marked by an increase in split length and the development of more cracks which separate the beam into two or more parts along the grains at the end of the beam (Figure 4. 1). Shear failure was common in members having side checks which combined into a large crack during the test; as for example in beams 4A, 10A, 10C, 14A, 14C and 16A.

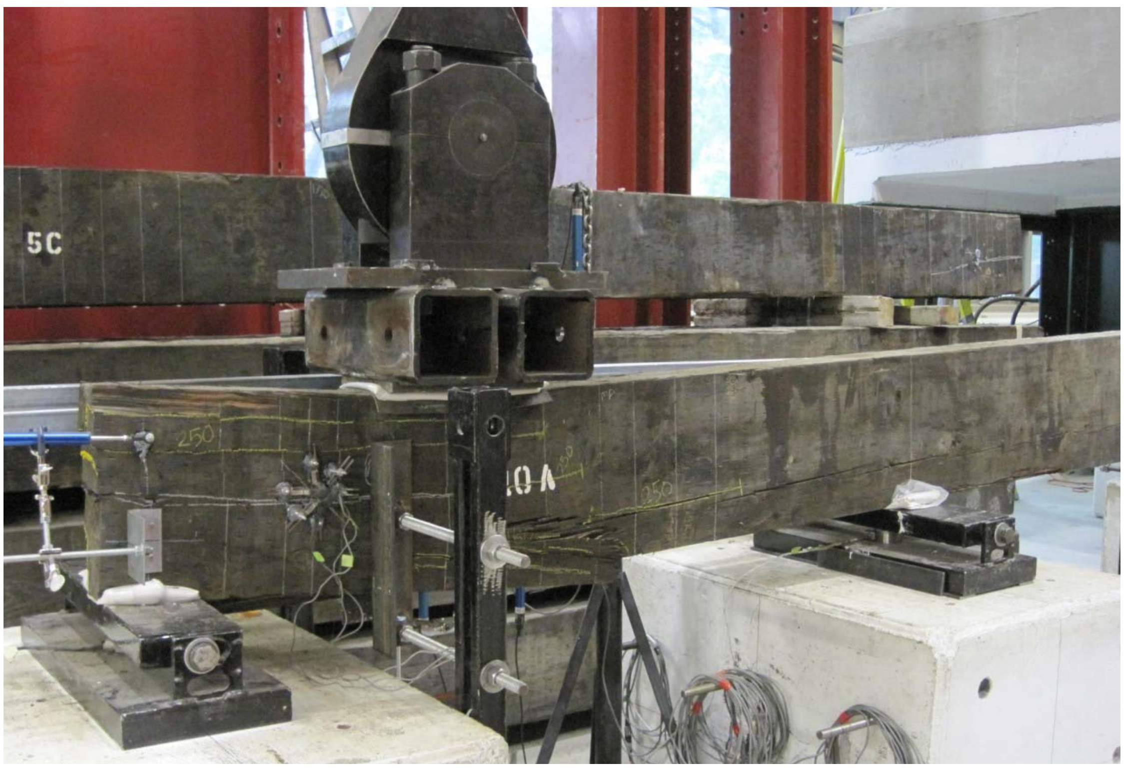

Figure 4. 1 Shear failure of Group 2 beam 10A

Every time a crack was formed, the applied load dropped. In Group 1, the split extended up to the support. During testing split propagated further beyond the support towards the location of the load. However, in one test out of 17 tests in Group 1 (beam 13C) the split length did not propagate further. The average split length prior to testing was 618 mm and the average increase in split length attained was 451 mm for Group 1 beams, except beam 13C. After reaching the peak load, the beams developed further cracks at the end and ultimately were split into several parts.

In Group 2 specimens, the split length was extended up to the load point. During testing, the splits did not increase as much as those in Group 1 specimens. In 7 tests out of 19 tests in Group 2 beams, the split length did not propagate further. The average split length prior to testing was 620 mm and average split length propagation was 183 mm for the rest of this group of beams. In this group, some of the beams disintegrated at their ends through vertical cracks along the annual rings at the end. Similarly to the behaviour of beams in Group 1, the beams also developed further cracks at the end and broke into several parts. The static test results for these two groups are shown in Table 4.1 and Table 4.2.

4.3 Beam Stiffness

The flexural stiffness, EI, of the specimens was calculated from the load-deflection graphs using the following equation (Wood Design Manual, 2001):

$$EI = \left(\frac{\Delta P}{\Delta \delta}\right)\frac{a^2 b^2}{3L} \tag{4.1}$$

Table 4. 1: Group 1 Static Test Results

Beam*	Grade	Flexural Stiffness, EI	Ultimate Load	Nominal Shear stress	Failure Mode
		($x10^9$ $kNmm^2$)	kN	MPa	
7A	No. 2	1.69	**211**	4.96	Bearing failure
23A	No. 1	2.01	**187**	4.39	Bearing failure
23C	No. 1	2.16	**162**	3.80	Bearing failure
21A	No. 2	1.82	**163**	3.83	Bearing failure
21C	No. 2	2.35	**167**	3.92	Shear Failure
17A	No. 2	2.22	**239**	5.62	Bearing failure
17C	No. 2	2.63	**231**	5.43	Shear Failure
16A	UTILITY	2.39	**233**	5.47	Shear Failure
16C	UTILITY	2.16	**227**	5.33	Bearing failure
4A	No. 2	2.30	**240**	5.64	Shear Failure
4C	No. 2	2.62	**262**	6.16	Flexural Failure
28A	No. 2	2.01	**183**	4.30	Bearing Failure
28C	No. 2	1.86	**178**	4.18	Shear Failure
13A	No.1	3.00	**222**	5.22	Shear Failure
13C	No.1	2.94	**275**	6.47	Bearing Failure
2A	No. 2	2.59	**182**	4.28	Shear Failure
2C	No. 2	2.41	**201**	4.73	Shear Failure
Average		**2.31**	**209.57**	**4.93**	

Table 4. 2: Group 2 Static Test Results

Beam*	Grade	Flexural Stiffness, EI	Ultimate Load	Nominal Shear stress	Failure Mode
		($x10^9$ $kNmm^2$)	kN	MPa	
11C	No. 2	1.48	**172**	4.04	Shear Failure
15A	No.1	1.45	**167**	3.93	Shear Failure
15C	No.1	1.23	**195**	4.58	Shear Failure
5A	No. 2	1.15	**217**	5.10	Shear Failure
5C	No. 2	1.52	**183**	4.30	Shear Failure
10A	No. 2	1.47	**223**	5.24	Shear Failure
10C	No. 2	1.46	**181**	4.25	Shear Failure
22A	No.1	1.15	**198**	4.65	Shear Failure
22C	No.1	1.43	**177**	4.16	Shear Failure
41A	No.1	1.21	**187**	4.39	Shear Failure
41C	No.1	1.65	**158**	3.71	Shear Failure
44A	No.1	1.64	**178**	4.18	Shear Failure
44C	No.1	1.54	**229**	5.38	Shear Failure
50A	No.1	1.28	**166**	3.90	Shear Failure
50C	No.1	1.67	**211**	4.96	Shear Failure
49A	No.2	1.38	**177**	4.16	Shear Failure
49C	No.2	1.13	**178**	4.18	Shear Failure
14A	No.2	1.34	**223**	5.24	Shear Failure
14C	No.2	1.23	**214**	5.03	Shear Failure
Average		**1.39**	**191.26**	**4.49**	

*Beam number denotes the original beam numbers in “as received” state and A, C denotes the two ends of one timber beam.

where E is the modulus of elasticity, I is the moment of inertia, L is the total span, δ is the deflection measured at the load point, P is the maximum load corresponding to a linear load-deflection behaviour, a is the distance from the nearest support to the load point, and b is the distance from the farthest support to the load point as shown in Figure 4. 3.

For example, beam 4C had an initial slope of the load-deflection graph of 33.21 kN/mm using Excel trend line as shown in Figure 4. 2. The full graph is available in Figure 4. 5. The known values of Eq. 4.1 are: $\frac{\Delta P}{\Delta \delta}$ = 33.21 kN/mm, a = 555 mm, b = 1140 mm, L = 1695 mm. Therefore, the stiffness, EI, of beam 4C is 2.62×10^9 $kNmm^2$.

To calculate the stiffness of the specimens it was necessary to calculate the slope of the load-deflection graph which would give the value of $\frac{\Delta P}{\Delta \delta}$. For this, only the linear part of the load-deflection curve was considered. The results are shown in Table 4.1 and Table 4.2.

There is clear difference in beam stiffness between the two groups tested in this research. Group 1 beams with a support at the tip of the split had an average stiffness of 2.31×10^9 $kNmm^2$. Group 2 beams had a support at the end of the beam and the average stiffness was 1.39×10^9 $kNmm^2$. Group 1 beams had stiffness 66% higher than that of Group 2 beams, clearly a result of absence of split between the supports.

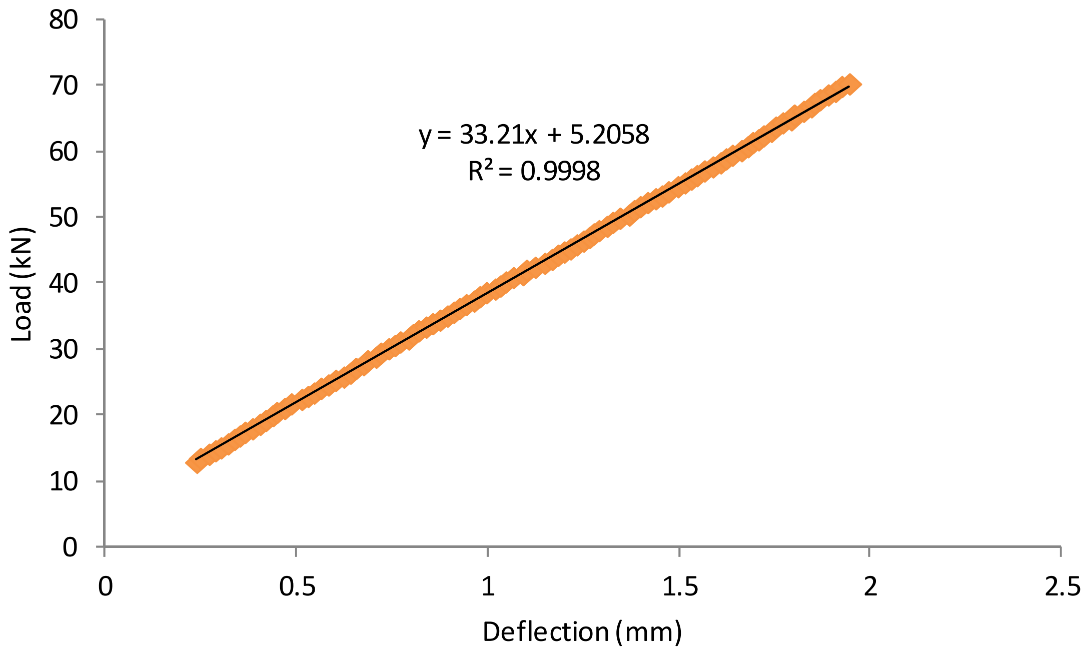

Figure 4. 2 Slope of the load-deflection graph of beam 4C.

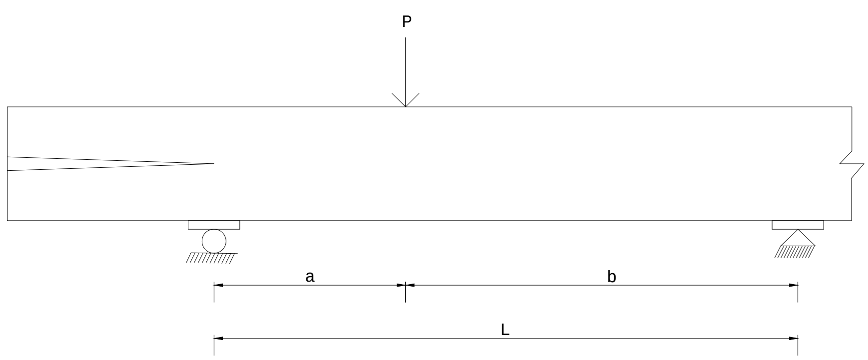

(a) Group 1 test setup

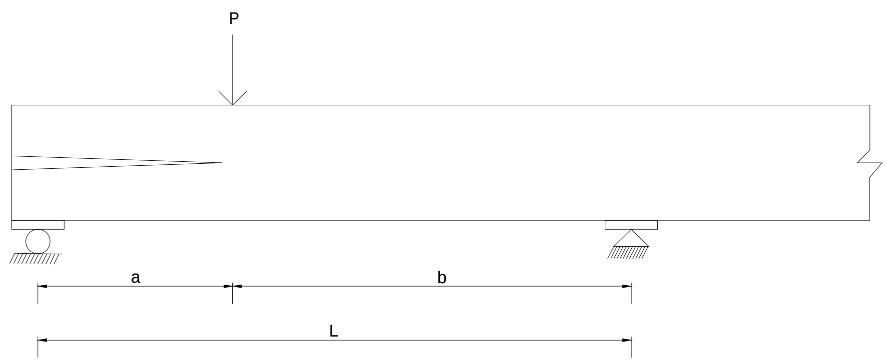

(b) Group 2 test setup

Figure 4. 3 Parameters used to calculate the flexural stiffness of the specimens

4.4 Load-Deflection Behaviour and Ultimate Load

Among the17 beams that were tested in Group 1 only one beam failed in flexure. Beam 4C that failed in flexure carried an ultimate load of 262 kN before failure. At 257 kN the beam developed a bottom tensile crack directly under the load point (Figure 4. 4) and following a drop in load, as seen in Figure 4. 5, the loads continued to increase. After reaching 262 kN, the beam developed some more cracks at mid height and the load dropped.

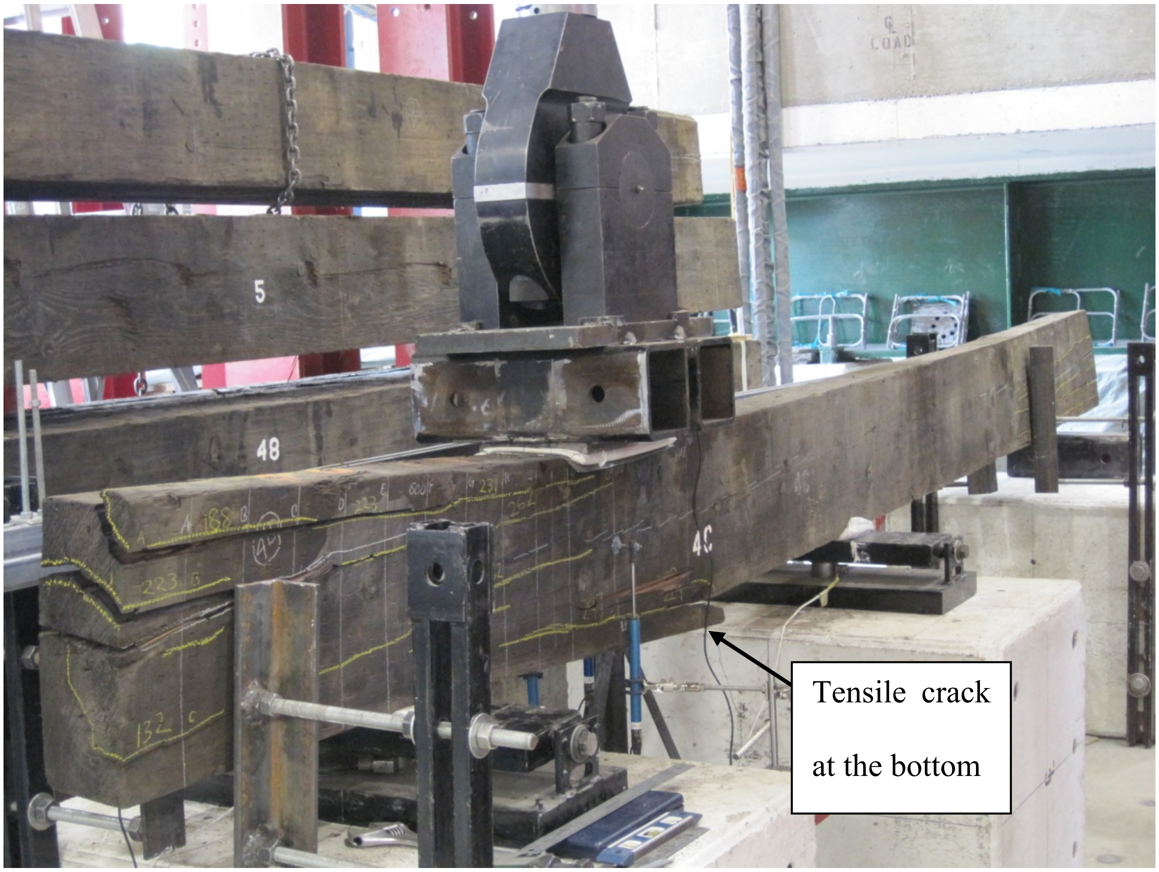

Figure 4. 4 Flexural failure of Group 1 beam 4C

Eight specimens in Group 1 failed in bearing. The load-deflection curve was initially linear up to 50 % of the ultimate load. Beams having bearing failures had a flat portion of load-deflection curve without much increase in load in the load deflection curves, for example beam 7A, 23A, 21A and 28 A, as can be seen in Figure 4. 6 and Figure 4. 7. The beams continued to deflect and had crushing under the load plates.

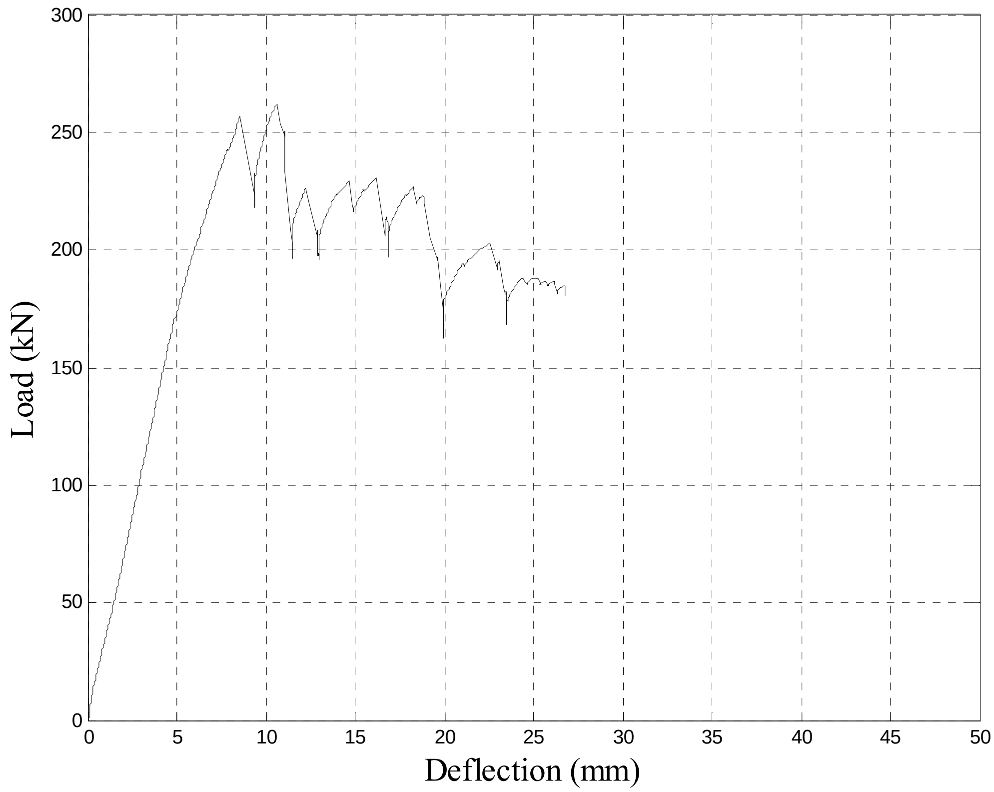

Figure 4. 5 Load-deflection curve for specimen 4C (Group 1) having flexure failure

The beams that failed in bearing had a maximum load carrying capacity of 275 kN in beam 13C and a minimum load carrying capacity of 162 kN in beam 23C. It is recalled that the beams were taken from an old bridge. It is likely that due to prolonged exposure of moisture from the wood deck, the top layers of the beams had softened, leading to bearing failure.

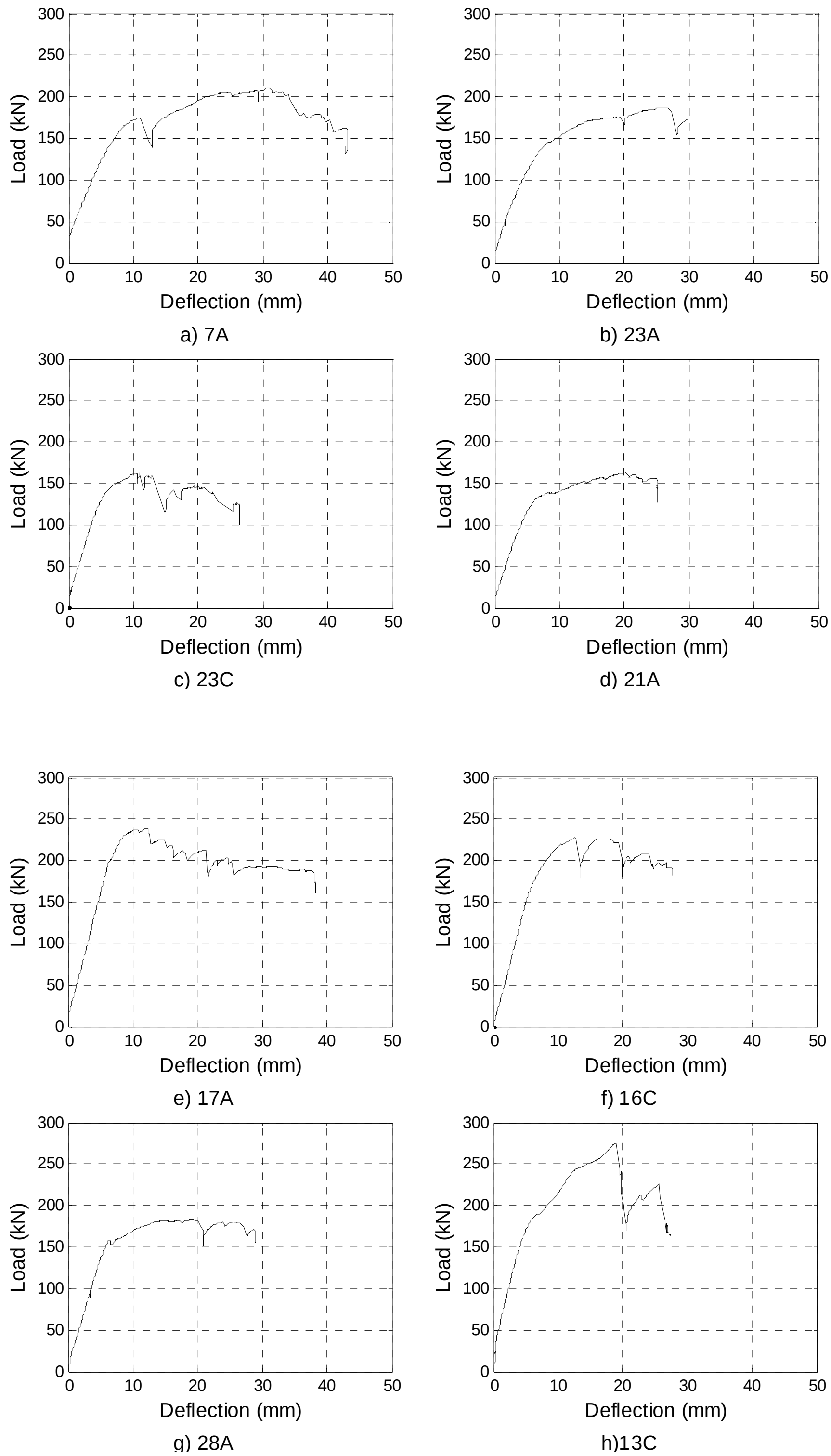

Figure 4. 6 Load-deflection curves for Group 1 beams that failed in bearing

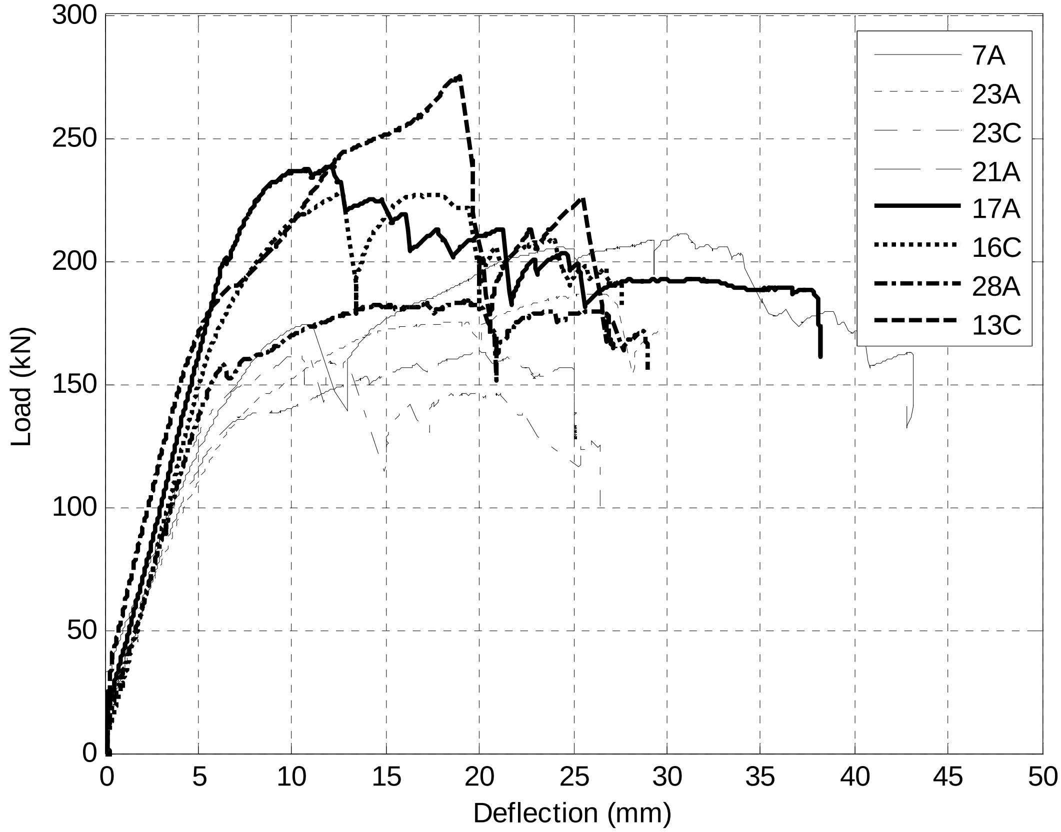

Figure 4. 7 Load-deflection curves for Group 1 beams that failed in bearing

The load-deflection behaviour of beams that failed in shear, did not display the typical linear-elastic behaviour up to failure except beam 17C, 4A, 13A and 2A as seen in Figure 4. 8 and Figure 4. 9. The curve dropped whenever cracks developed and could not recover the load.

In Group 1 beams, the maximum shear failure load was 240 kN and minimum shear failure load was 167 kN. The average ultimate load for this group of beams was 209 kN. The average deflection to reach peak load for this group was 15 mm.

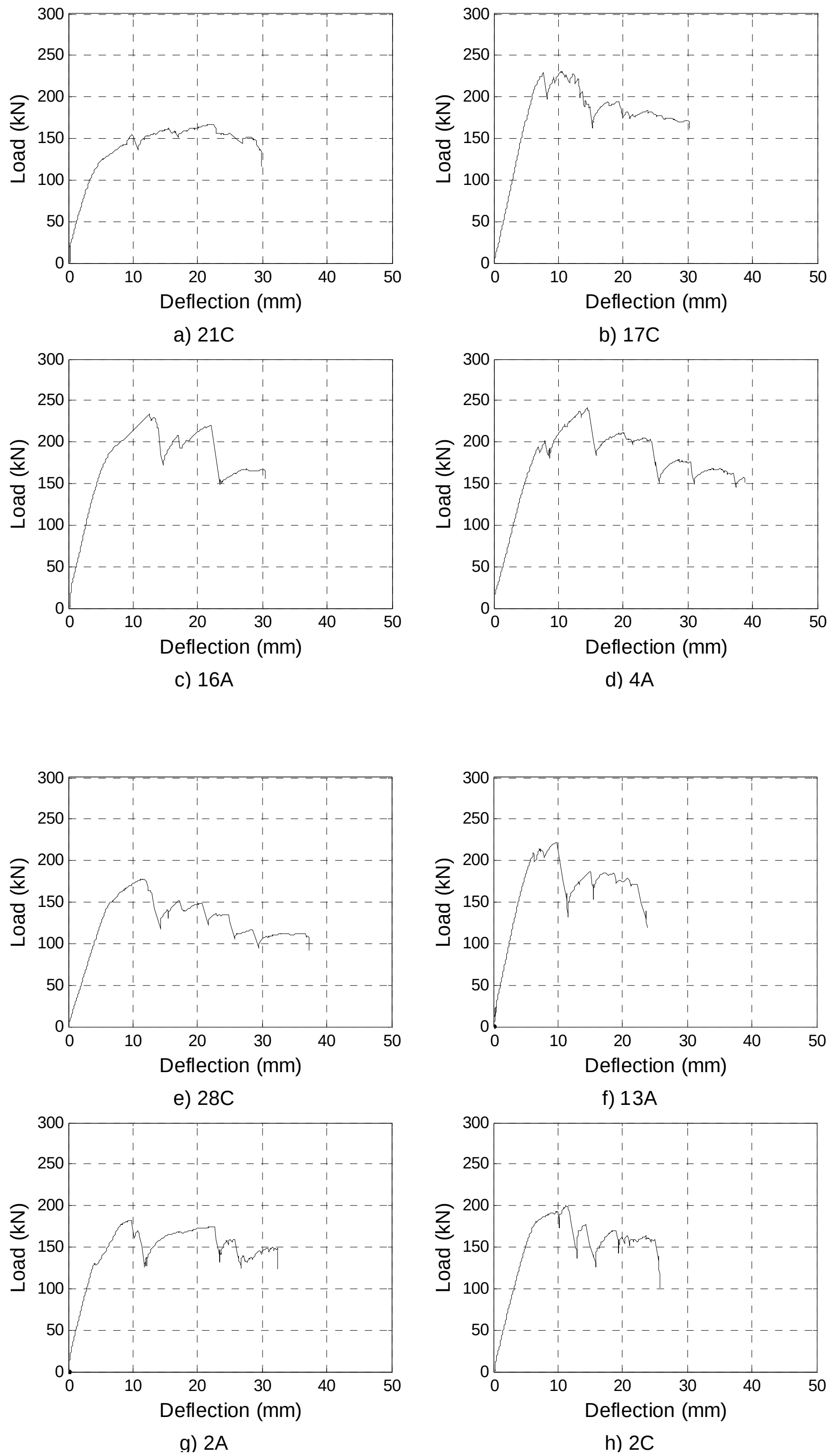

Figure 4. 8 Load-deflection curves for Group 1 specimens that failed in shear

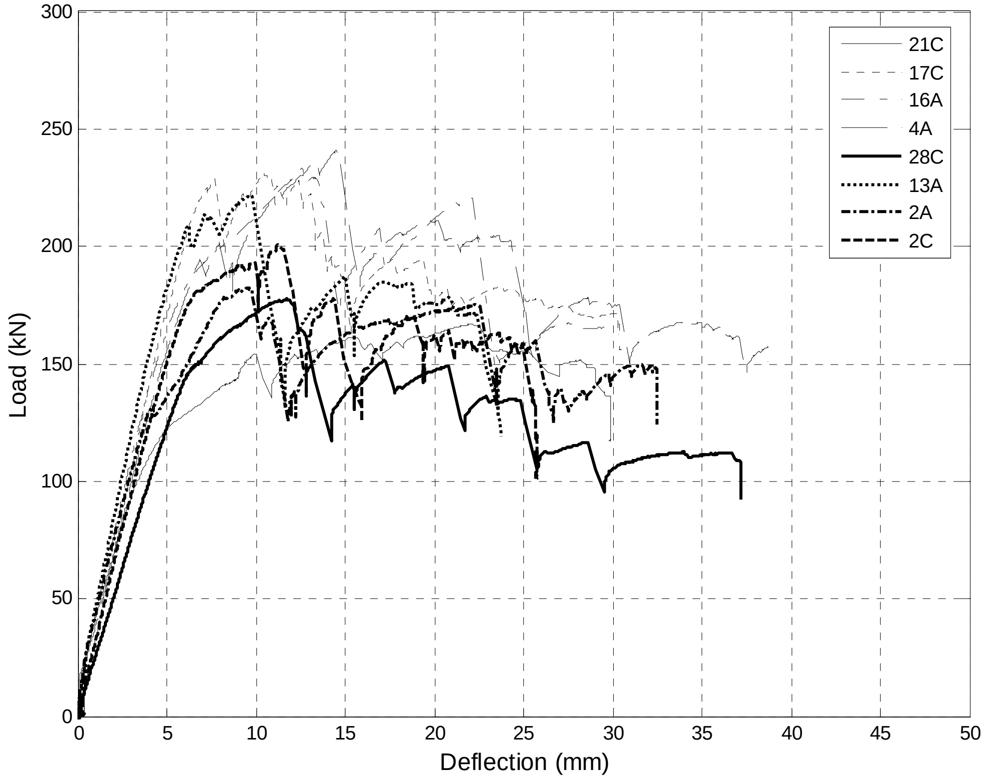

Figure 4. 9 Load-deflection curves for Group 1 specimens that failed in shear

In Group 2 beams, the maximum and minimum failure loads were 229 kN and 158 kN, respectively. The average ultimate load for this group was 191 kN. The average deflection to reach peak load for this group of beam was 16.50 mm. Group 1 beams carried on average 10 % higher load than that of Group 2. The load-deflection graphs for Group 2 beams can be seen in Figure 4. 10 and Figure 4. 11.

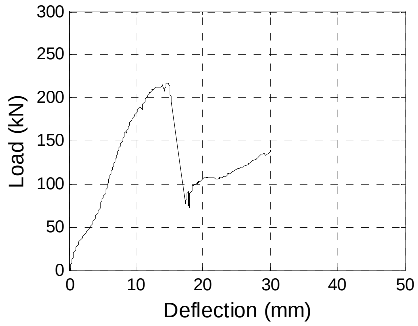

a) 5A

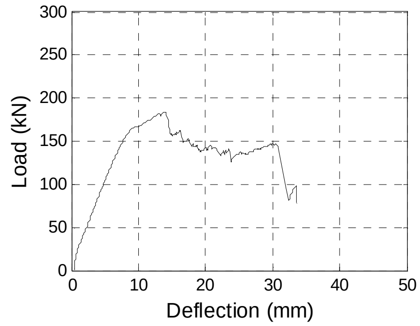

b) 5C

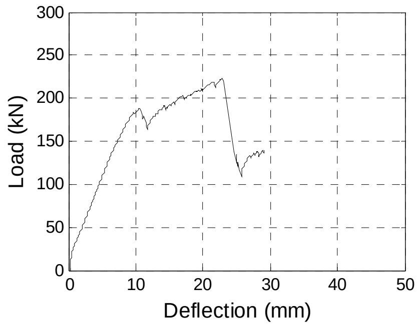

c) 10A

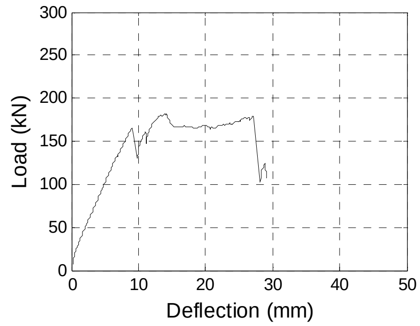

d) 10C

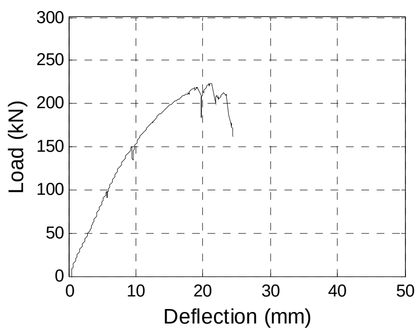

e) 14A

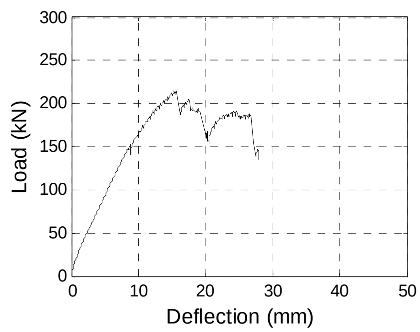

f) 14C

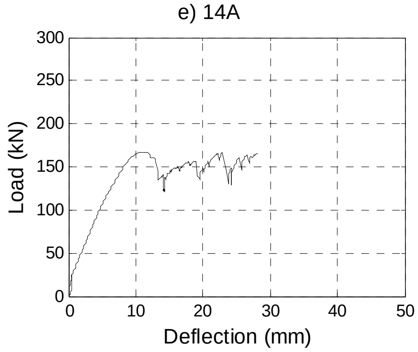

g) 15A

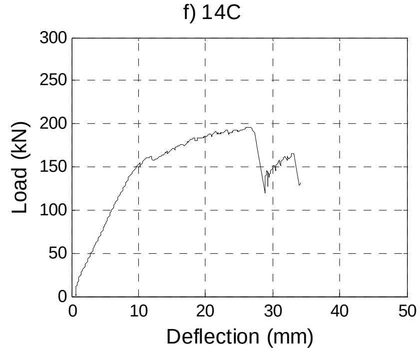

h) 15C

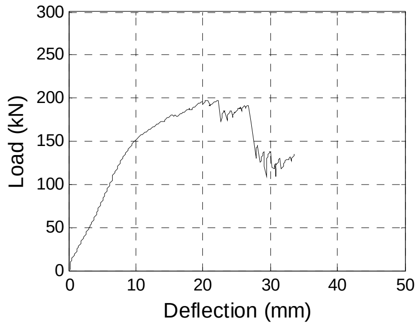

i) 22A

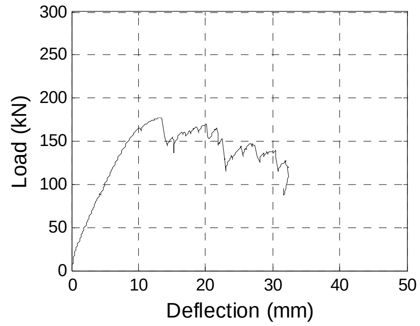

j) 22C

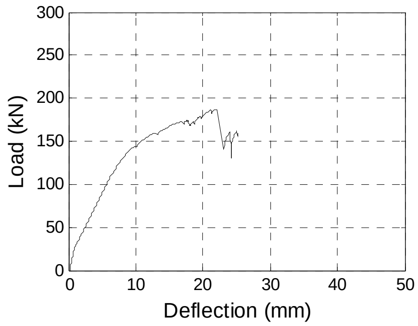

k) 41A

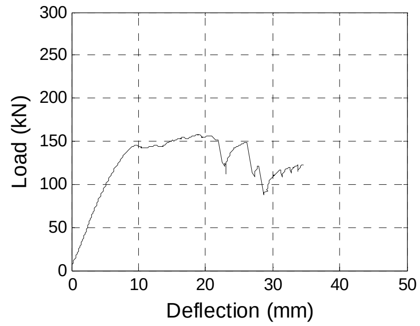

l) 41C

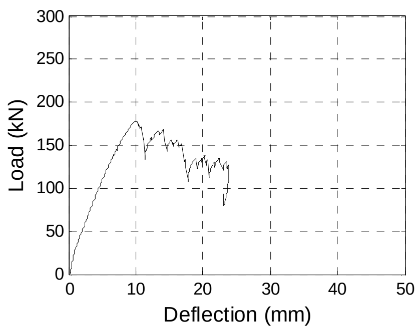

m) 44A

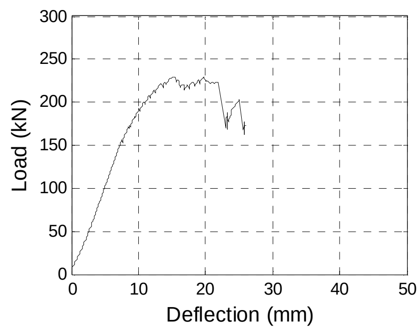

n) 44C

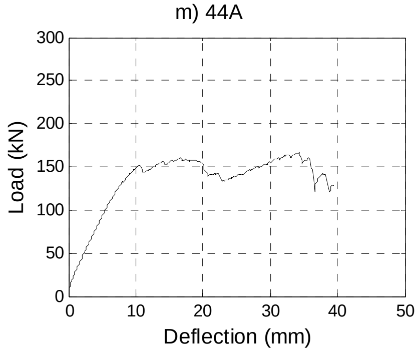

o) 50A

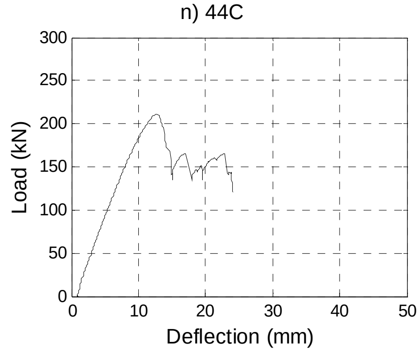

p) 50C

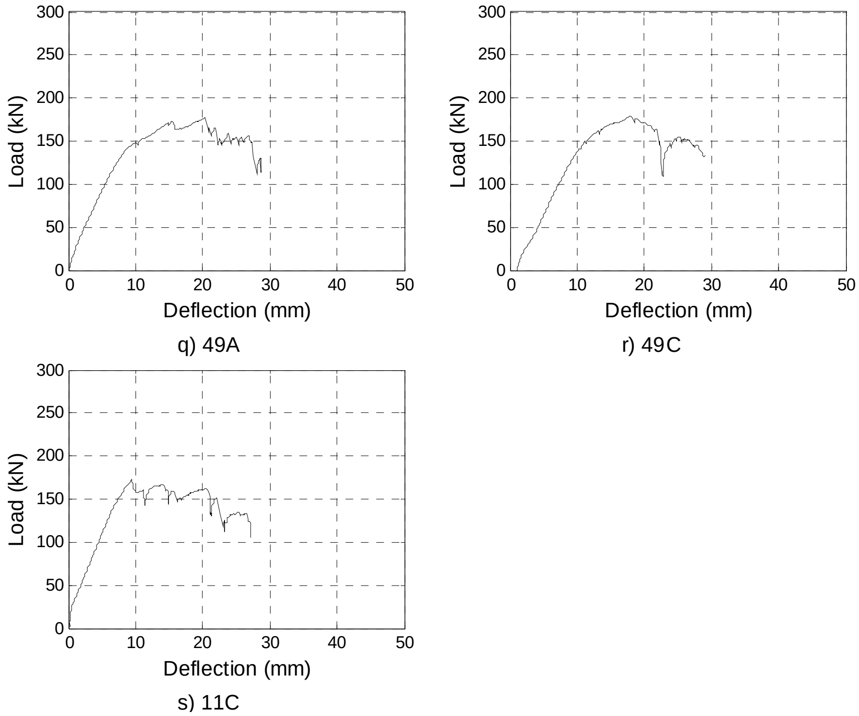

Figure 4. 10 Load-deflection curves for Group 2 specimens failing in shear

4.5 Shear Stress Calculation

From elementary mechanics the expression for principal strain is as follows (Timoshenko & Goodier, 1970):

$$\varepsilon_1 = \frac{\varepsilon_{x+}\varepsilon_y}{2} + \frac{\varepsilon_x - \varepsilon_y}{2} cos2\theta + \frac{\gamma_{xy}}{2} \sin 2\theta$$

$$= \frac{\varepsilon_x}{2}(1 - cos2\theta) + \frac{\varepsilon_y}{2}(1 - cos2\theta) + \gamma_{xy} sin\theta cos\theta$$

$$= \varepsilon_x cos^2\theta + \varepsilon_y sin^2\theta + \gamma_{xy} sin\theta cos\theta$$

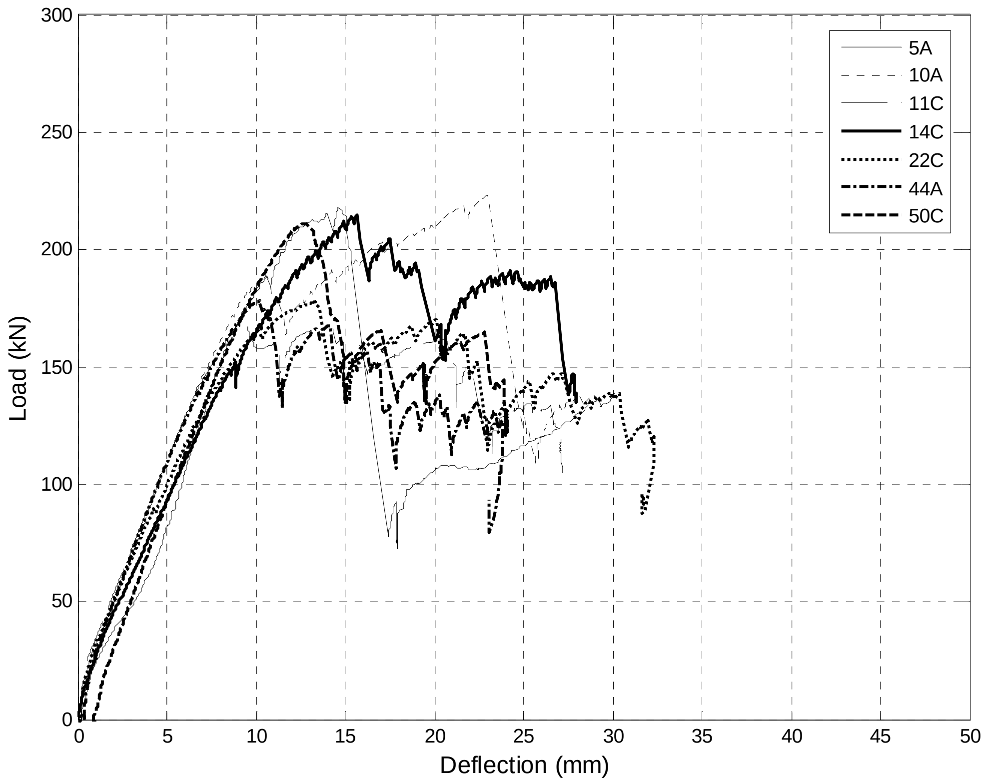

Figure 4. 11 Load-deflection curves for some Group 2 beams failing in shear

For three different angles of θ of pi-gauges, for example 0, 90, and 45°, as seen in Figure 4. 12, the above equation can be expressed as follows:

for θ = 0°; $\varepsilon_1 = \varepsilon_x$

for θ = 90°; $\varepsilon_2 = \varepsilon_y$

for θ = 45°; $\varepsilon_3 = \frac{\varepsilon_x + \varepsilon_y + \Upsilon_{xy}}{2}$

Substituting ε_x and ε_y with ε_1 and ε_2 gives the expression for the shear strain as follows:

$\Upsilon_{xy} = 2\varepsilon_3 - \varepsilon_1 - \varepsilon_2$

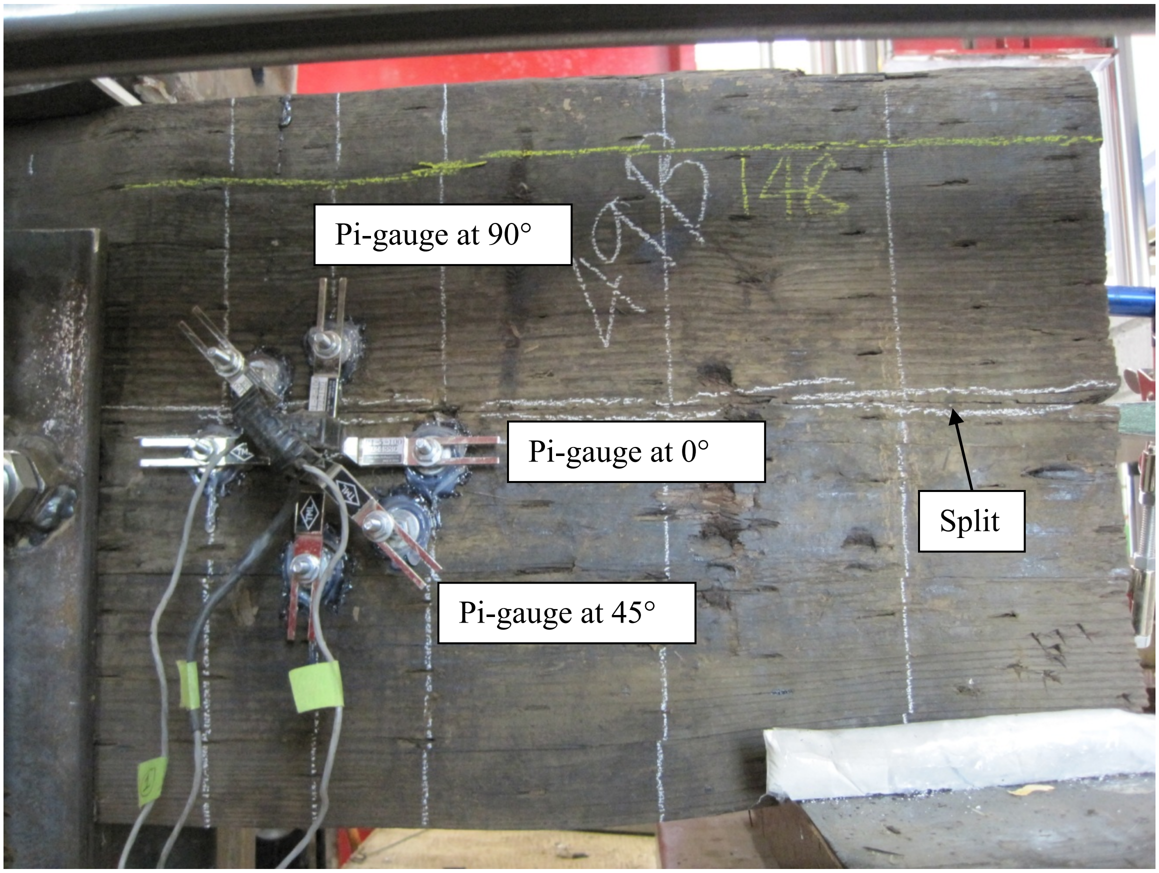

Figure 4. 12 Placement of pi-gauges on split in a Group 2 specimen

Assuming timber as a linear elastic isotropic material shear stress can be calculated as follows: $\tau = G\gamma_{xy}$

Here, G is the shear modulus of timber. The CHBDC code (Canadian Highway Bridge Design Code, CAN/CSA-S6-06, 2006) specifies shear modulus G as, $G = 0.065*E_L$.

For this research the modulus of elasticity, E_L, is calculated from the experimental load-deflection curves of timber. Shear stress values calculated using this method is available in Table 4.3 and Table 4.4.

Table 4. 3 Shear stress results for Group 1

Beam	Maximum linear load (kN)	Ultimate load (kN)	% of Ultimate load	Shear stress, τ_{pi} (MPa)	Ultimate Shear stress, τ (MPa)
7A	-	211	100	-	4.96
23A	135	187	72	1.46	4.39
23C	-	162	100	-	3.80
21A	-	163	100	-	3.83
21C	90	167	54	0.29	3.92
17A	200	239	84	1.37	5.62
17C	185	231	80	1.79	5.43
16A	-	233	100	-	5.47
16C	150	227	66	2.16	5.33
4A	-	240	100	-	5.64
4C	198	262	76	3.21	6.16
28A	-	183	100	-	4.30
28C	145	178	81	1.31	4.18
13A	199	222	90	1.90	5.22
13C	150	275	55	1.64	6.47
2A	130	182	71	1.79	4.28
2C	160	201	80	1.99	4.73

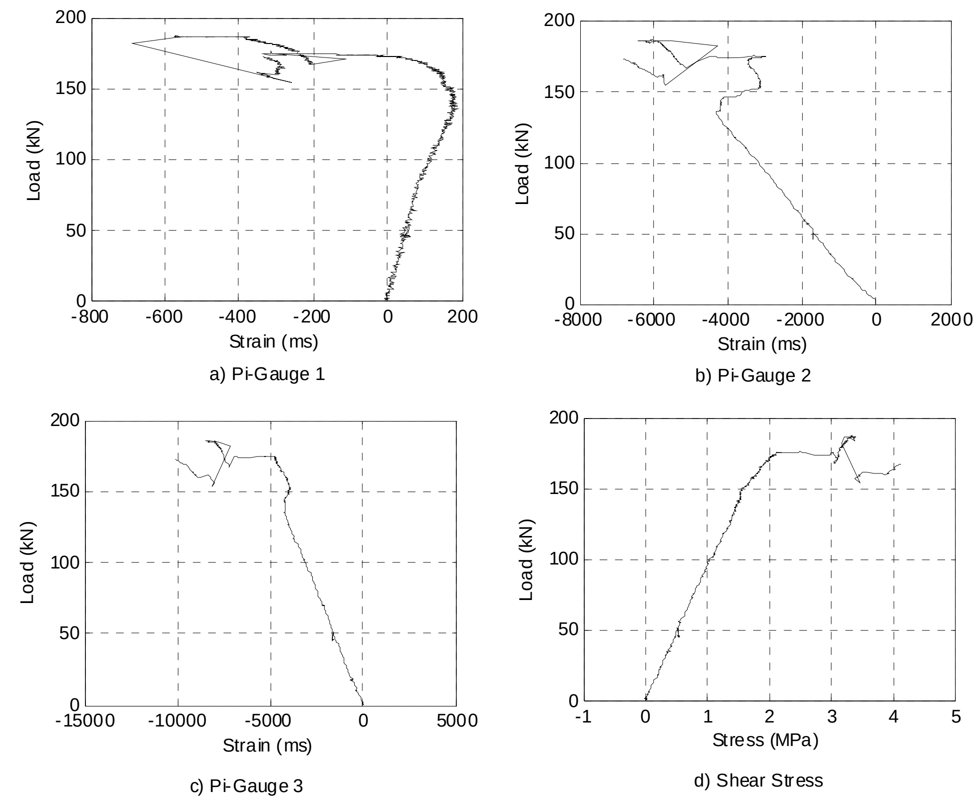

Figure 4. 13 Strain profile and shear stress of beam 23A (Group 1)

The shear stress graph of beam 23A, as seen in Figure 4. 13, has a linear ascending curve up to 135 kN. At this load the shear stress value from the graph is 1.46 MPa. The shear stress graph of beam 5C, as seen in Figure 4. 14, has a linear ascending curve up to 150 kN. At this load the shear stress value from the graph is 7.99 MPa. The shear stress values of Group 1 beams ranged from 0.29 MPa to 3.21 MPa. The shear stress values of Group 2 beams ranged from 3.00 MPa to 7.99 MPa, considering only the linear portion of the curves.

Table 4. 4 Shear stress results for Group 2

Beam	Maximum linear load (kN)	Ultimate load (kN)	% of Ultimate load	Shear stress, τ_{pi} (MPa)	Ultimate Shear stress,τ (MPa)
11C	140	172	81	6.63	4.04
15A	100	167	60	4.20	3.93
15C	-	195	100	-	4.58
5A	-	217	100	-	5.10
5C	150	183	82	7.99	4.30
10A	145	223	65	7.14	5.24
10C	-	181	100	-	4.25
22A	-	198	100	-	4.65
22C	-	177	100	-	4.16
41A	144	187	77	5.30	4.39
41C	70	158	44	3.00	3.71
44A	137	178	77	5.41	4.18
44C	155	229	68	6.48	5.38
50A	115	166	69	5.50	3.90
50C	-	211	100	-	4.96
49A	-	177	100	-	4.16
49C	141	178	79	4.99	4.18
14A	-	223	100	-	5.24
14C	129	214	60	6.32	5.03

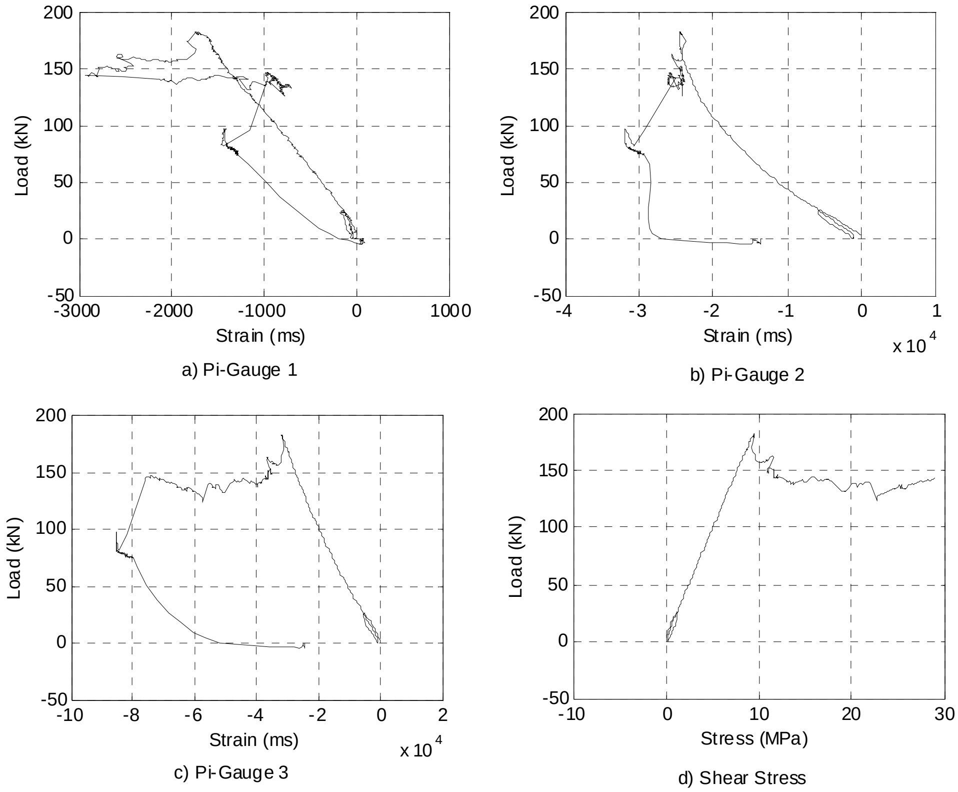

Figure 4. 14 Strain profile and shear stress of beam 5C (Group 2)

It is to be noted that, Group 2 beams have splits along their span at mid height and the pi gauges were placed on those splits as shown in Figure 4. 12. The strain profile and shear stress curves for Group 1 and Group 2 beams are available in Appendix B.

4.6 Fatigue Tests

Eight beams were tested under fatigue, four tests in each group. As in the case of static tests, Group 1 specimens had splits outside the span and Group 2 specimens had splits within the span.

To evaluate the fatigue capacity of the timber specimens, the first test was conducted with an applied load of 150 kN, which was about 72% of the average static strength of Group 1 specimens and 78% of the average static strength of Group 2 specimens. The minimum-to -maximum load ratio was chosen to be 0.1. Before starting a fatigue test, a load of 150 kN was applied to the specimens. The remaining specimens were loaded to 100 kN load, which is about 48% of static strength of Group 1 and 52% of static strength of Group 2, before the start of the fatigue test.

4.6.1 Fatigue test of Group 1 specimens

In Group 1, the support was located at 600 mm from the end of the beam, i.e. at the tip of the split. The specimen 6A, as seen in Figure 4. 15, had a split length of 642 mm prior to the start of the test. The first test on this group was done using 150 kN of load to get an initial value for the fatigue capacity of this group of beams. The first cycle was completed using a static test of 150 kN which is about 71 % of the average ultimate load carrying capacity of this group of beams. The ratio of minimum and maximum loads was kept constant to 0.1. Therefore the beam experienced a loading range of 15 to 150 kN. The deflection recorded at 100 kN was 3.8 mm and at 150 kN it was 5.5 mm. During the static test the split length increased from 642 to 1730 mm. However the beam was able to sustain 150 kN of load despite this long crack.

After the static test, the fatigue test was started at a frequency of 0.3 Hz. The ratio of minimum to maximum loads was kept constant at 0.1 After 500 cycles, the beam started showing signs of fibre softening under the load. At 1750 cycles, there was a 40 mm increase in the split length and at 2820 cycles, there was a 100 mm increase in the split length. The beam continued to soften more under the load with increase in deflections. At 3387 cycles, there was a crack at the top part of the beam which originated from the end and propagated beyond the load point as shown in Figure 4. 15. After this crack the beam could no longer sustain the load and the test stopped at 3720 cycles. The maximum deflection recorded for this beam was 20.5 mm as seen in Figure 4. 16.

The fatigue test of beam 6A at 150 kN could sustain only 3720 cycles, producing an early failure of the beam. For the later tests on this group of beams 100 kN load was applied to prevent such failures.

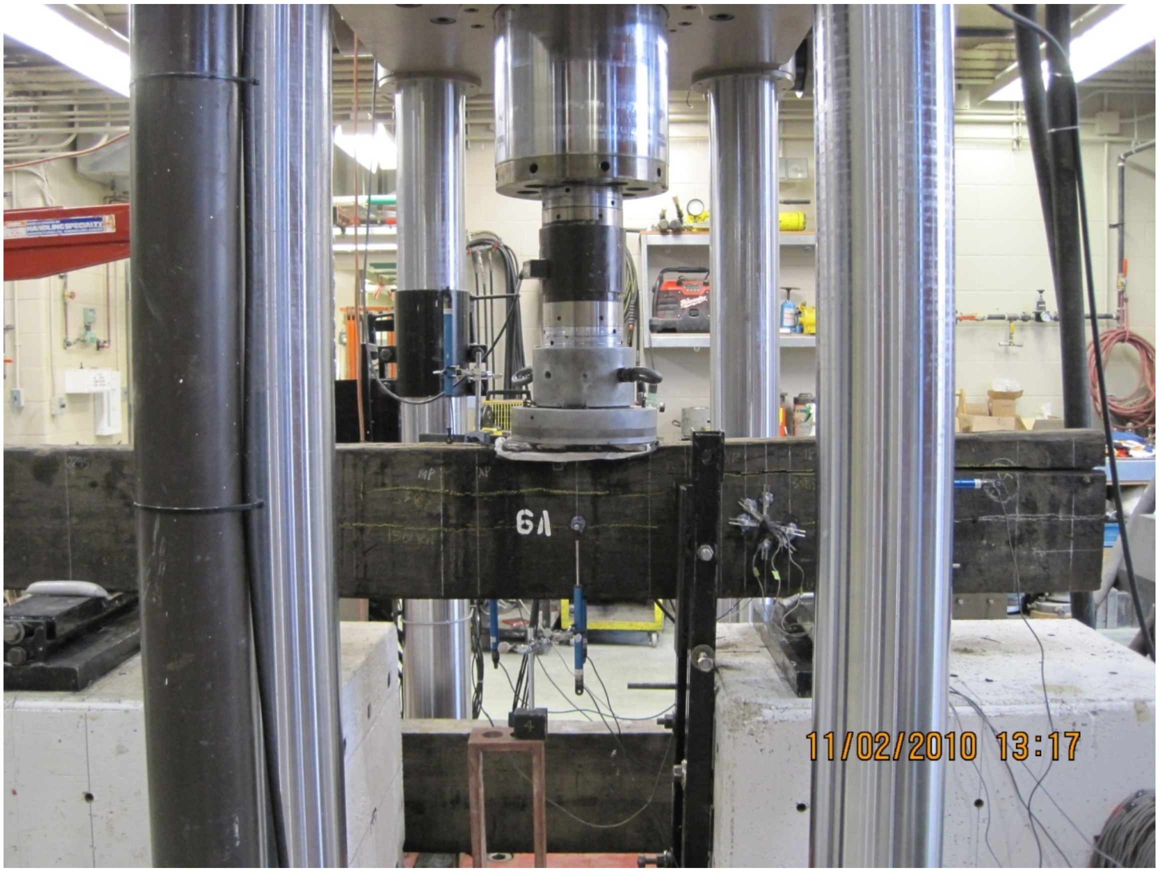

Figure 4. 15 Fatigue test of beam 6A after the test

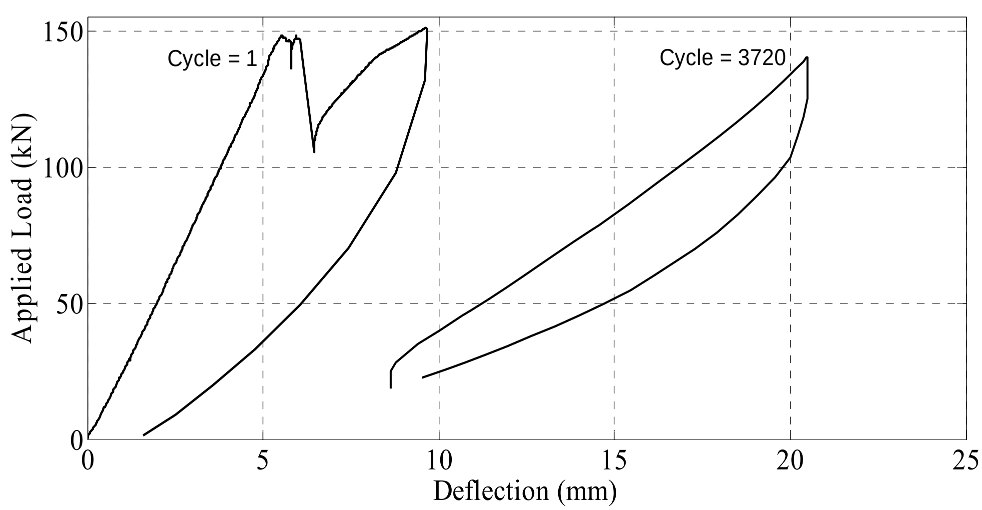

Figure 4. 16 Load-deflection curves for beam 6A

Beam 6C was tested first at a static load of 100 kN. This load represents about 48% of the static load capacity of this group of beams. The beam deflected 3.3 mm at 100 kN applied static load. The frequency used for this fatigue test was 0.5 Hz. The ratio of minimum to maximum loads was kept constant to 0.1. Therefore the beam experienced a fatigue loading range of 10 kN to 100 kN. The beam sustained a total of 240,813 cycles.

The initial split length for this beam was 610 mm. When the fatigue test started the increase in split length was 650 mm after 46,000 cycles. At 95,000 cycles there was another 100 mm increase in split length. The beam was not able to sustain load after 240,000 cycles and the test was stopped. The beam experienced a maximum deflection of 16 mm, as seen in Figure 4. 17.

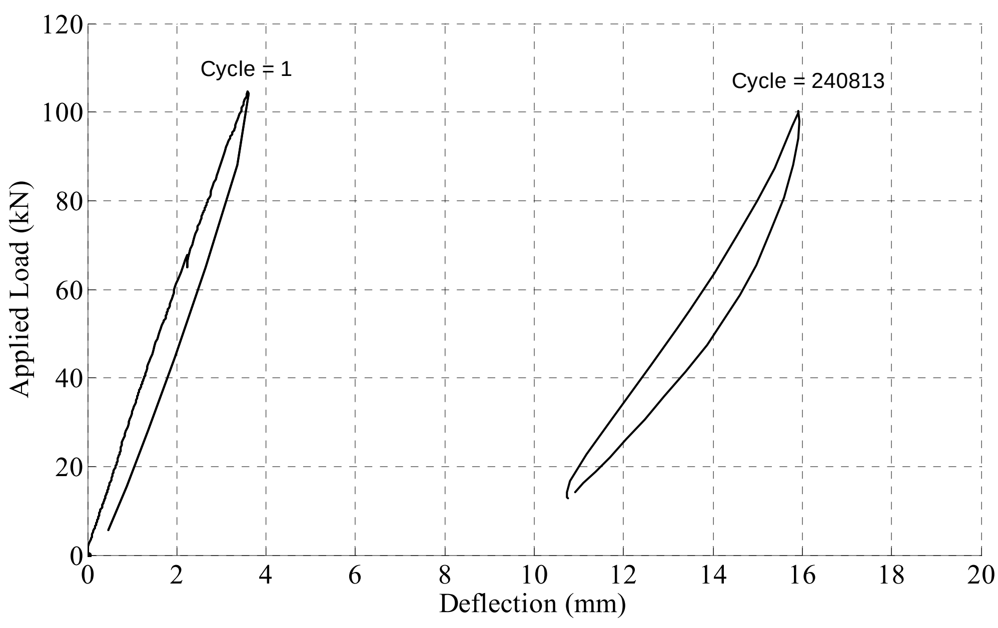

Figure 4. 17 Load-deflection curves for beam 6C

Similarly to beam 6C, beam 3A was also tested first at a static load of 100 kN. The deflection recorded at 100 kN was 3.5 mm. The beam was twisted sideways and also had side checks at 145 mm height. The split was induced at 145 mm height and extended 687.5 mm in length. When the fatigue test started, the beam had very little increase in deflection with cycles. After 40,000 cycles the split length increased by 400 mm. However the deflection was only 3.7 mm compared to 3.5 mm deflection at the beginning. The beam continued to sustain more cycles without much increase in deflection. After one million cycles the deflection was only 7.5 mm (Figure 4. 18).

The beam was later tested under static load to find its residual strength after one million cycles. The beam reached an ultimate load of 233 kN. The beam developed some bottom tensile crack around a knot at 200 kN and at 180 kN the beam cracked at top which continued to the load point and the load dropped to 134 kN as shown in Figure 4. 19.

Beam 3C was also tested first in static mode for up to 100 kN. The beam deflected about 3 mm at 100 kN. The beam had side checks all along the length at one side of the beam at 120 mm height from bottom. During the fatigue test there was no increase in split length. After applying one million cycles the beam had only 9.8 mm deflection (Figure 4. 20) and had no increase in split length. There were also no signs of failure. The fatigue test was stopped after one million cycles and was tested later under static load to failure to find its residual strength.

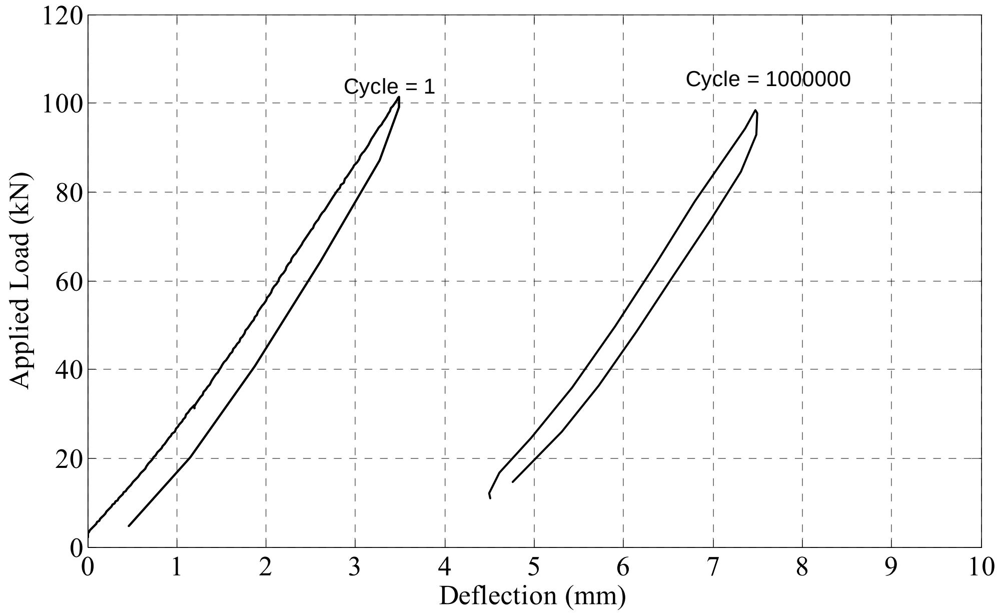

Figure 4. 18 Load Deflection curve for beam 3A

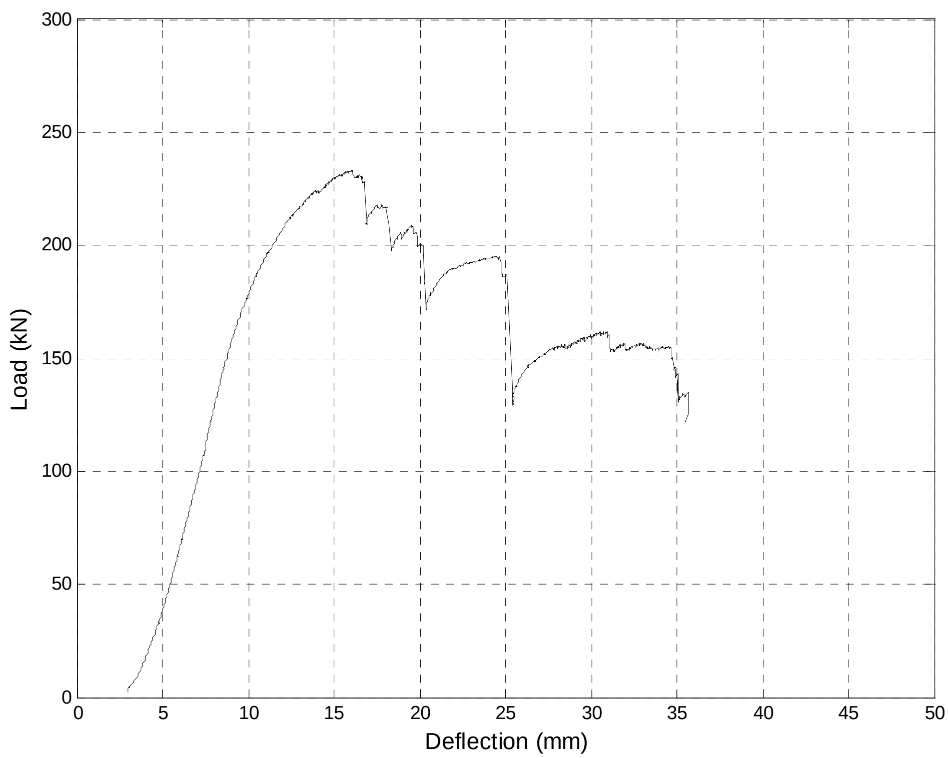

Figure 4. 19 Static failure test of beam 3A

The beam reached a maximum load of 226 kN as seen in Figure 4. 21. After reaching the maximum load, the load dropped to 200 kN due to shear cracks. Another shear crack caused the load to drop to 145 kN. Later the beam continued to lose its strength due to tensile splitting of fibres at the bottom under the load point.

The fatigue test results of Group 1 beams are also summarised in Table 4. 5.

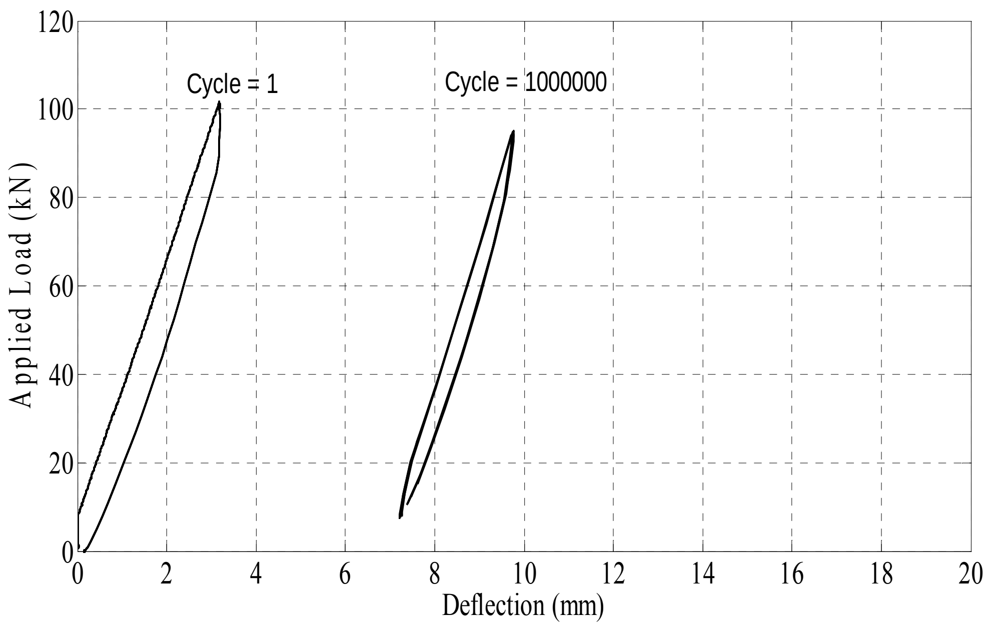

Figure 4. 20 Load-deflection curves for beam 3C

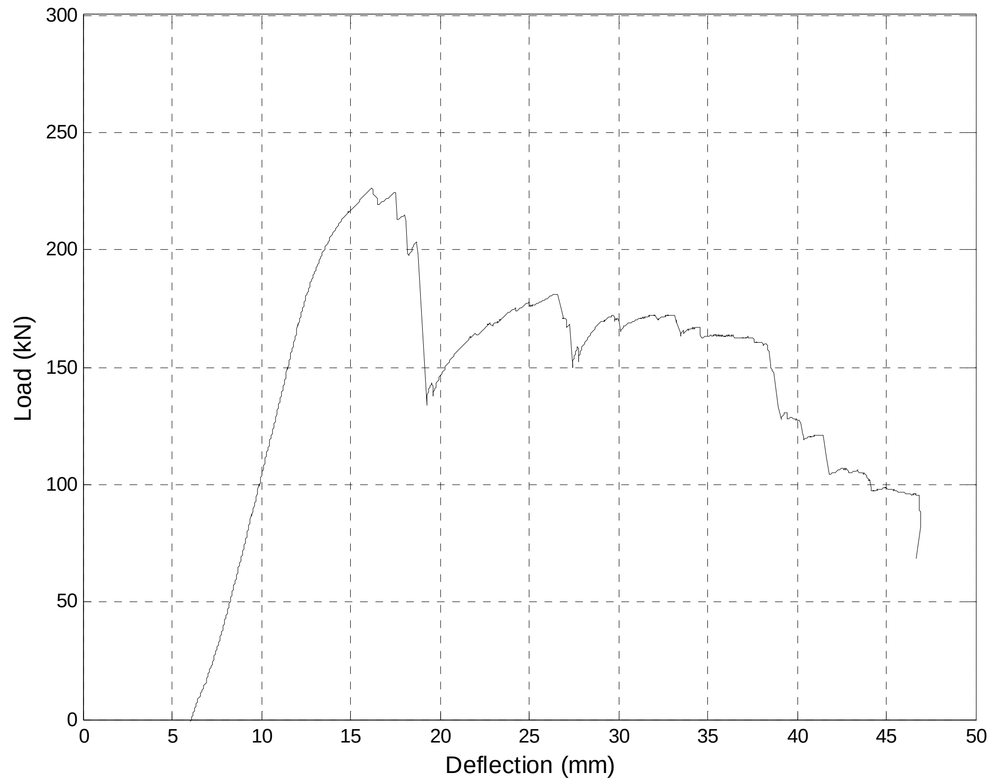

Figure 4. 21 Static failure test of beam 3C

Table 4. 5 Fatigue test results for Group 1 beams

	Beam	Grade	Load (kN)		Frequency (Hz)	Total Cycles	Failure Mode
			min	max			
1	**6A**	No.2	15	150	0.3	3,720	LP Bearing failure
2	**6C**	No.2	10	100	0.5	240,813	Shear Failure
3	**3A**	Utility	10	100	0.5	1,000,000	-
4	**3C**	Utility	10	100	0.5	1,000,000	-

4.6.2 Fatigue test of Group 2 specimens

The first test in Group 2 specimens was conducted with an applied load of 150 kN which represents 78% of the average static strength of specimens in this group. The ratio of minimum and maximum load was kept constant at 0.1. Therefore the beam experienced a loading range of 15 to 150 kN.

Before the start of the fatigue test a static load of 150 kN was applied. When the fatigue tests started with beam 42A, the beam could not sustain many cycles of loading at 150 kN and could reach only 395 cycles. The beam had an initial split length of 700 mm. The split length propagated further with additional cycles of load. During the static test the split length propagated 80 mm. When the fatigue test started, the split length propagated another 50 mm within the first 200 cycles. Within 200 to 395 cycles the split length propagated 160 mm more.

There was a knot at the very bottom of the beam under the load plate. One crack originated from this knot as the fatigue test started. One low level crack also developed from the end of the beam during 200 to 395 cycles. Because of these cracks the beam could not sustain 150 kN load and the test was stopped after 395 cycles. The load deflection curve of the beam 42A is shown in Figure 4. 22. The maximum deflection recorded for this beam was 32 mm. For the remaining tests, 100 kN load was applied to the beams which is about 52% of the static strength of the beams.

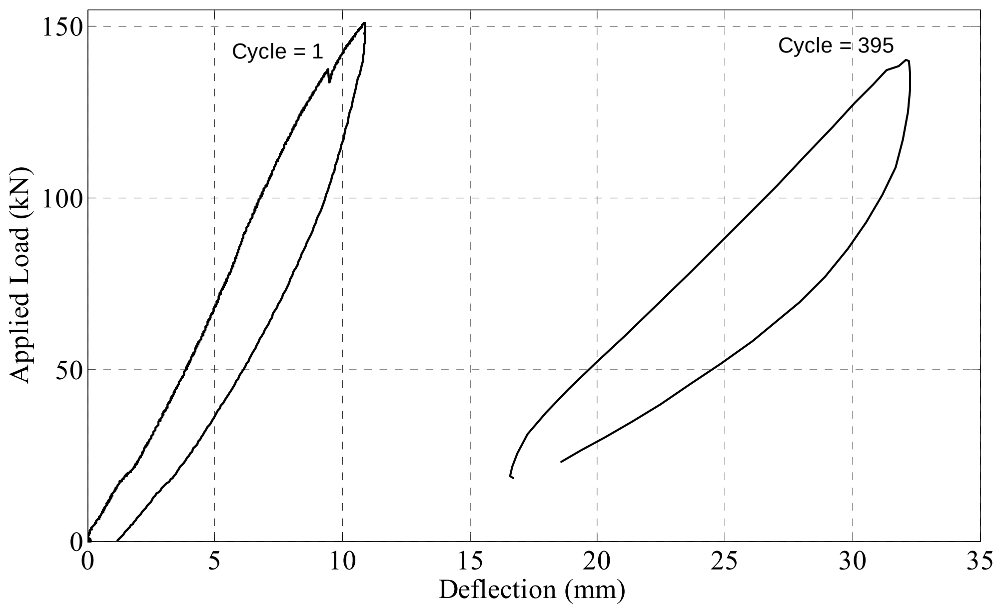

Figure 4. 22 Load-deflection curves for beam 42A

Beam 42C as seen in Figure 4. 23, sustained a total of 136,268 cycles of load prior to failure. After 100,000 cycles of loading the beam developed some cracks at the lower end of the beam. One crack also originated from the bottom of the support. With cycles of loading, these cracks at the end started opening up big. The end part disintegrated more and more and one crack also developed at the top end of the beam (Figure 4. 24). At this point the beam could not sustain the desired load and the test was stopped. The original split length of the beam was 760 mm at mid height. The split length propagated additional 170 mm from the start to the end of the test. There were no signs of fibre softening or bearing failure under the support or at the load point, however there was disintegration at the support of the beam. The maximum deflection recorded for this beam was 43 mm as seen in Figure 4. 25.

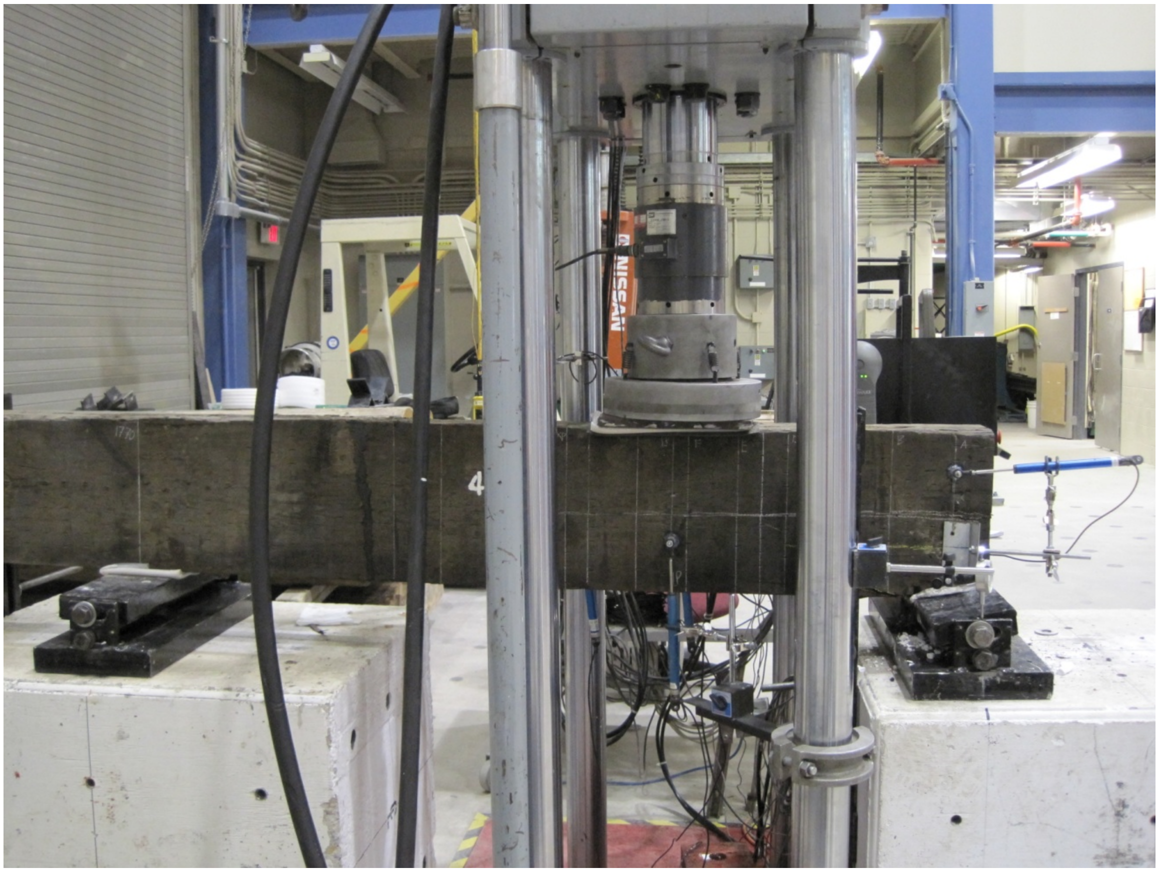

Figure 4. 23 Fatigue test of beam 42C

Beam 9A sustained a total of 22,186 cycles of loading. The beam had a wane at the bottom corner (Figure 4. 26) and plaster was used to make the beam level. After, 500 cycles of loading, the split length increased by 80 mm and the beam developed a crack along the grain at the lower end of the beam. The split length continued to increase with cycles of loading. Cracks also developed along the grain at the lower end of the beam. Due to the presence of a wane, the beam disintegrated more and more at the end of the beam. The total increase in split length was 327 mm. The maximum deflection recorded for this beam was 23 mm, as seen in Figure 4. 27.

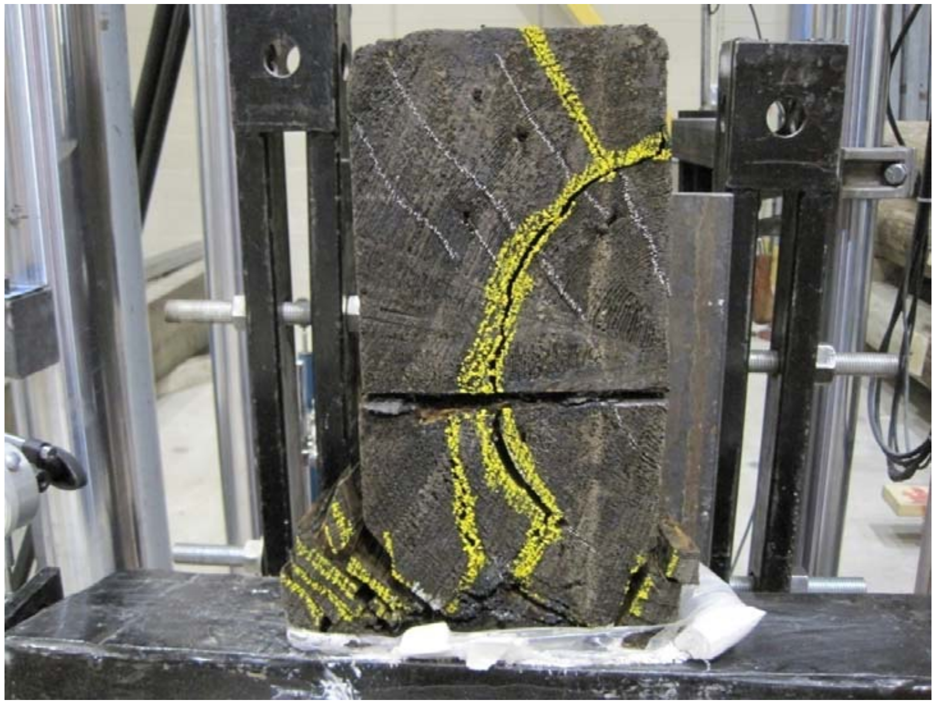

Figure 4. 24 End section of beam 42C after the test

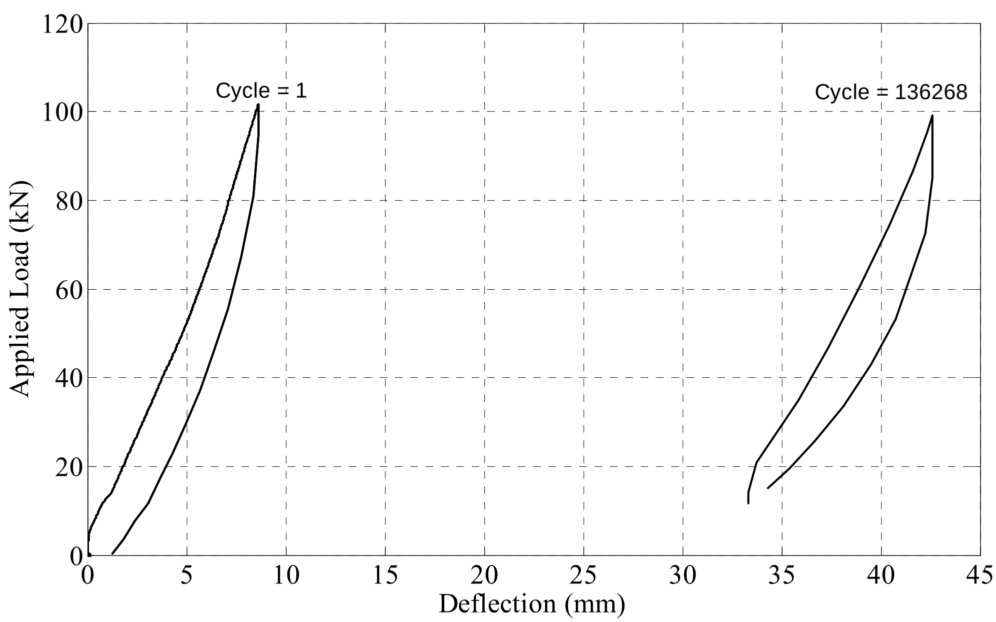

Figure 4. 25 Load-deflection curves for beam 42C

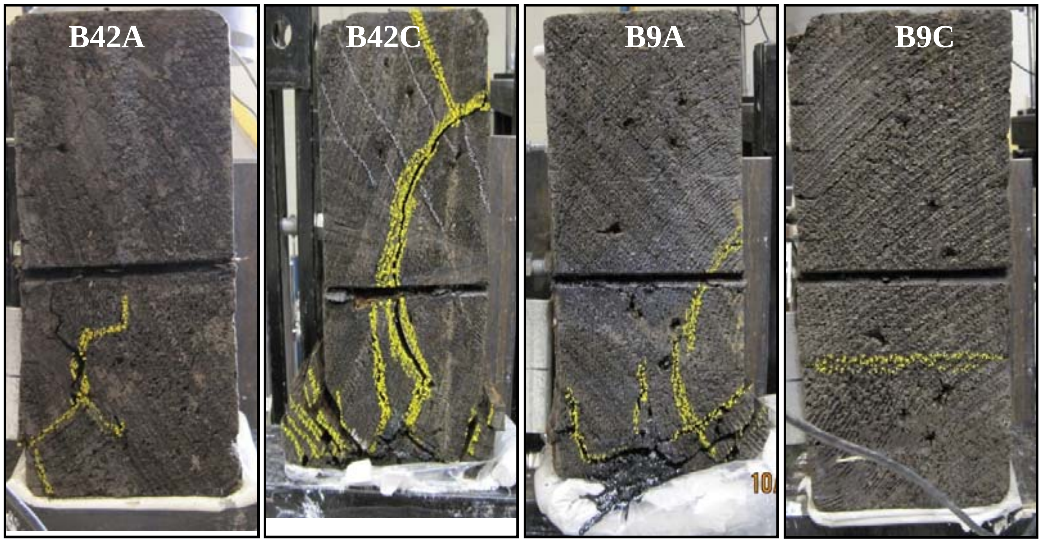

(a) 42A (b) 42C (c) 9A (d) 9C

Figure 4. 26 End section of the Group 2 beams after fatigue test

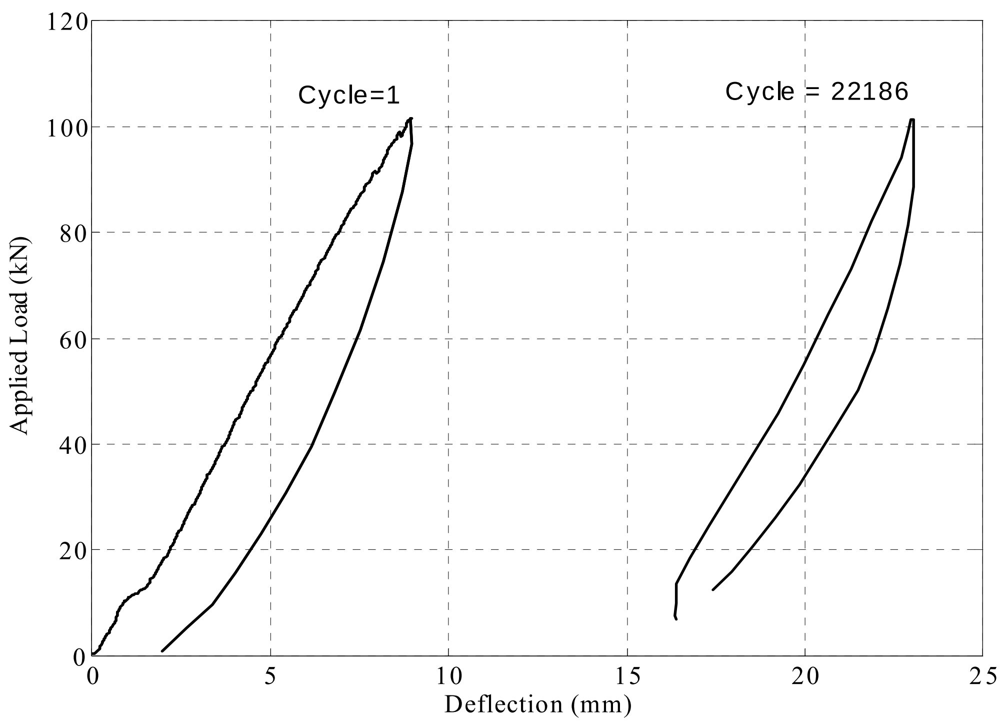

Figure 4. 27 Load-deflection curves for beam 9A

Beam 9C was tested in a different MTS machine which had a 5000 kN load capacity and 360 mm deflection capacity. The maximum frequency achieved with this machine was 0.3 Hz. After 50 cycles of loading, the beam developed a longitudinal crack at 110 mm height from the end and propagated up to 800 mm. Another crack originated under the load point at the bottom of the section at 183 cycles. The split length also increased 300 mm within the first 500 cycles of loading. The low height cracks continued to increase with the number of cycles. After 7500 cycles the beam was not able to sustain any more load and the test was stopped after 7697 cycles. The maximum deflection recorded for this beam was 28 mm, as seen in Figure 4. 28. Table 4. 6 gives a summary of fatigue test results of Group 2 beams.

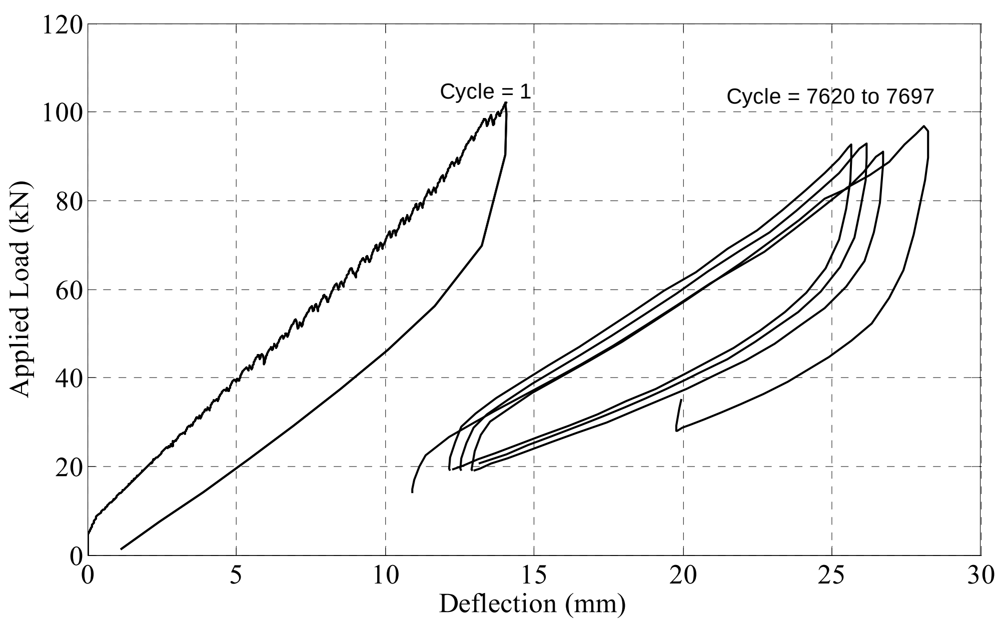

Figure 4. 28 Load-deflection curves for beam B9C

Table 4. 6 Fatigue test results for Group 2 beams

	Beam	Grade	Load (kN)		Frequency	Total Cycles	Failure Mode
			min	max	Hz		
1	**42A**	No.2	15	150	0.5	395	Shear Failure
2	**42C**	No.2	10	100	0.75	136,268	End Disintegration*
3	**9A**	No.2	10	100	0.75	22,186	End Disintegration*
4	**9C**	No.2	10	100	0.3	7,697	Shear Failure

* See Figure 4. 26 for a view of the ends of the beam at failure.

Chapter 5

Data Analysis

5.1 General

This chapter focuses on the strength properties of timber as found from the experimental test results. Both static and fatigue test results were analysed to obtain an overview of the timber beam shear strength. Static test results were used here to determine the shear strength and bearing strength of the beams tested and were compared with the specified strength in the CAN/CSA-S6-06 standard. Fatigue test results are used to develop the fatigue strength of the beams tested.

5.2 Static Test Data

5.2.1 Shear Stress

The main objective of this research project was to determine the shear strength of beams having a split at their end and the effect of the support location on their strength. The present CAN/CSA-S6-06 standard specifies the longitudinal shear strength, f_{vu}, for Douglas-fir beams to be 1.5 MPa. This longitudinal shear strength value is the same for select structural, No.1 and No. 2 beams and stringers. According to NLGA (Standard Grading Rules for Canadian Lumber, 2007), a select structural beams and stringers can have split with length equal to half width of the section. No. 1 beams and stringers can have a short split that is equal in length to the width of the member. No. 2 beams and stringers are allowed to have a medium split that is equal in length to twice the width of the piece. The split length used in this research was 600 mm which is more than four times the width of the beam.

However, the Canadian Highway Bridge Design Code (CHBDC) does not specify anything regarding the location of the support and therefore the split can be outside of the loading span, as in Group 1 beams, or within the loading span as in Group 2 beams. The CHBDC (2006) specified value is therefore assumed to be 1.5 MPa for both groups.

Using the theory of solid mechanics the longitudinal shear stress in a rectangular beam at mid height is:

$$f_{vu} = \frac{VQ}{It} = 1.5\frac{V}{bh}$$

where,

f_{vu}= longitudinal shear stress

V= Vertical shear force

Q = Shear area of the member

I = Moment of inertia

t = thickness of the member

b = width of the member

h = depth of the member

The shear stress results are summarised according to failure type in Table 5.1. The average shear stress for the Group 1 beams was 4.93 MPa (Table 4.1). Considering only the beams with shear failure, the beams had an average shear strength value of 4.86 MPa (Table 5. 1) compared to CHBDC (2006) specified value of only 1.5 MPa. It is noted that the beams that did not fail in shear had higher shear strength than that corresponding to the failure loads.

The maximum and minimum shear strengths for Group 1 were 6.47 MPa and 3.8 MPa respectively and have a standard deviation of 0.82 MPa. The fifth percentile value of shear stress for this group is 3.82 MPa based on normal distribution.

Table 5. 1: Summary of static test results for two groups

Beam Diagram	Failure Type	Shear Strength (MPa)	Ultimate Load (kN)	No of Beams
Group 1 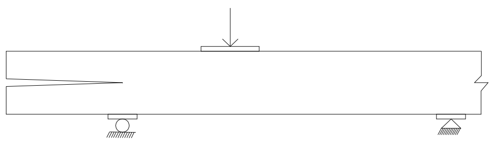	Flexural Failure	>6.16	262	1
	Bearing Failure	>4.84	206	8
	Shear Failure	4.86	207	8
Group 2 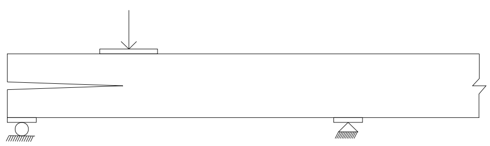	Shear Failure	4.49	191	19

For Group 2 beams, as seen in Table 5. 1, the average shear stress is 4.49 MPa which is still higher than the CHBDC (2006) specified value of 1.5 MPa. The maximum and minimum shear strengths for this group are 5.38 MPa and 3.71 MPa and have a standard deviation of 0.52 MPa. The fifth percentile value of shear stress for this group is 3.88 MPa. It is to be noted that this group of beams had split length along its loading span which is higher than the permitted split length in NLGA (2007). The 5th percentile values for both groups are very comparable.

5.2.2 Bearing Stress

The beams were supported on two steel plates which were 150 mm in width. The load was applied to the beams using a 300 mm wide steel plate. To avoid bearing failure, both a neoprene pad and plaster were used. Although adequate bearing lengths were provided, there were eight bearing failures observed in Group 1.That represent 47 % of the total number of tests completed in this group. The bearing failures occurred under the load due to softening of fibres which continued to increase with the increase in load. In some beams, fibre softening was also observed at the support locations, as for example in beam 23A and beam 23C. The current Canadian Highway Bridge Design Code (CHBDC 2006) limits the specified compressive stress perpendicular to grain to 4.7 MPa for Douglas-fir species irrespective of their grades.

Table 5. 2 represents a comparison of experimental bearing stress and the CHBDC (2006) specified bearing stress. The highest bearing stress is 7.05 MPa and the lowest bearing stress is 4.16 MPa. The average bearing stress is 5.28 MPa and a fifth percentile value of bearing stress is 4.17 MPa only. It is to be noted that, the average experimental bearing stress is not very high compared to the CHBDC specified value and the 5th percentile value of bearing stress falls below the CHBDC specified specified bearing stress.

The beams in this research originated from a bridge that was removed from service, so that may be the reason for the low value of the 5th percentile strength. Moreover in real world, timber beams in bridges are not supported on steel plates. Rather timber beams are connected to decks and piers using fasteners and more likely timber to timber connection. The bearing stresses in these situations should be smaller.

Table 5. 2 Bearing stress results for Group 1 beams

	Beam	Grade	Ultimate Load	Bearing Stress	CHBDC Bearing Stress
			kN	MPa	MPa
1	**7A**	No. 2	**211**	5.41	4.7
2	**23A**	No. 1	**187**	4.79	4.7
3	**23C**	No. 1	**162**	4.16*	4.7
4	**21A**	No. 2	**163**	4.19*	4.7
5	**17A**	No. 2	**239**	6.12	4.7
6	**16C**	UTILITY	**227**	5.82	4.7
7	**28A**	No. 2	**183**	4.69*	4.7
8	**13C**	No.1	**275**	7.05	4.7
	Average		**206**	**5.28**	**4.70**

* Less than the code limits for bearing stress

5.3 Fatigue Strength

The purpose of the fatigue tests was to determine the fatigue life of split timber beams with different support location. From the test results it was possible to construct load-cycle (P-N) curves to understand the fatigue behaviour of timber beams. Memon (2005) used a modified Matsui (2001) formula to construct the P-N curve for the fatigue strength of concrete deck slabs. The equation is as follows:

$$log_{10}n = C(\frac{1}{\left(\frac{P}{P_u}\right)} - 1)^{\alpha} \tag{5.1}$$

where,

n = number of cycles

P = applied cyclic load

P_u = static failure load.

C and α in Eq. 5.1 are two factors which depend on the fatigue curve of the member.

5.3.1 Fatigue Strength of Group 1 and Group 2 Beams

To find the fatigue strength of the timber beams using Eq. 5.1, it is necessary to find the values of C and α. For example, Beam 6A of Group 1 was subjected to a fatigue load of 150 kN which represents 72% of the static strength of the group (Table 5.3). The beam sustained a total of 3,720 cycles. The variations of deflection with the number of cycles for Group 1 specimens are available in Figure 5. 1. The best fit curve using Excel gives a linear equation of the order 1 for beam 6A (Table 5.4). The value of α is therefore 1 (α = 1/ order of polynomial). Using a value of α = 1, n = 3,720 and P/P_u = 0.72 yields the value of C = 8.99.

Knowing the values of C and α, Equation 5.1 can be used to draw the fatigue strength curve of beam 6A. The values of C and α for all the specimens of Group 1 and Group 2 are available in Table 5.3. The best fit equations are available in Table 5.4 and in Figure 5. 1 and Figure 5. 2. Fatigue strength curves for Group 1 and Group 2 specimens using this method are available in Figure 5. 3 and Figure 5. 4.

Beam 3A and 3C of Group 1 sustained one million cycles of load and showed no signs of failure. Due to time constraint, fatigue tests were stopped after one million cycles of repeated loads. It is assumed that these beams would sustain more cycles of load and therefore, have not been used in this method as they did not fail.

Table 5. 3 α and C values for Group 1 and Group 2 specimens

Beam	% of Static strength (P/P_u)	No. of cycles (n)	$\log_{10}n$	α	C
Group 1					
6A	0.72	3,720	3.57	1.00	8.99
6C	0.48	240,813	5.38	0.33	5.22
3A	0.48	>1,000,000	-	1.00	-
3C	0.48	>1,000,000	-	0.33	-
Group 2					
42A	0.78	395	2.60	0.50	4.95
42C	0.52	136,268	5.13	0.33	5.29
9A	0.52	22,186	4.35	1.00	4.76
9C	0.52	7,697	3.89	0.33	4.01

Table 5. 4 Best fit equations of fatigue curves for Group 1 and Group 2 specimens

Specimen	Polynomial equation	Degree of polynomial	α
Group 1			
6A	$y = 0.0015x + 10.294$	1	1.00
6C	$y = 3E\text{-}15x^3 - 1E\text{-}09x^2 + 0.0002x + 5.3187$	3	0.33
3A	$y = 4E\text{-}06x + 3.7208$	1	1.00
3C	$y = 3E\text{-}17x^3 - 5E\text{-}11x^2 + 3E\text{-}05x + 4.1564$	3	0.33
Group 2			
42A	$y = 0.0001x^2 - 0.0305x + 12.135$	2	0.50
42C	$y = 2E\text{-}14x^3 - 4E\text{-}09x^2 + 0.0003x + 9.8878$	3	0.33
9A	$y = 0.0005x + 8.8398$	1	1.00
9C	$y = 4E\text{-}11x^3 - 5E\text{-}07x^2 + 0.0019x + 14.247$	3	0.33

*See Figure 5. 1 and Figure 5. 2 for a view of the best fit curves

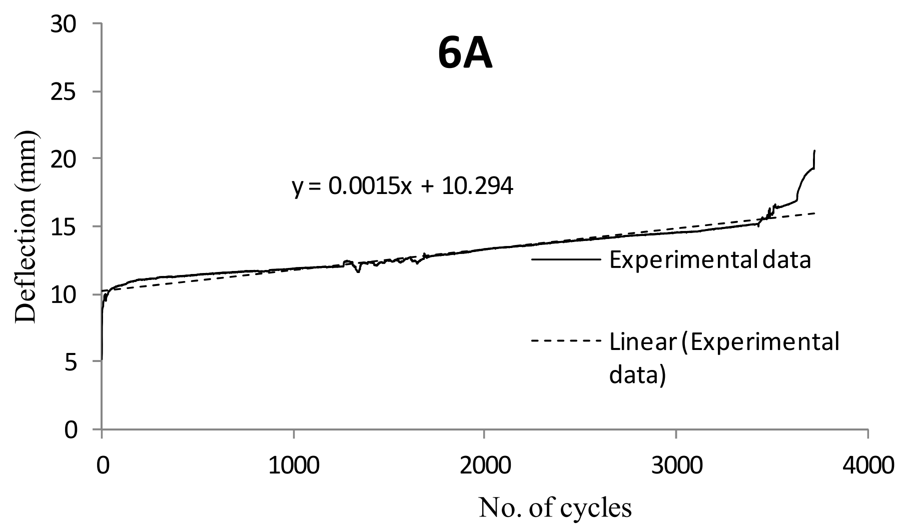

a) Fatigue curve of beam 6A

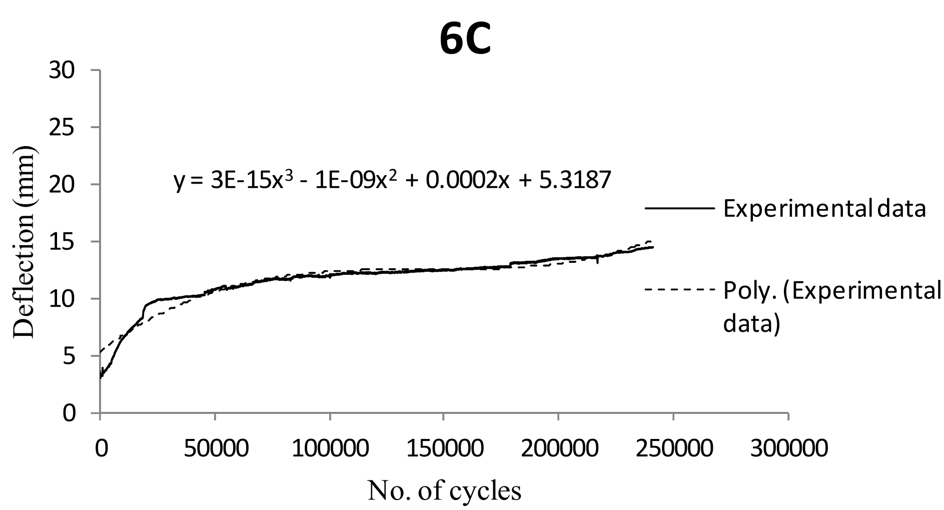

b) Fatigue curve of beam 6C

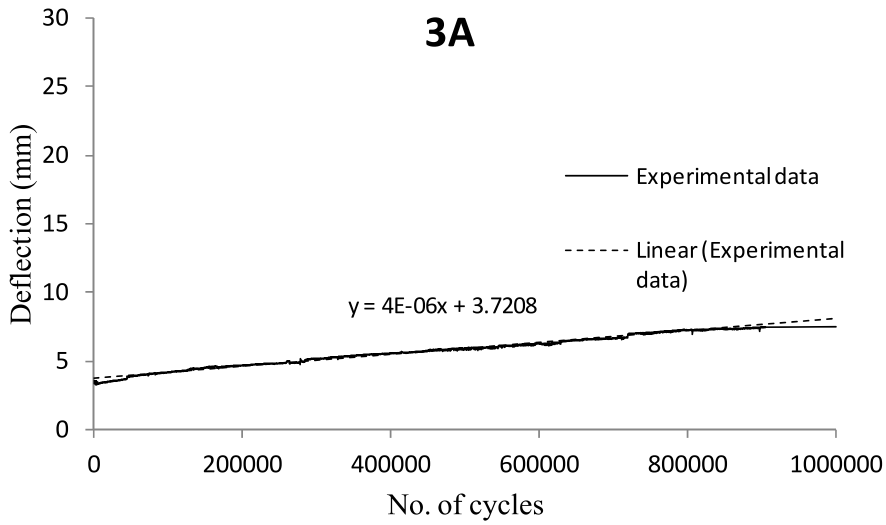

c) Fatigue curve of beam 3A

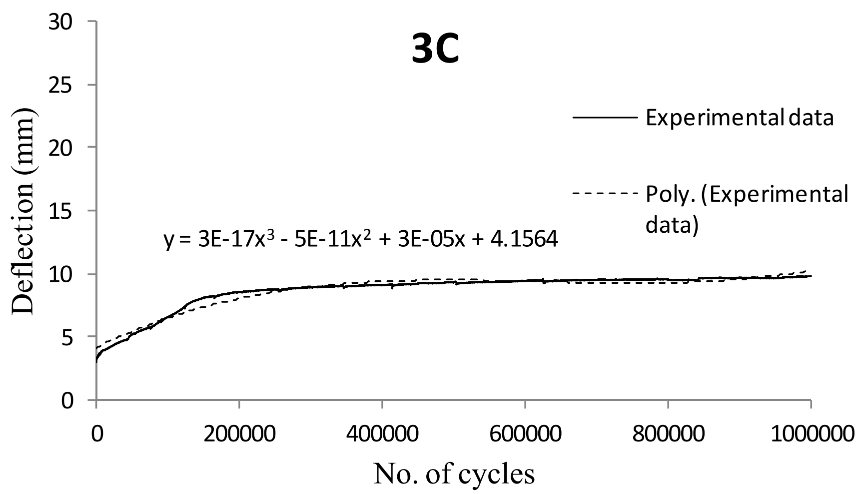

d) Fatigue curve of beam 3C

Figure 5. 1 Fatigue curves of Group 1 beams

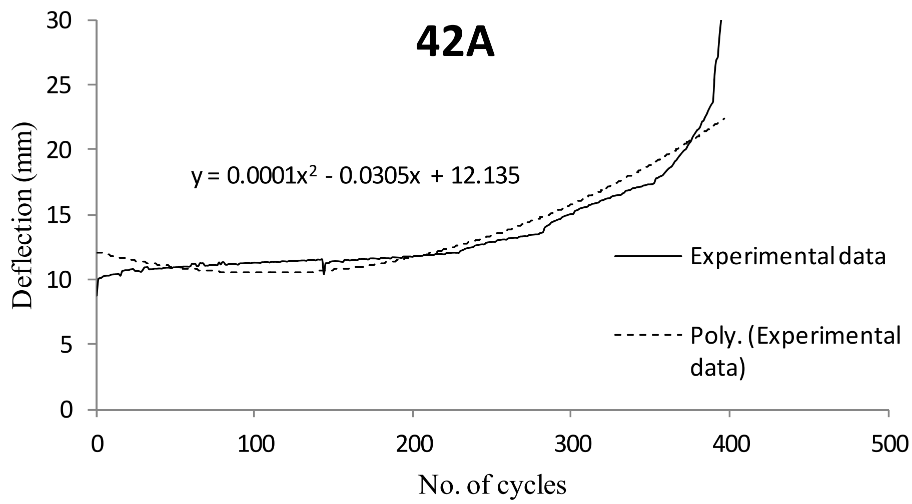

a) Fatigue curve of beam 42A

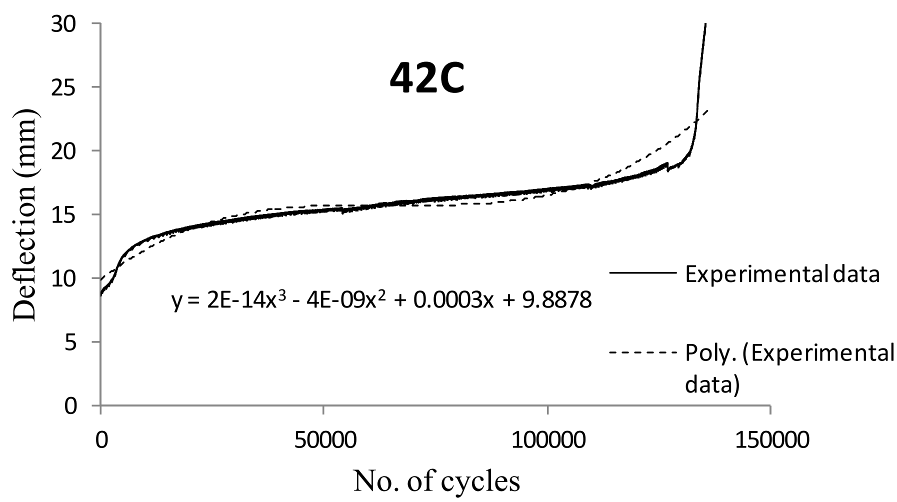

b) Fatigue curve of beam 42C

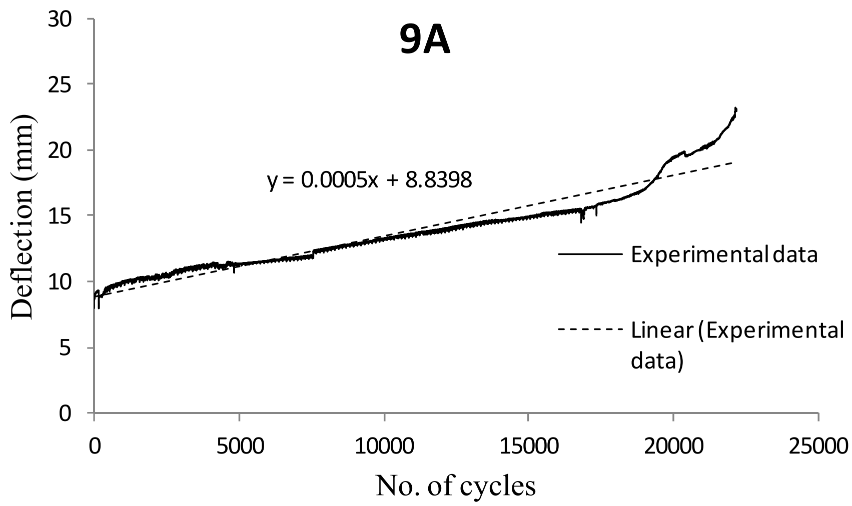

c) Fatigue curve of beam 9A

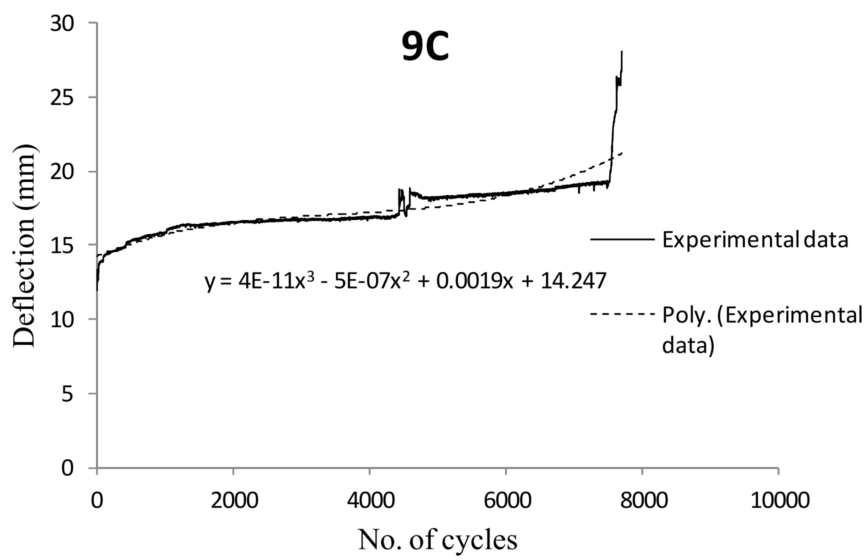

d) Fatigue curve of beam 9C

Figure 5. 2 Fatigue curves of Group 2 beams

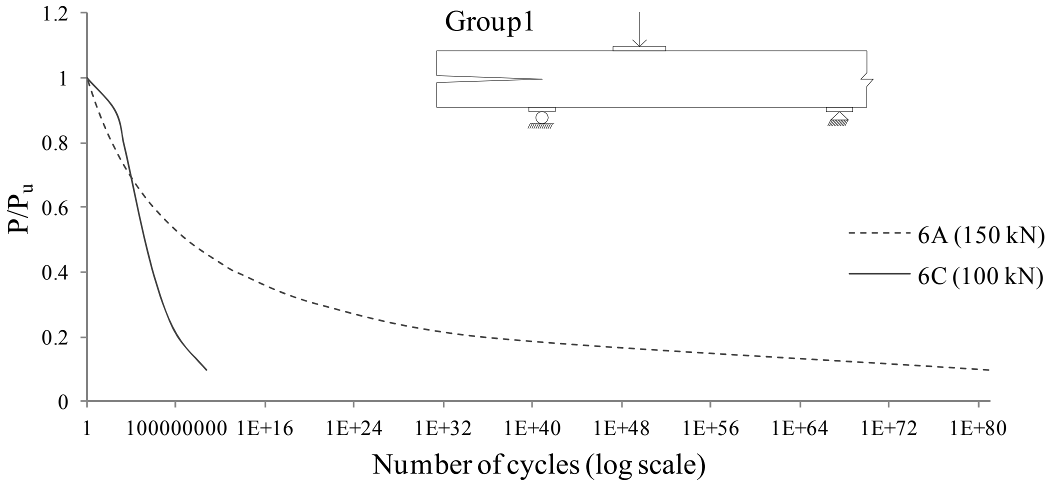

Figure 5. 3 Fatigue strength curves for beam 6A and 6C of Group 1

Fatigue strength curves of timber beams are non-linear (Figure 5. 3 and Figure 5. 4). As the percentage of static strength (P/P_u) decreases along the fatigue curves, the number of cycles increases. As seen from the curves, at 52 % of static strength beam 9A sustained about 22,186 cycles of repeated load during test and at 42 % of static strength the beam would have sustained about 3.7 million cycles of repeated load (Figure 5. 4). According to the nature of the curves, only a small decrease in the percentage of static strength can result into many cycles of fatigue load.

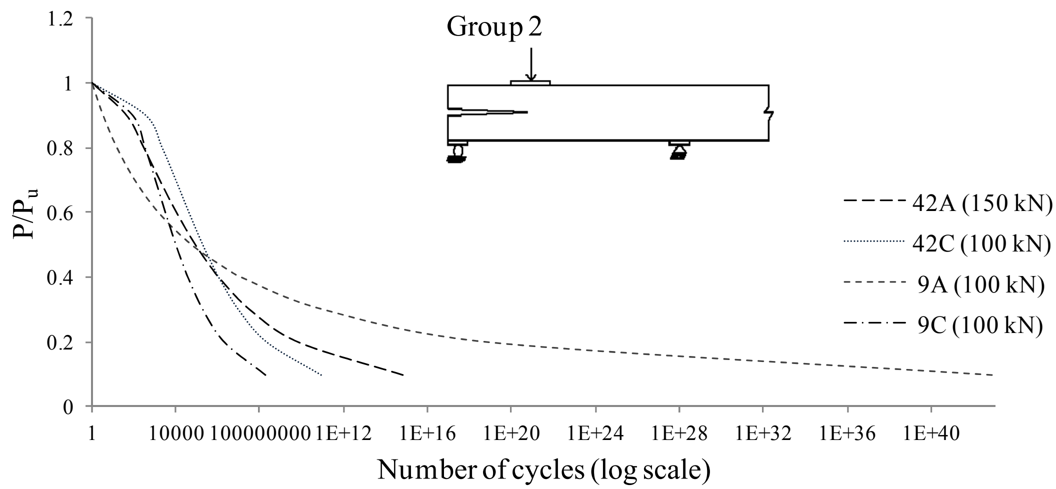

Figure 5. 4 Fatigue strength curves of Group 2 beams

Chapter 6

Summary and Conclusions

6.1 Conclusions

Timber beams with end splits were investigated for their shear strength in a three-point bending test setup. End splits in the timber specimens were artificially created to a length of 600 mm at mid height of the section. The beams were divided into two groups based on their support location: Group 1 had support at 600 mm away from the end and Group 2 had support at the end of the beam. Thirty six static tests were performed to determine the shear strength of Douglas fir timber beams with end splits having two different support locations. Eight fatigue tests were also performed to evaluate the fatigue life of the split timber specimens having two different support locations.

The main objective of this research was to find the shear strength of timber beams that have splits at their ends. The static test results showed that, Group1 and Group 2 beams had an average shear strength of 4.93 MPa and 4.49 MPa, respectively. The research yielded a fifth percentile shear strength value of 3.82 MPa for Group 1 and 3.88 MPa for Group 2 which are higher than the Canadian Highway Bridge Design Code (2006) specified value of 1.5 MPa.

Based on the static test results, it was determined that shear failures dominate when the support is located at the end of the beam with splits within the loading span. All the beams in this study failed in shear when the support was located at the end of the beam.

Some specimens in Group 1 failed in bearing at a relatively low bearing stress. The fifth percentile value of bearing stress was only 4.17 MPa which is lower than the CHBDC (2006) specified value of 4.7 MPa.

This research also showed that in both groups of specimens tested, the split propagated further with loading. It was also observed that side checks, when present, formed into large cracks during testing and the beams failed in shear, which confirms the findings by Uppal et al. (2001).

During the fatigue testing of Group 1 specimens, two beams sustained one million cycles of repeated loading without failure. One of the four beams of this group failed in shear and another failed in bearing under load plate. In Group 2, two of the four beams failed in shear failure and the other two beams failed due to disintegration at their ends.

Group 2 beams could not sustain as many cycles of load compared to Group 1 beams. At an applied load of 150 kN, Group 1 beams sustained nine times higher cycles than beams in Group 2.

At an applied load of 100 kN, all the beams in Group 1 sustained a higher number of cycles than that of beams in Group 2. In general beams having support at the inside end of the split sustain higher cycles than beams having support at the outside end of the beam.

The fatigue strength curves of the timber beams tested were developed using Memon's (2005) formula. The fatigue strength curve is an approximate way to find the fatigue life of a member at a given load. The curves also showed that at a very low load the member could sustain an indefinite number of cycles. Since the number of fatigue tests conducted in this research is very small, a definite conclusion can not be drawn.

6.2 Recommendation for future research

In this experiment Douglas fir beams having end splits were investigated. Two groups of beams were investigated under static and fatigue loading. In Group 1 the splits were outside the loaded span while in Group 2 the splits were located within the loaded span. A total of 17 tests were performed in Group 1. Among these 17 beams, one beam failed in flexure, eight failed in bearing and eight failed in shear. In Group 2, a total of 19 beams were tested and all of them failed in shear. However no control beams were tested in these two groups. Therefore, the shear strength of these kinds of beams without any split could not be found and the experimental test results were compared only with CHBDC (2006). For future research the author would like to recommend tests on control beams without any split.

Due to shortage of the number of beams and time constraint the number of fatigue tests performed in this research is very small. Therefore test results obtained from these few tests does not necessarily reflect the real strength of timber beams. For future experimental work the author would like to recommend larger number of tests including some fatigue tests on control beams without any splits. The results from control beam tests can be used to compare data with test results from beams having splits.

References

ASTM. (1976). Standard method of testing plywood in rolling shear (shear in the plane of plies). D 2718-76. American Society for Testing and Materials, Philadelphia, Pa .

ASTM. (1927-1975 editions). Standard methods for establishing structural grades for visually graded lumber, D245. American Society for Testing and Materials .

ASTM. (1978). Standard methods of evaluating the properties of wood-base fiber and particle panel materials, D1037-78. American Socirty for Testing and Materials, Philadelphia, Pa .

ASTM. (1987). Standard methods of testing small clear specimens of timber, D143-87. American Society for Testing and Materials, Philadelphia, Pa .

ASTM. (1996). Standard methods of testing small clear specimens of timber, D143-94. American Society for Testing and Materials, West Conshohocken, Pa .

ASTM. (2005). Standard Test Methods of Static Tests of Lumber in Structural Sizes, D198-05a. ASTM International, West Conshohocken, PA .

Aghayere, A., & Vigil, J. (2007). Structural Wood Design- A practice-oriented approach using the ASD method. New Jersey: John Wiley & Sons, Inc.

Barrett, J. D., & Foschi, R. O. (1977). Shear strength of uniformly loaded dimension lumber. Canadian Journal of Civil Engineering, 4 , 86-95.

Bateman, J. H., Hunt, M. O., & Sun, C. T. (1990). New inrerlaminar shear test for structural wood composites. Forest Products Journal, 40(3) , 9-14.

Buchanan, A. H. (1990). Bending Strength of Lumber. Journal of Structural Engineering, Vol. 116, No.5 , 1213-1229.

Canadian Highway Bridge Design Code, CAN/CSA-S6-06. (2006). Canadian Standards Association.

Cramer, S. M., & Goodman, J. R. (1983). Model for Stress Analysis and Strength Prediction of Lumber. Wood and Fiber Science, 15(4) , 338-349.

Davids, W. G., Richie, M., & Gamache, C. (2005). Fatigue of glulam beams with fiber-reinforced polymer tension reinforcing. Forest Products Journal, 55(1) , 93-101.

Ethington, R. L., Galligan, W. L., Montrey, H. M., & Freas, A. D. (1979). Evolution of Allowable Stresses in Shear for Lumber. Gen. Tech. Rep. FPL-23. Madison, WI: U.S. Department of Agriculture, Forest Service, Forest Products Laboratory .

Foschi, R. O., & Barrett, J. D. (1976). Longitudinal Shear Strength of Douglas Fir. Canadian Journal of Civil Engineering, 3 , 198-208.

Hansen, L. P. (1991). Experimental investigation of fatigue properties of laminated wood beams. Proceeding of the 1991 International Timber Engineering Conference , 4.203-4.210.

Huggins, M. W., Aplin, E. N., & Palmer, J. H. (1966). Evaluation of the Effect of Delamination. Engineering Journal , 49(2) , 32-41.

Iyengar, K. T. (1962). Two-Dimensional Theories of Anchorage Zone Stresses in Post-Tensioned Prestressed Beams. ACI Journal Proceedings, Vol. 59, No. 10 , 1443-1466.

Keenan, F. J. (1974). Shear Strength of Wood Beams. Forest Products Journal, 24(9) , 63-70.

Keenan, F. J., Kryla, J., & Kyokong, B. (1985). Shear strength of spruce glued-laminated timber beams. Canadian Journal of Civil Engineering, 12 , 661-672.

Kyanka, G. F. (1980). Fatigue Properties of wood and wood composites. International Journal of Fracture, 16(6) , 609-616.

Lam, F., Yee, H., & Barrett, J. D. (1997). Shear Strength of Canadian Softwood Structural Lumber. Canadian Journal of Civil Engineering, 24 , 419-430.

Legget, F. R. (2010) "Bridges." The Canadian Encyclopedia. Historica Foundation. http://www.thecanadianencyclopedia.com

Liu, J. Y., & Floeter, L. H. (1984). Shear Strength in Principal Plane of wood. Journal of Engineering Mechanics, ASCE, 110(6) , 930-936.

Longworth, J. (1977). Longitudinal shear strength of timber beams. Forest Products Journal, 27(8) , 19-23.

Madsen, B. (1992). Structural Behaviour of Timber. North Vancouver, British Columbia: Timber Engineering Ltd.

Matsui, S., & Tei, K. (2001). Researches and Japanese Developments on Highway Bridge Slabs and Contribution of Wheel Running Machines. Proceedings, Third International Conference on Concrete under Severe Conditions, (pp. Vol.1:992-1008). Vancouver, B.C.

Matsui, S., Tokai, D., Higashiyama, H., & Mizukoshi, M. (2001). Fatigue durability of fibre reinforced concrete decks under running wheel load. Proceedings Third International Conference on Concrete Under Severe Conditions, CONSEC 01, (pp. Vol.1:982-991). Vancouver, B.C.

Memon, A. H. (2005). "Comparative Fatigue Performance of Steel-Reinforced and Steel-Free Concrete Bridge Deck Slabs." Doctor of Philosophy in Civil Engineering thesis. University of Manitoba, Winnipeg, Manitoba, Canada.

Murphy, J. D. (1979). Strength of wood beams with end splits. Res. Pap. FPL 347, U.S. Dept. of Agr., Forest Products Laboratory, Madison, Wis.

Newlin, J., Heck, G., & March, H. (1934). New method of calculating longitudinal shear in checked wooden beams. American Society of Mechanical Engineers-Transactions, 56(10) , 739-744.

Norris, & Erickson. (1951). The effect of end checks on the strength of wood beams. Int. Rep. Madison, WI: U.S. Department of Agriculture, Forest Service, Forest Products Laboratory. 14 p.

Ritter, M. A. (1990). Timber Bridges: Design, Construction, Inspection and Maintenance. Washington, DC: United States Department of Agriculture Forest Service.

Riyanto, D. S., & Gupta, R. (1998). A comparision of test methods for evaluating shear strength of structural lumber. Forest Products Journal, 48(2) , 83-90.

Schwaighofer, J., Lee, C. S., & Microys, H. F. (1968). Stresses at Delaminations. Mechanics of the solid state, University of Toronto Press , 207-217.

Soltis, L. A., & Rammer, D. R. (1994). Shear strength of unchecked glued-laminated beams. Forest Products Journal, 44(1) , 51-57.

Standard Grading Rules for Canadian Lumber. (2007). BC, Canada: National Lumber Grades Authority.

Svecova, D., & Eden, R. J. (2004). Flexural and shear strengthening of timber beams using glass fibre reinforced polymer bars — an experimental investigation. Canadian Journal of Civil Engineering, 31 , 45-55.

Timoshenko, S. P., & Goodier, J. N. (1970). Theory of Elasticity. New York: McGraw Hill.

Tsai, K. T., & Ansell, M. P. (1990). The fatigue properties of wood in flexure. Journal of Materials Science, 25 , 865-878.

Uppal, A. S., Fry, G. T., & Byers, W. G. (2001). Fatigue strength of solid sawn timber railroad bridge structure. AREMA Annual Track and Structures Conference, Chicago, Illinois.

Weibull, W. (1939). A statistical theory of the strength of materials. Royal Swedish Institute for Engineering Research, Report No. 151 .

Wood Design Manual. (2001). Canadian Wood Council.

Yoshihara, H., & Suzuki, A. (2005). Shear Stress/Shear Strain Relation of Wood Obtained by Asymmetric Four Point Bending Test of Side-Tapered Specimen. Journal of Testing and Evaluation, 33(1) , 1-6.

Appendix A

Load deflection Graph

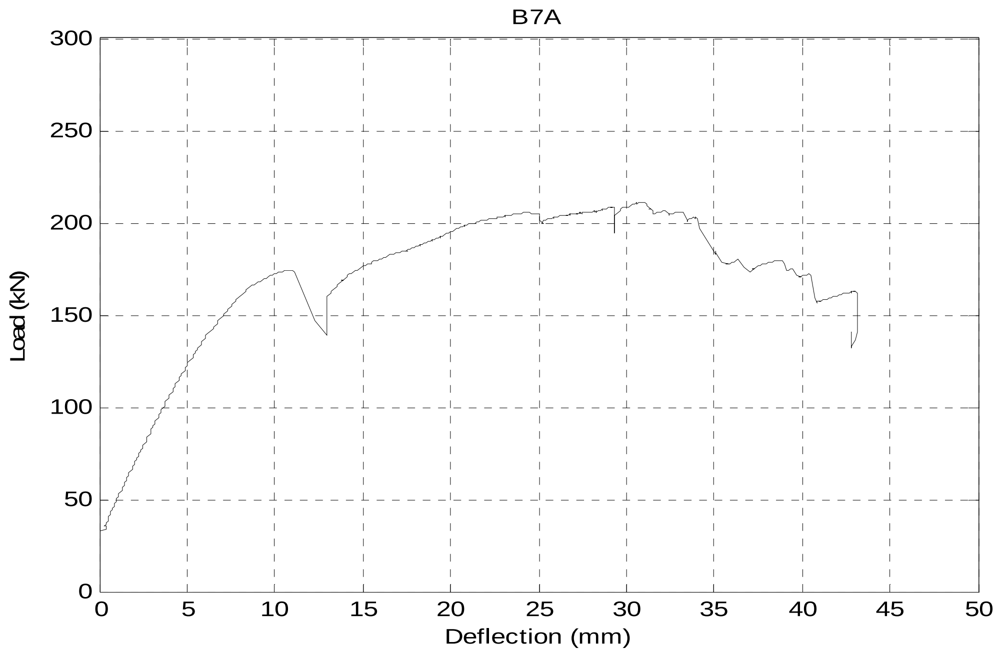

Figure A. 1 Load deflection graph of Group 1 Specimen B7A

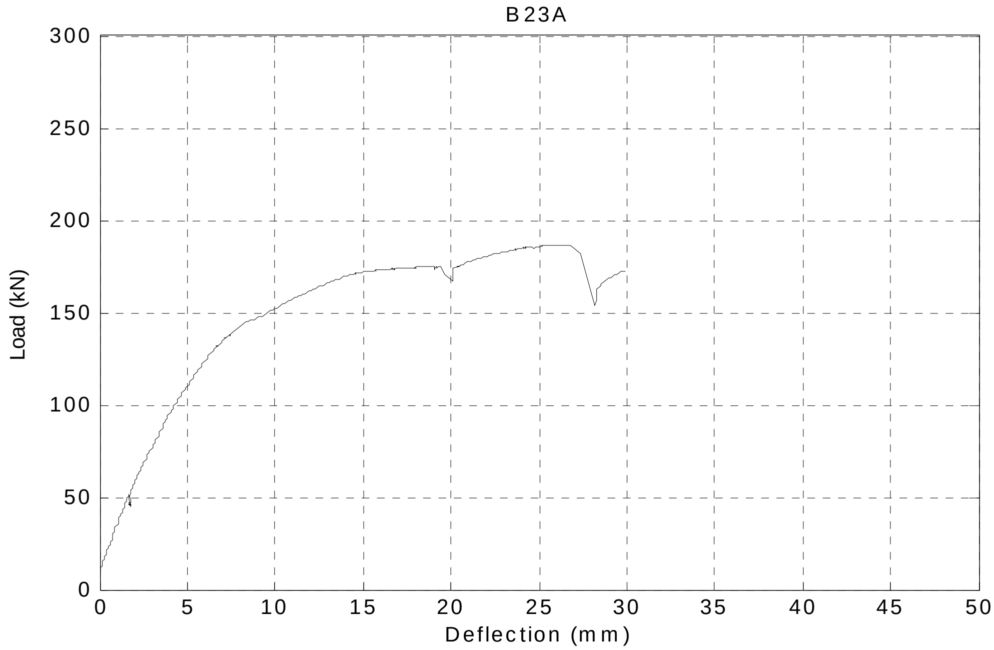

Figure A. 2 Load deflection graph of Group 1 Specimen B23A

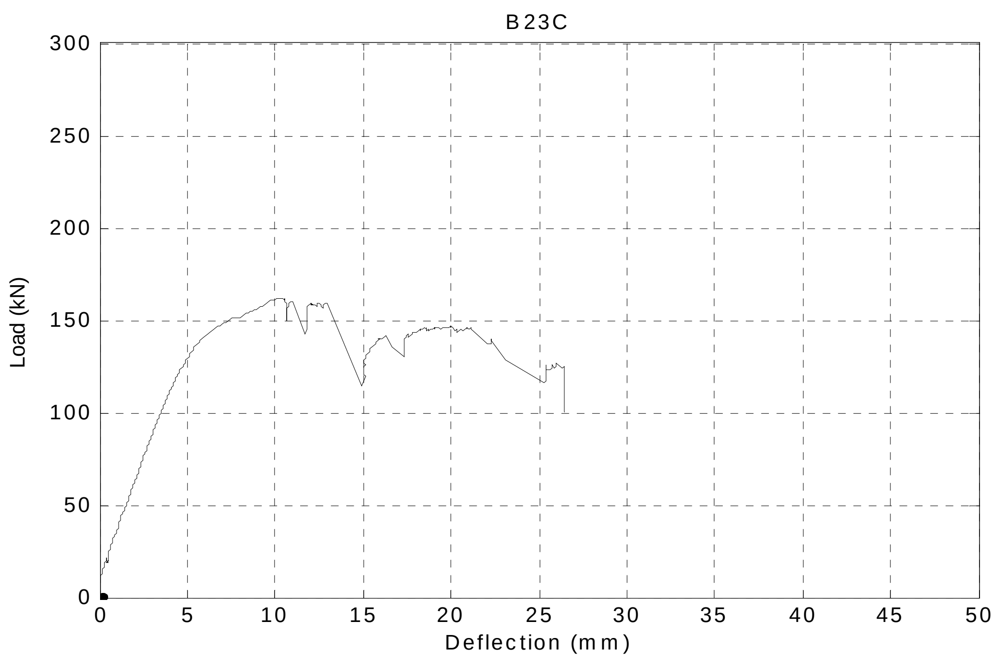

Figure A. 3 Load deflection graph of Group 1 Specimen B23C

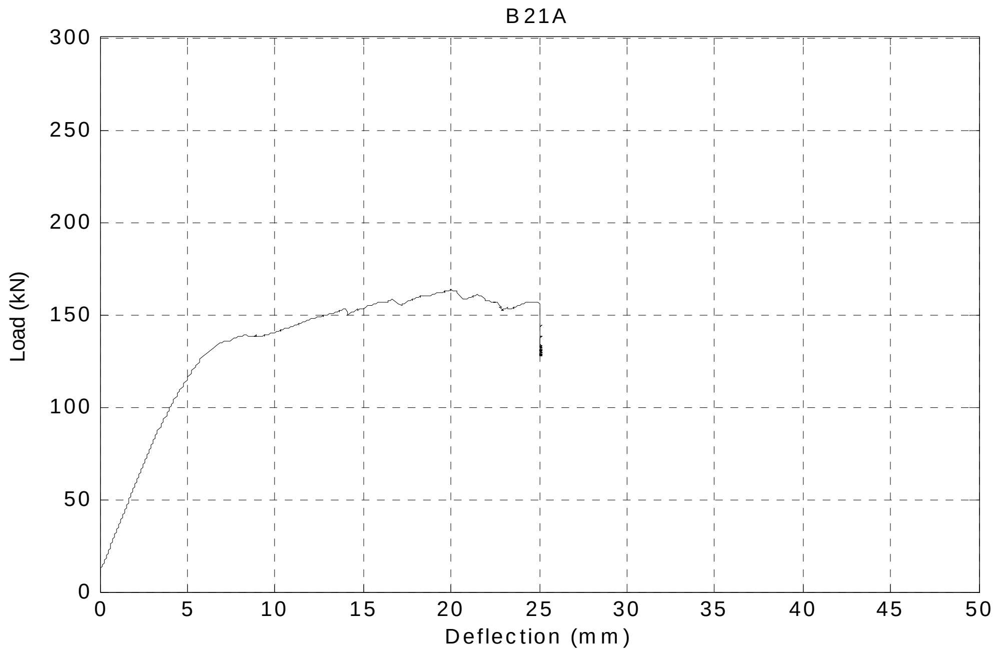

Figure A. 4 Load deflection graph of Group 1 Specimen B21A

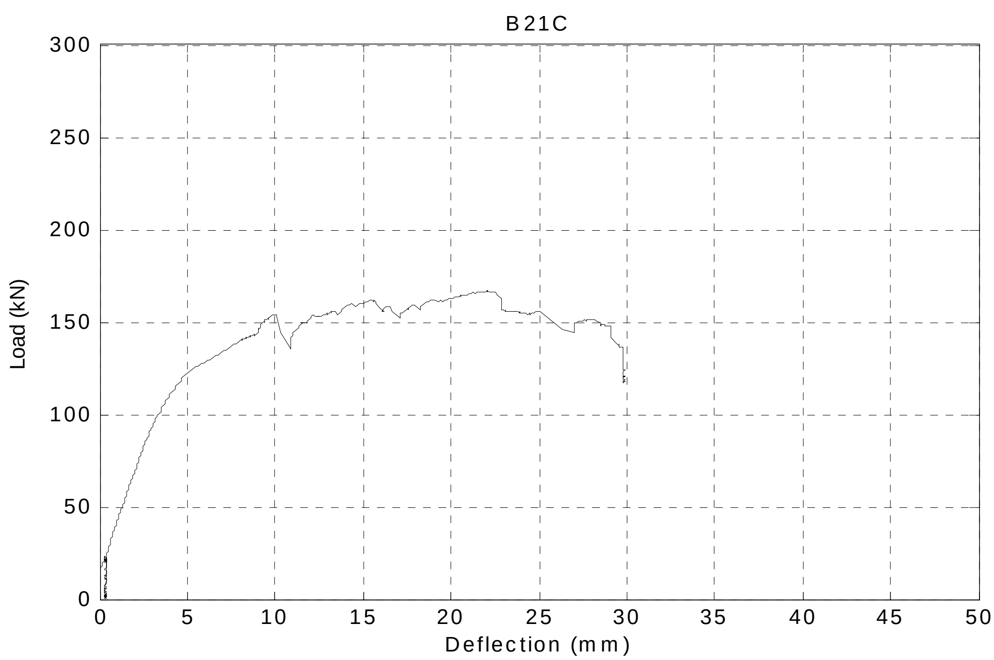

Figure A. 5 Load deflection graph of Group 1 Specimen B21C

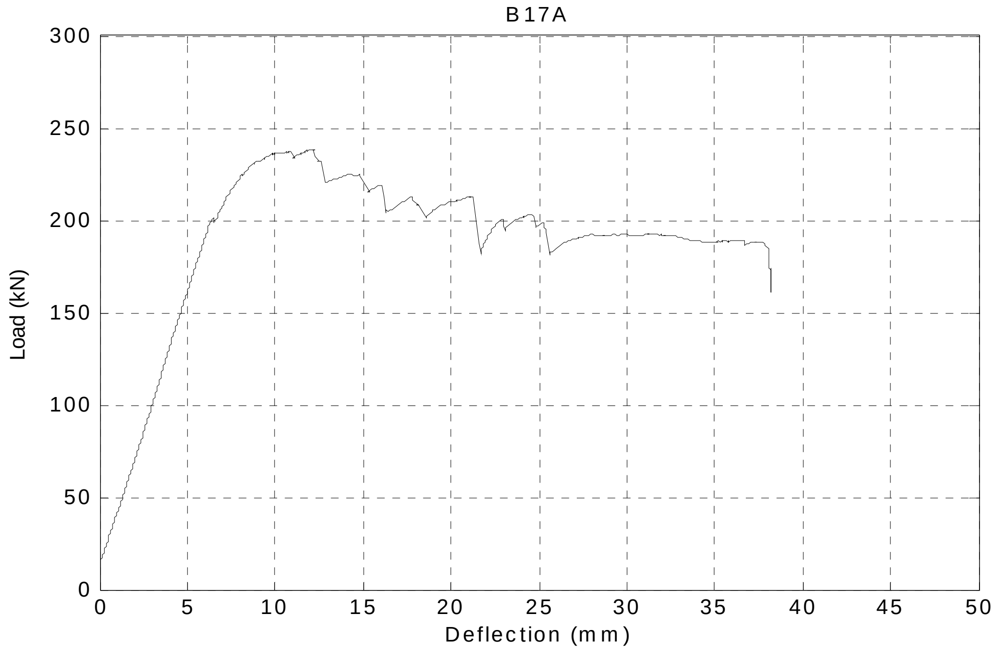

Figure A. 6 Load deflection graph of Group 1 Specimen B17A

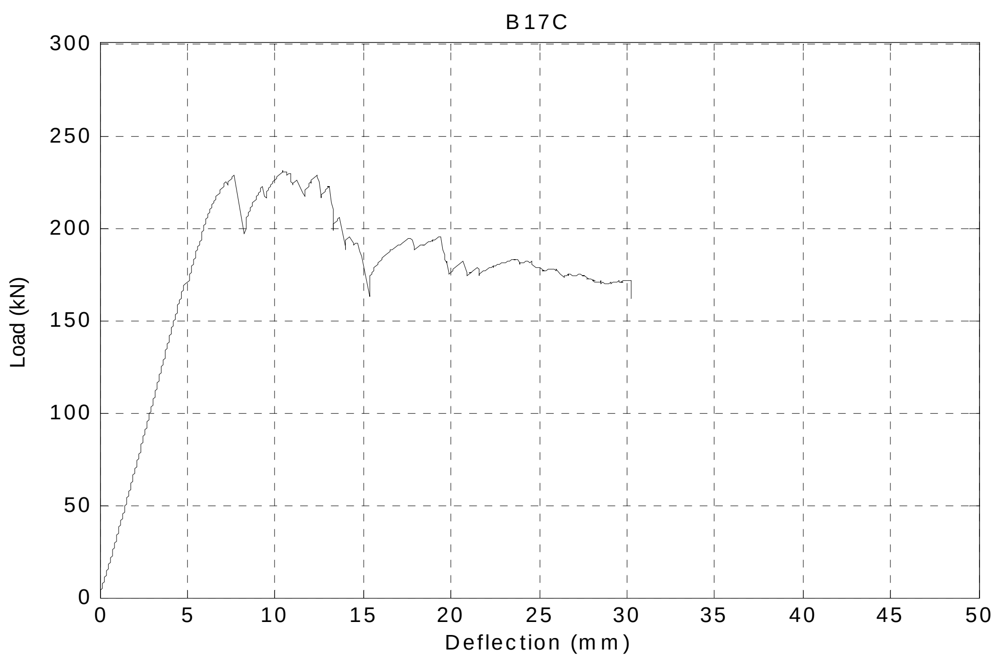

Figure A. 7 Load deflection graph of Group 1 Specimen B17C

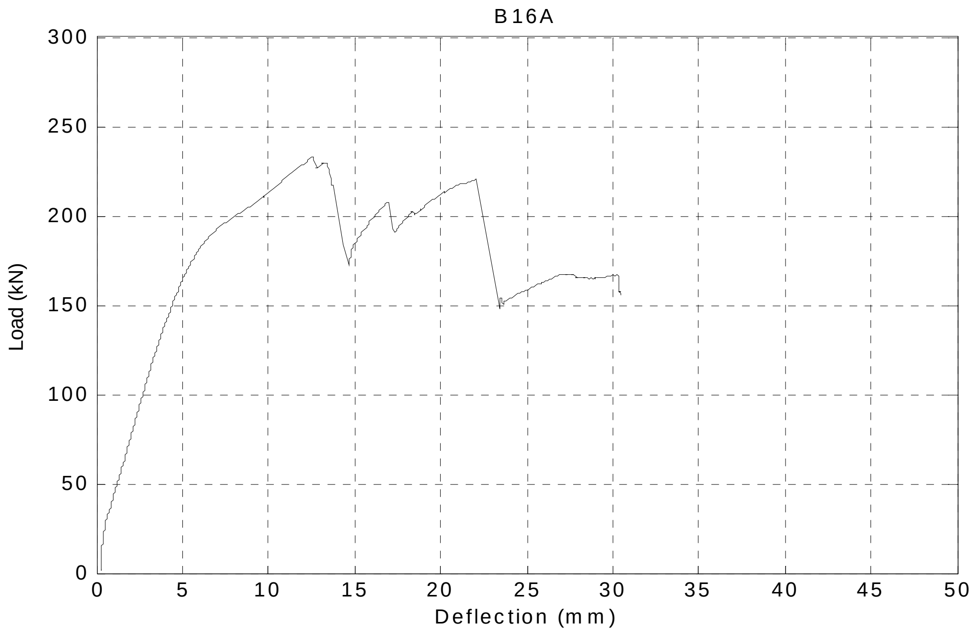

Figure A. 8 Load deflection graph of Group 1 Specimen B16A

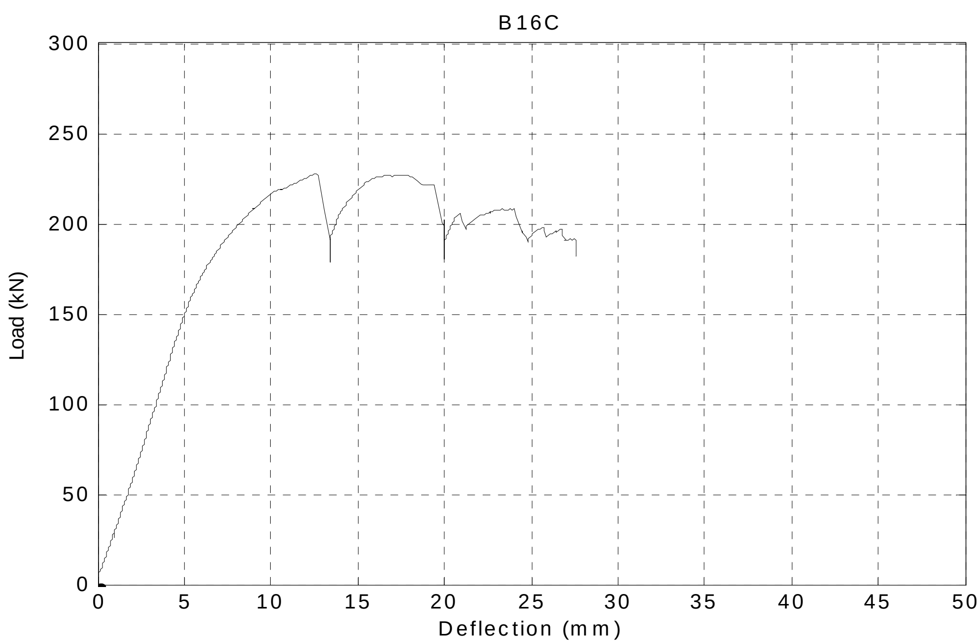

Figure A. 9 Load deflection graph of Group 1 Specimen B16C

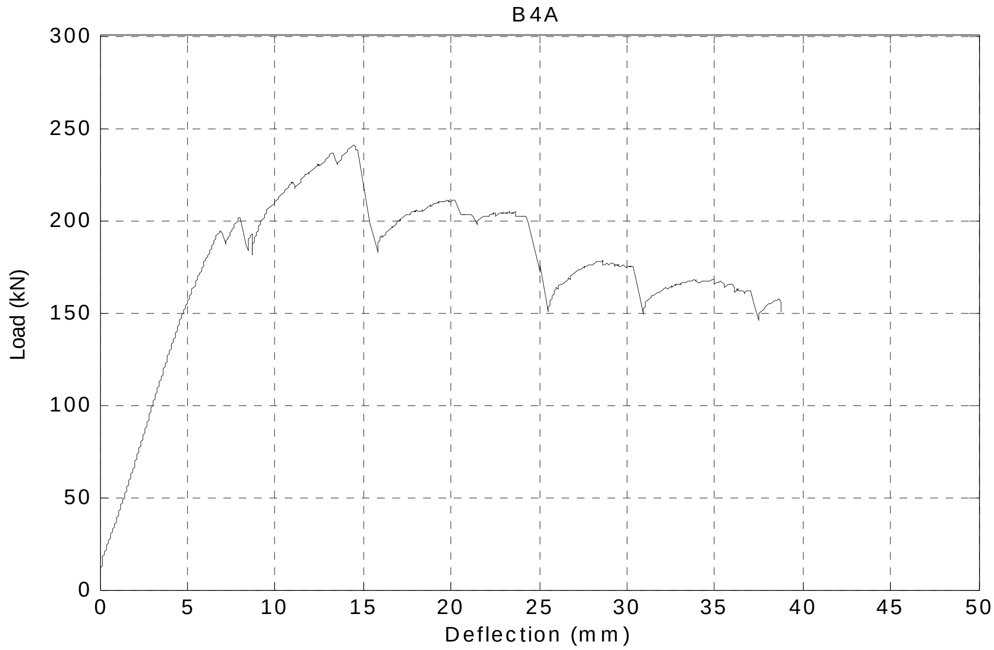

Figure A. 10 Load deflection graph of Group 1 Specimen B4A

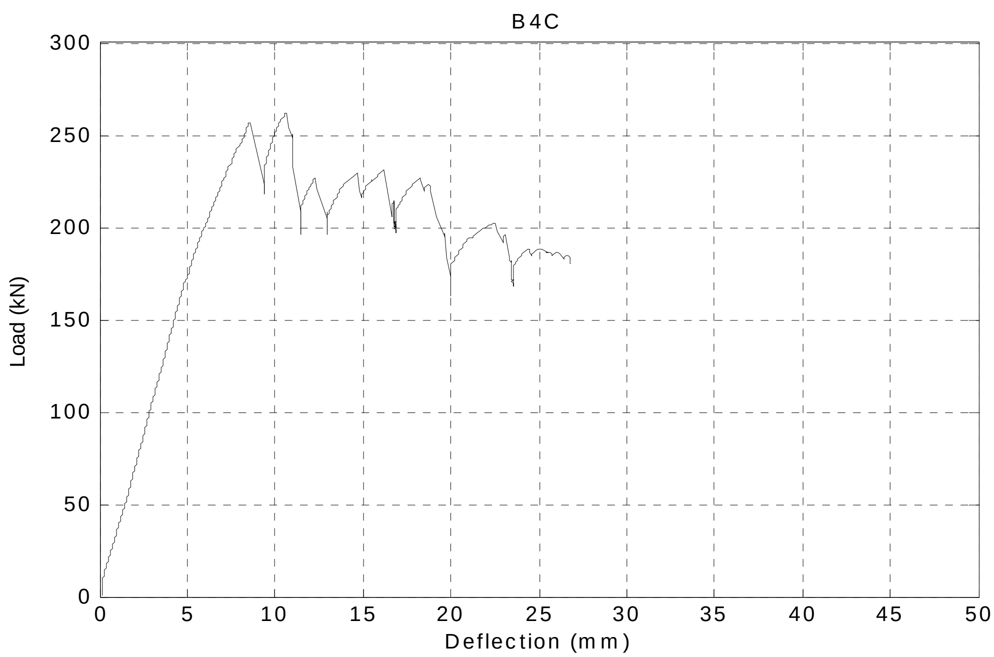

Figure A. 11 Load deflection graph of Group 1 Specimen B4C

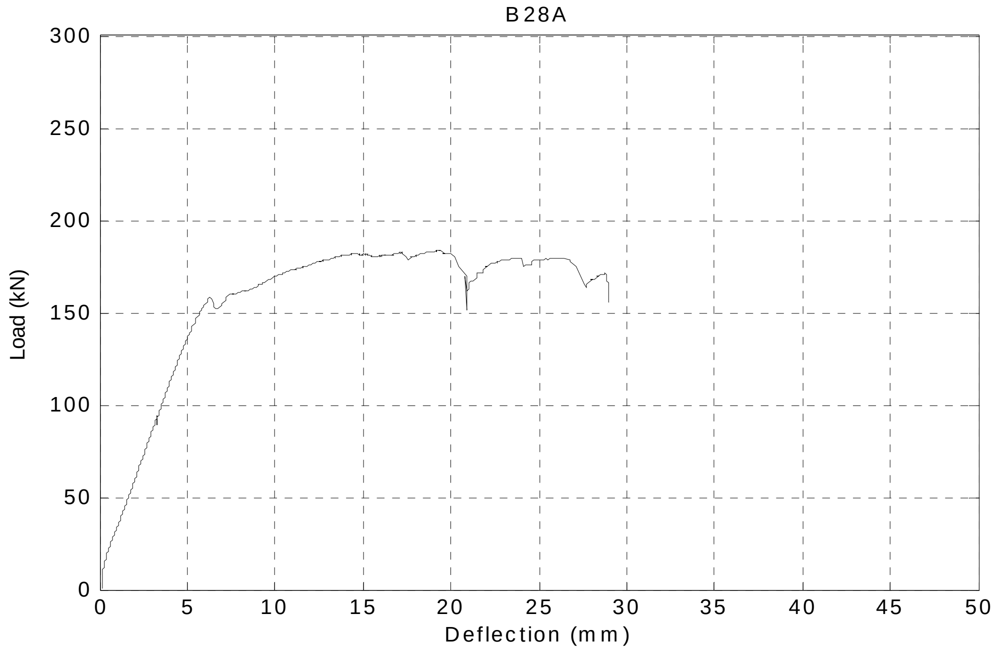

Figure A. 12 Load deflection graph of Group 1 Specimen B28A

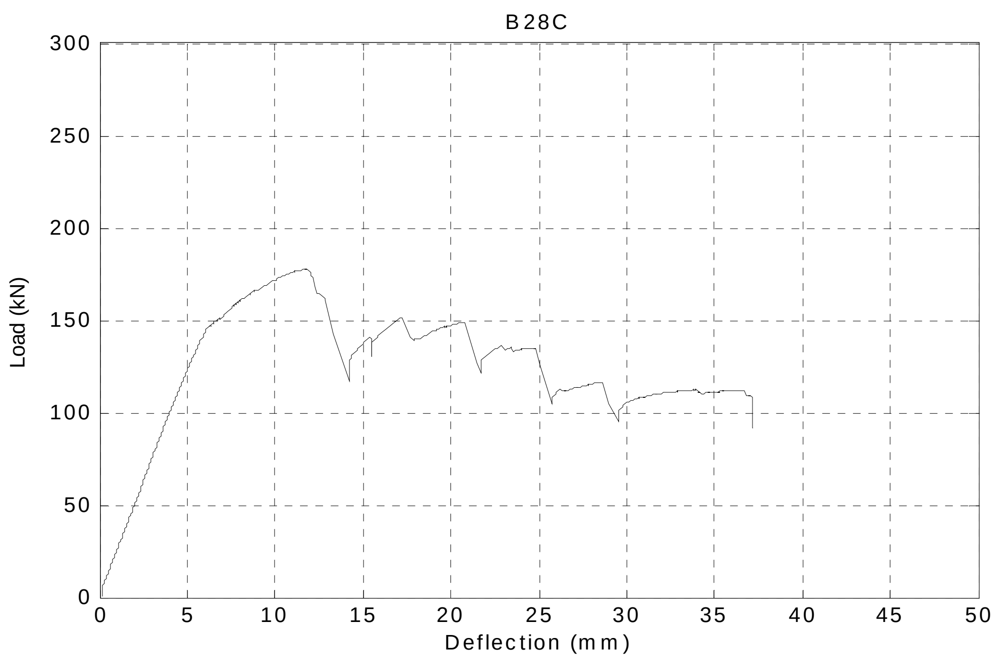

Figure A. 13 Load deflection graph of Group 1 Specimen B28C

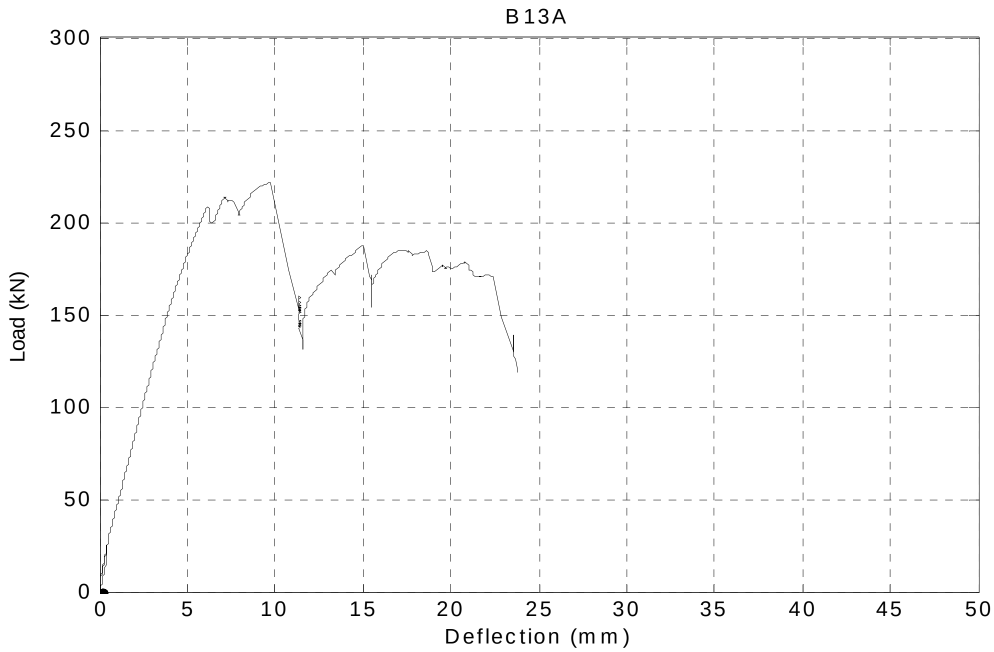

Figure A. 14 Load deflection graph of Group 1 Specimen B13A

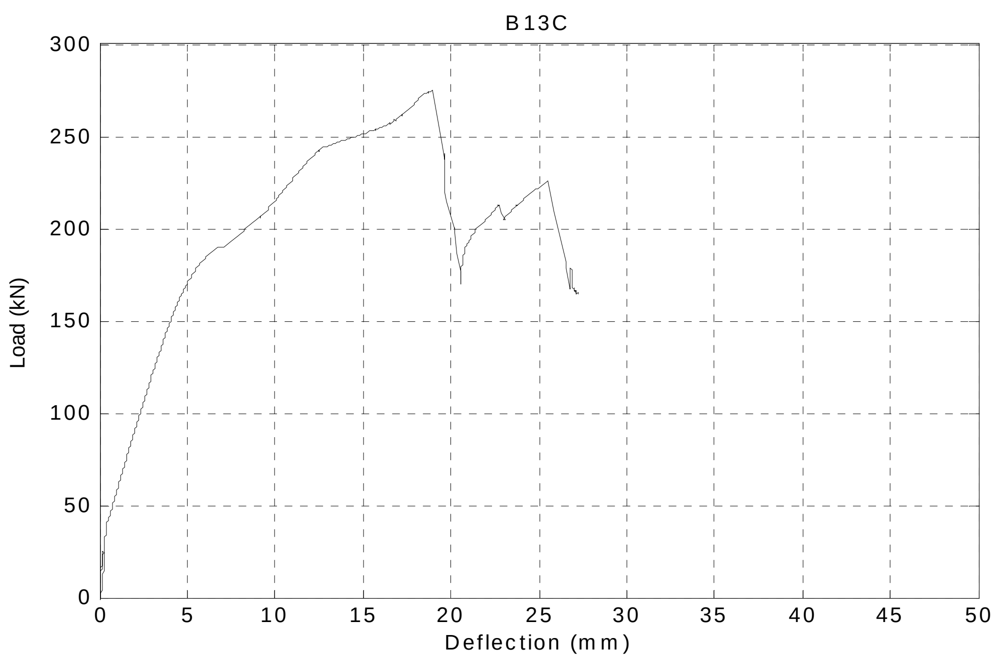

Figure A. 15 Load deflection graph of Group 1 Specimen B13C

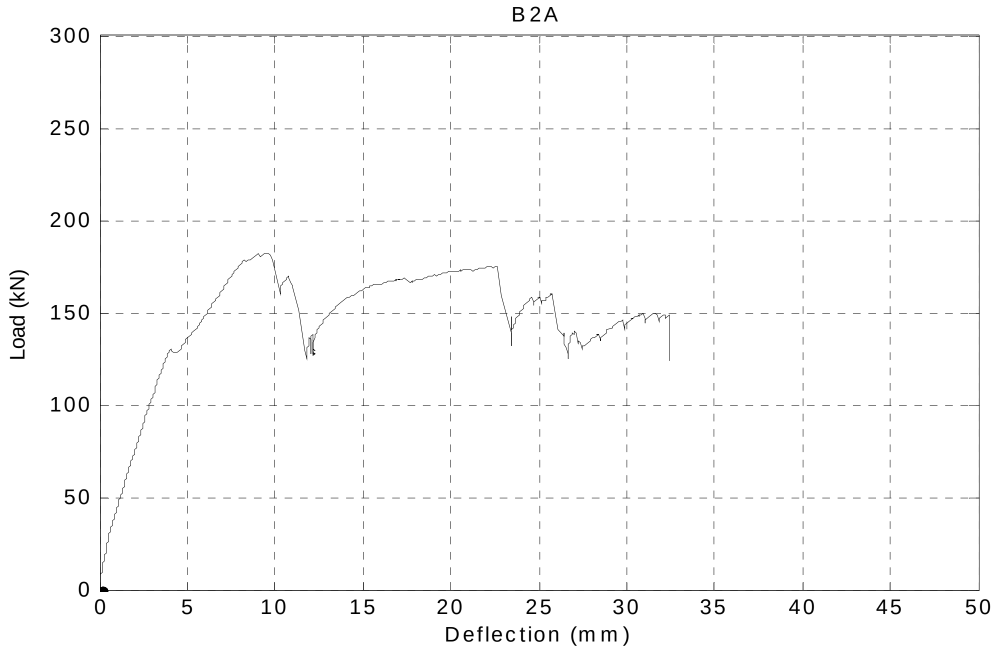

Figure A. 16 Load deflection graph of Group 1 Specimen B2A

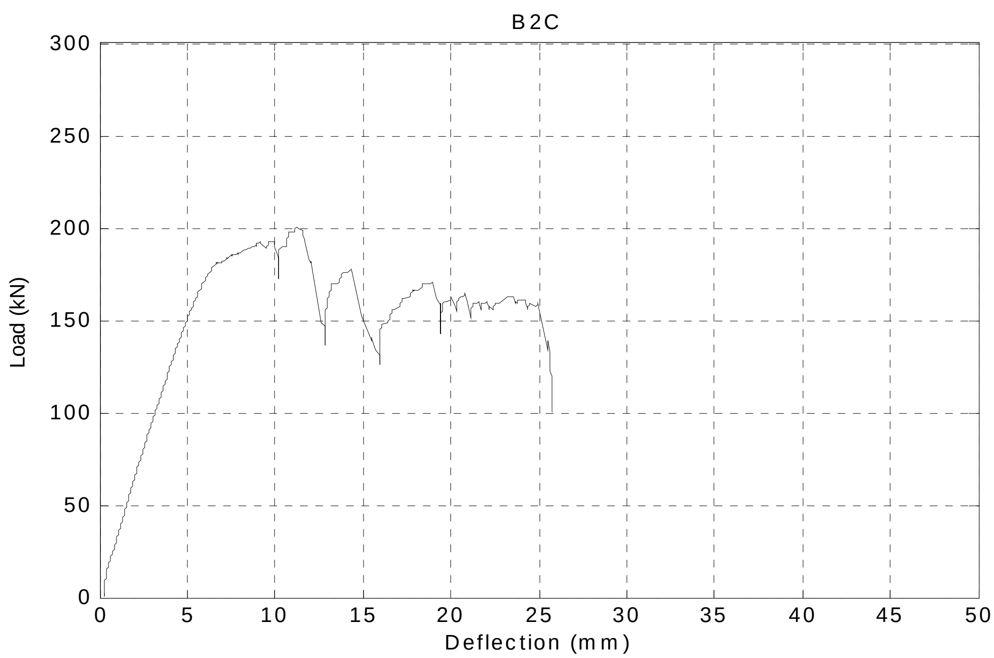

Figure A. 17 Load deflection graph of Group 1 Specimen B2C

Group 2

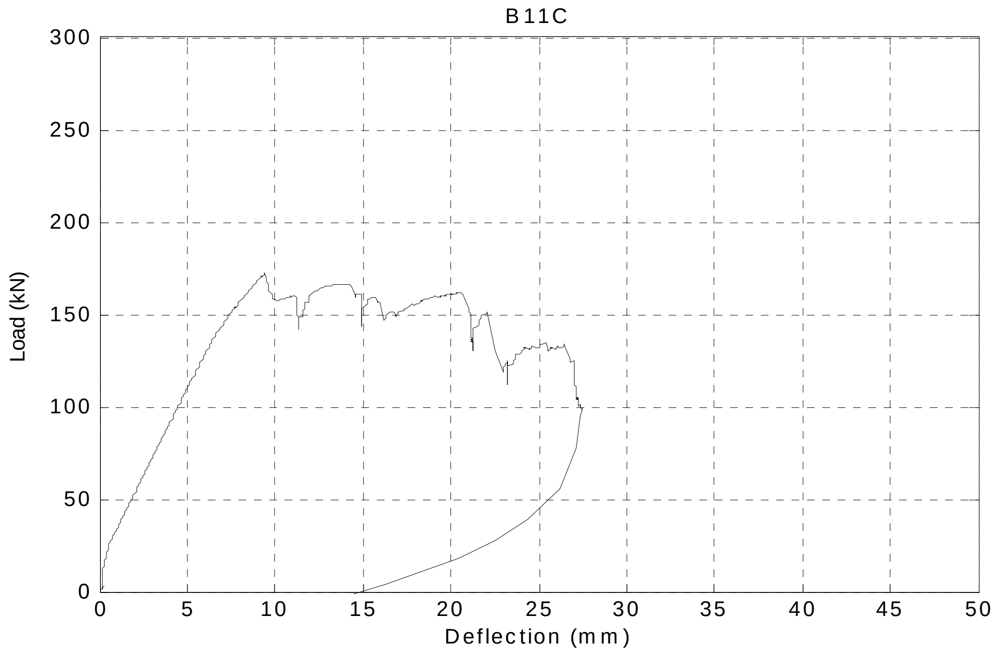

Figure A. 18 Load deflection graph of Group 2 Specimen B11C

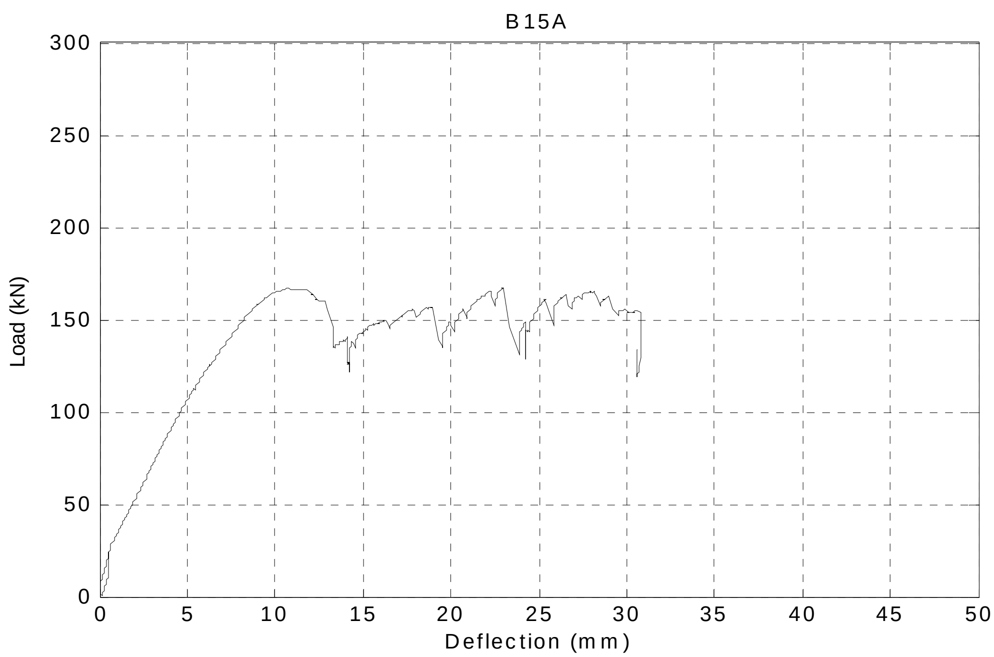

Figure A. 19 Load deflection graph of Group 2 Specimen B15A

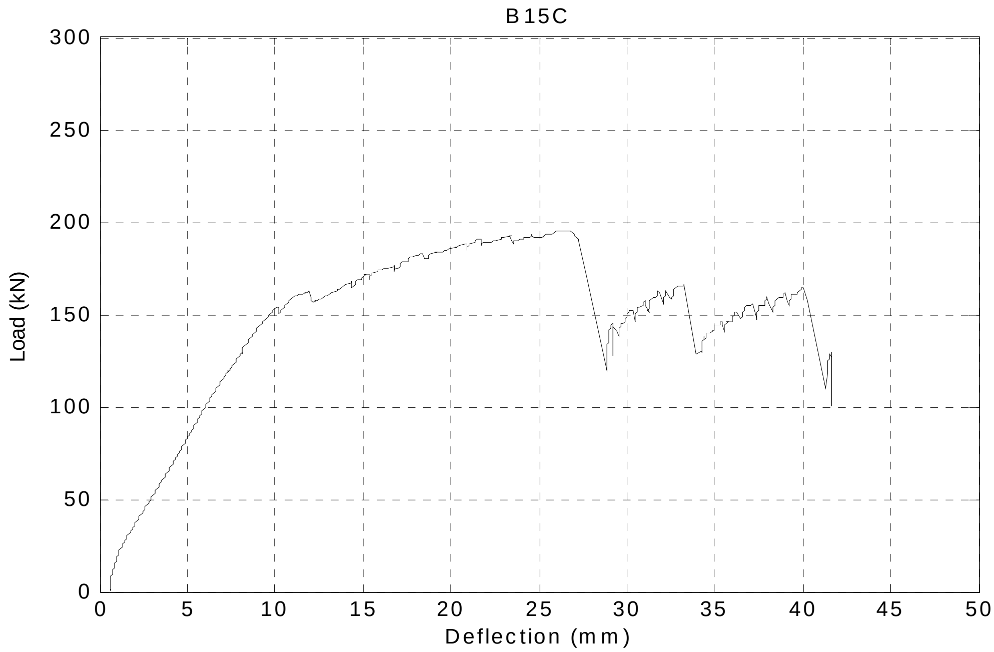

Figure A. 20 Load deflection graph of Group 2 Specimen B15C

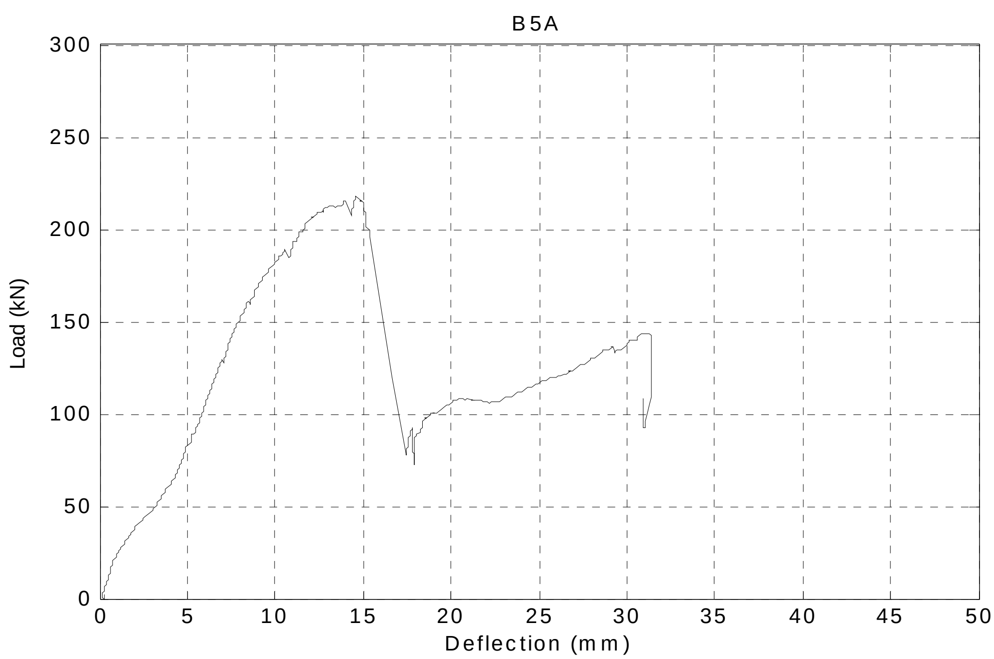

Figure A. 21 Load deflection graph of Group 2 Specimen B5A

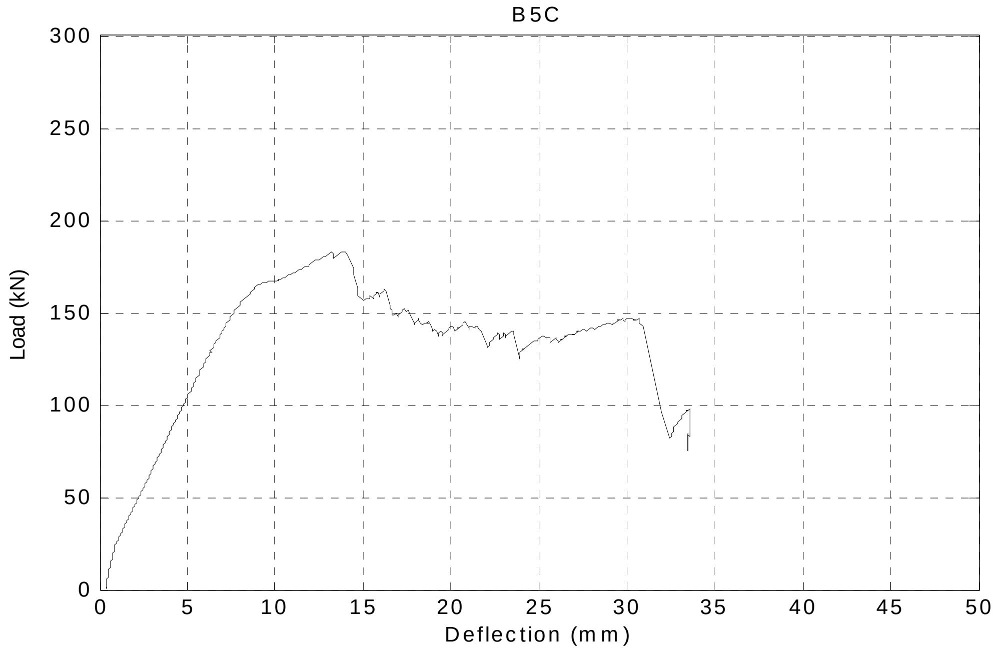

Figure A. 22 Load deflection graph of Group 2 Specimen B5C

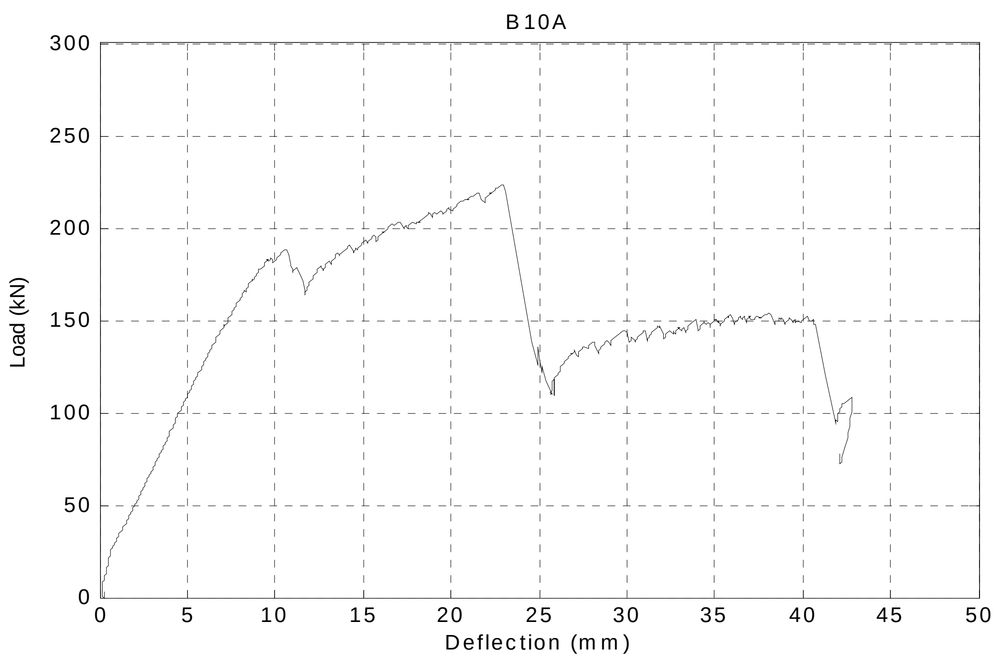

Figure A. 23 Load deflection graph of Group 2 Specimen B10A

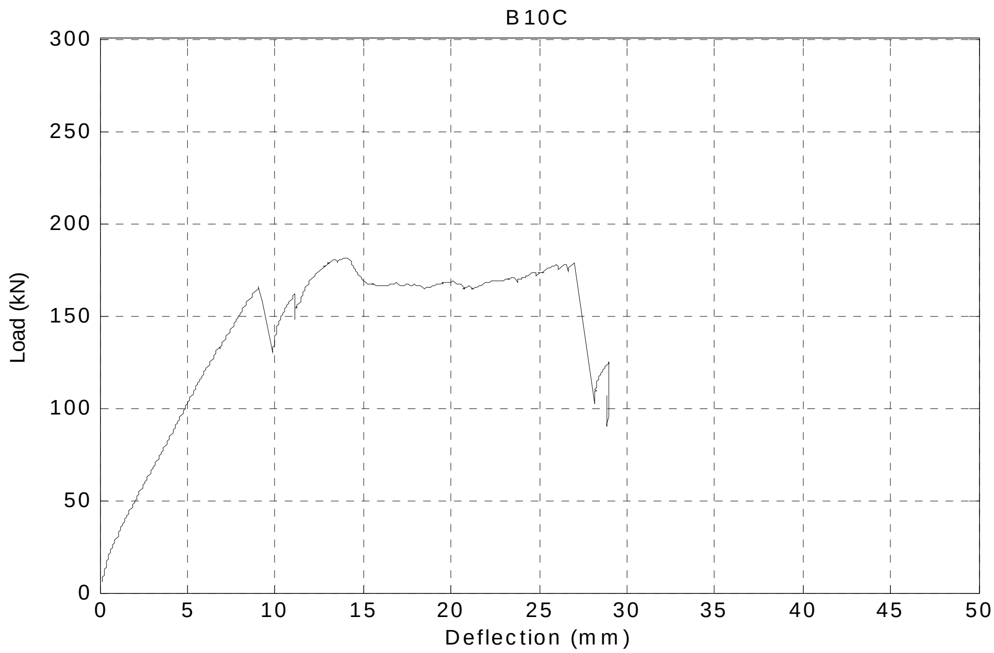

Figure A. 24 Load deflection graph of Group 2 Specimen B10C

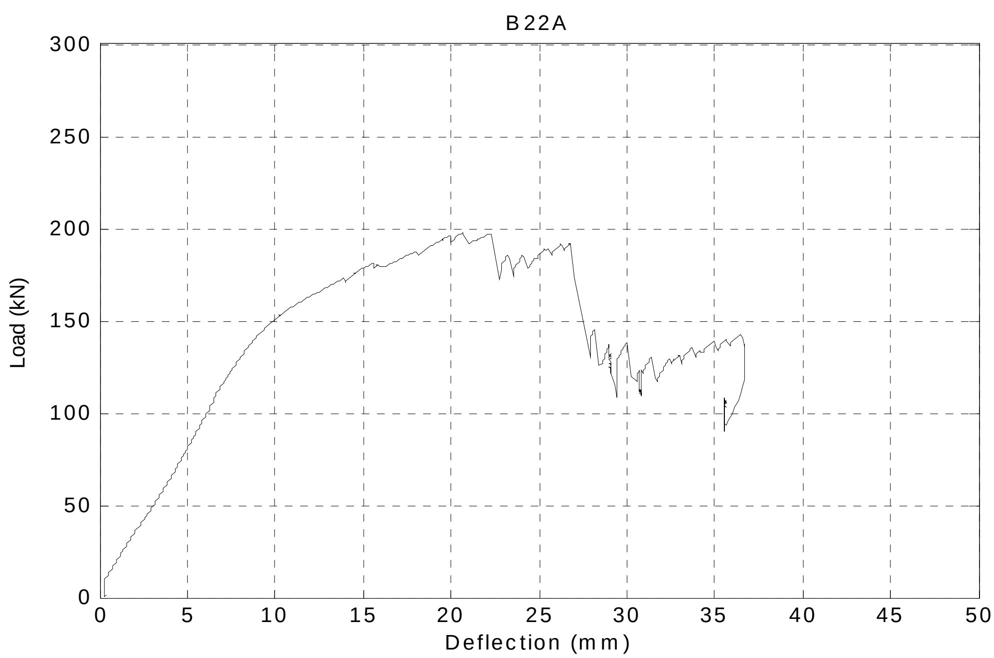

Figure A. 25 Load deflection graph of Group 2 Specimen B22A

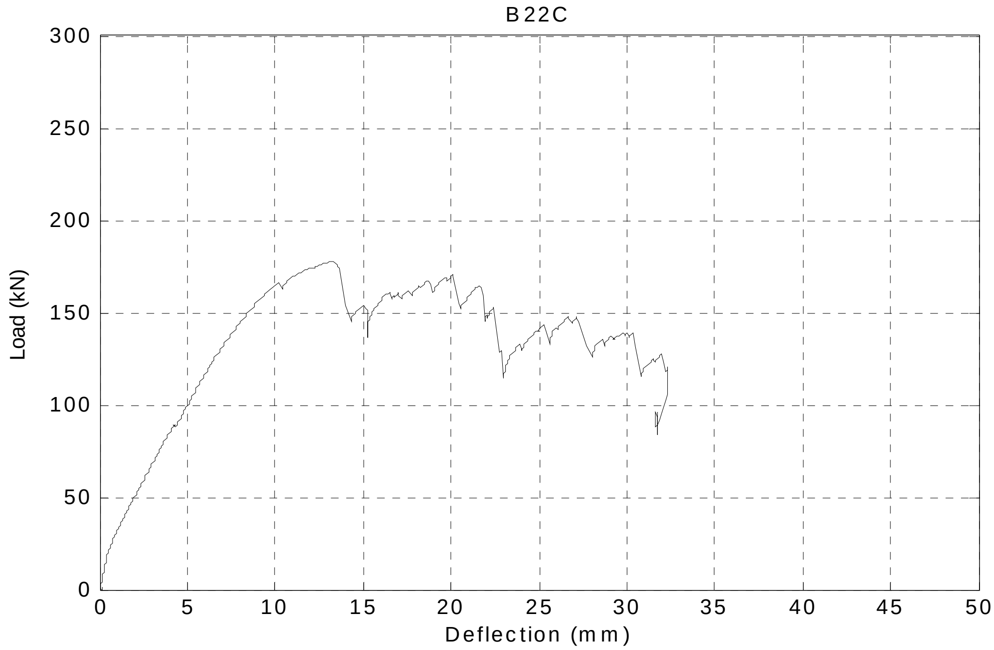

Figure A. 26 Load deflection graph of Group 2 Specimen B22C

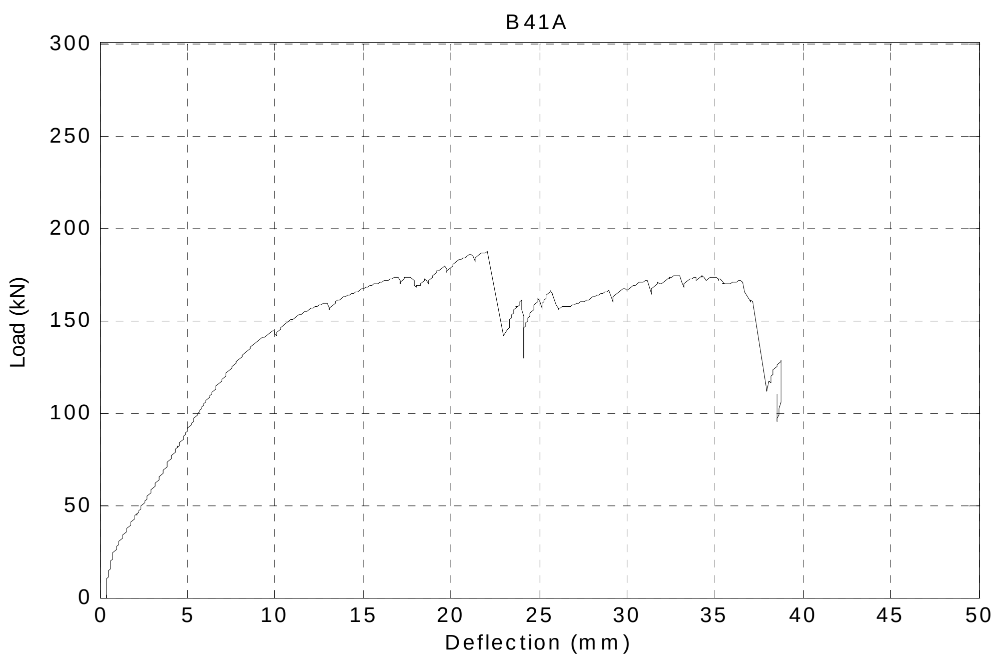

Figure A. 27 Load deflection graph of Group 2 Specimen B41A

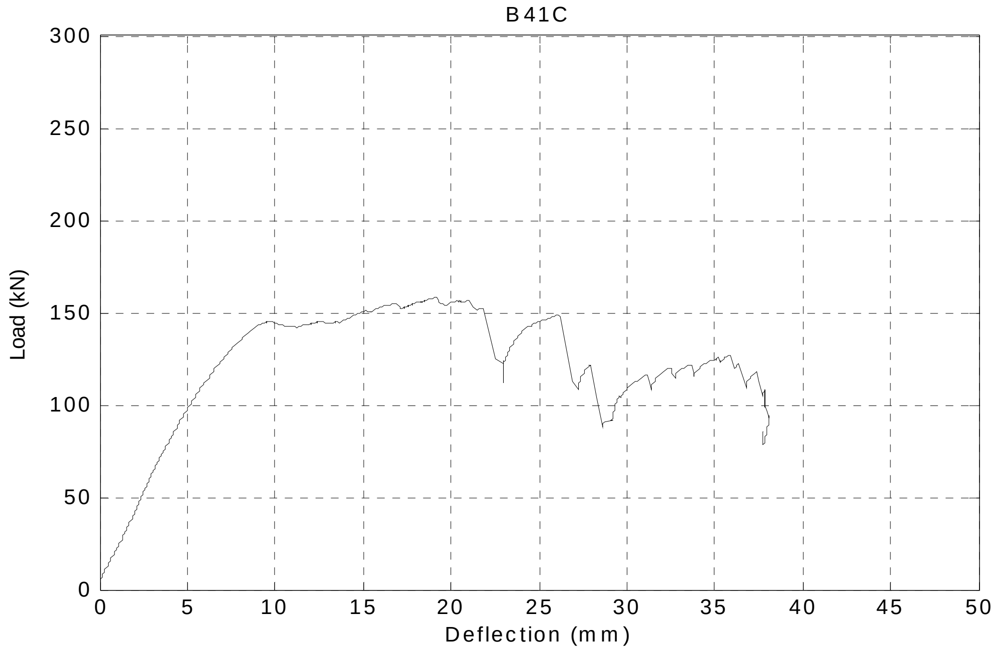

Figure A. 28 Load deflection graph of Group 2 Specimen B41C

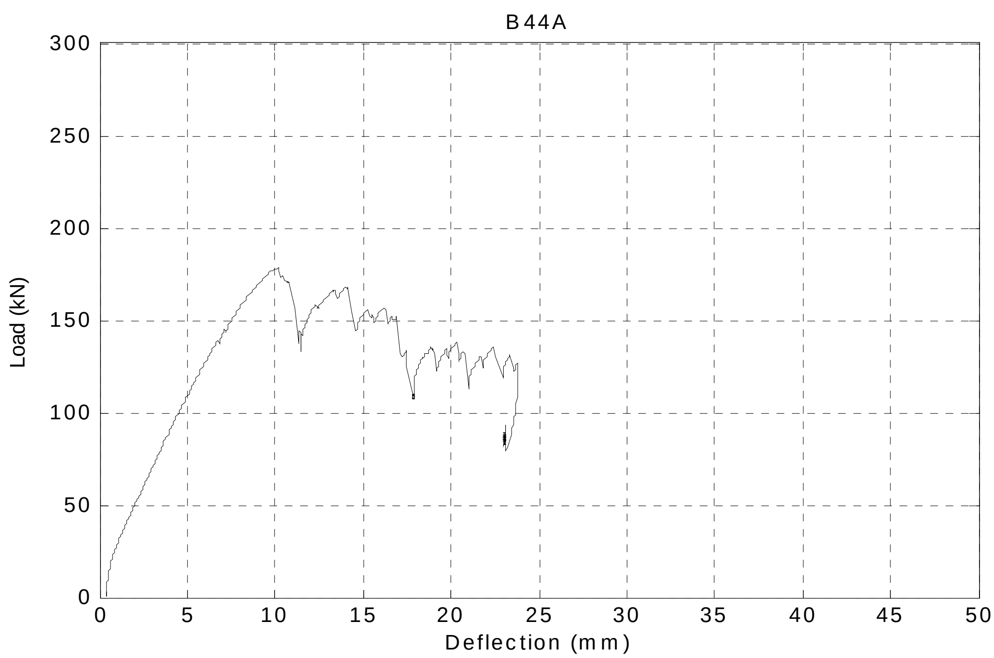

Figure A. 29 Load deflection graph of Group 2 Specimen B44A

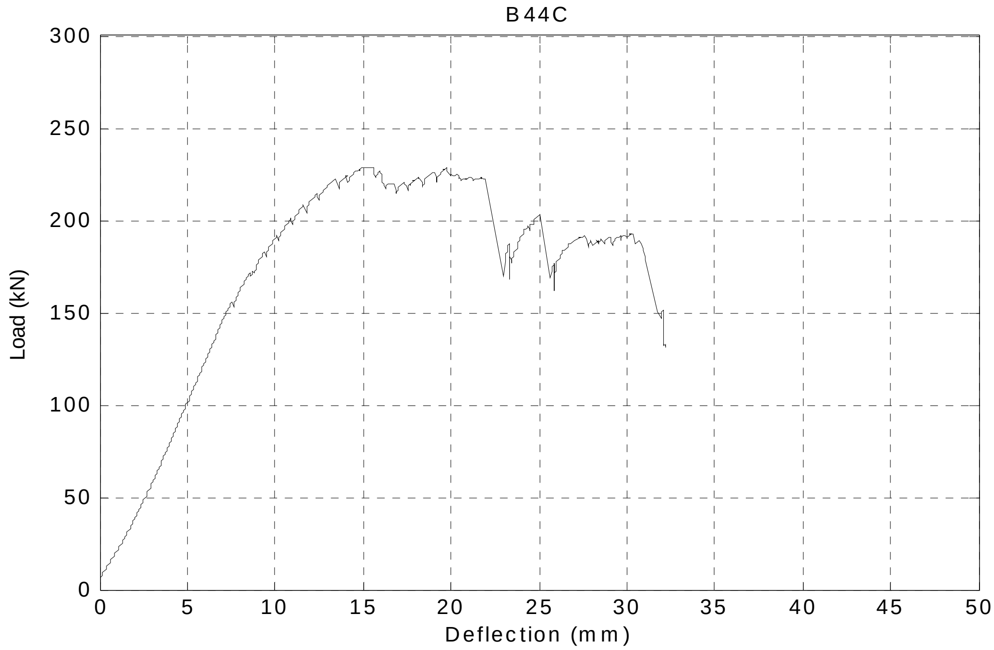

Figure A. 30 Load deflection graph of Group 2 Specimen B44C

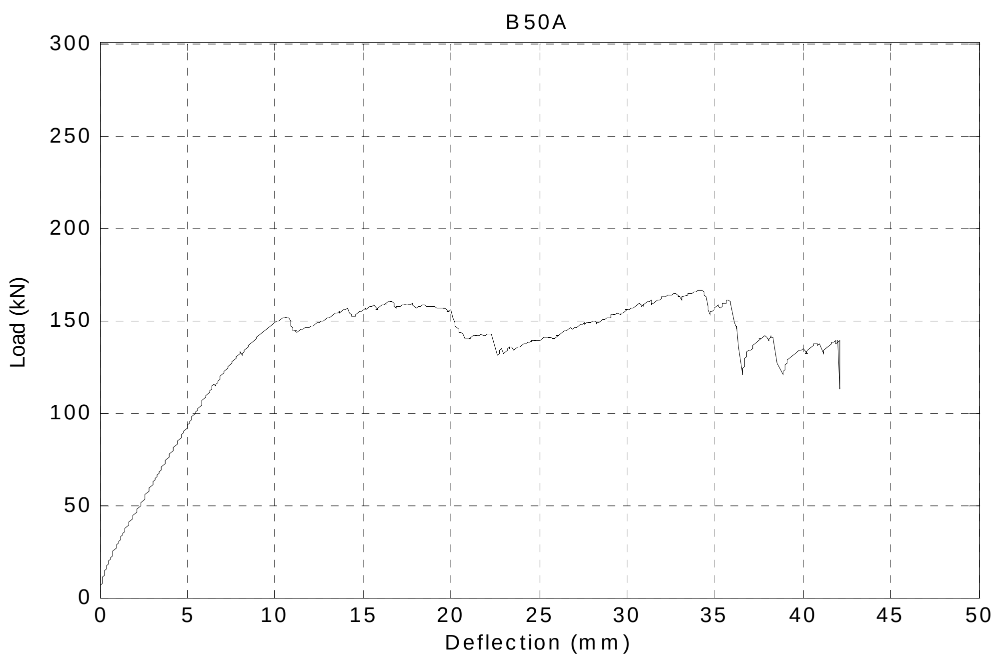

Figure A. 31 Load deflection graph of Group 2 Specimen B50A

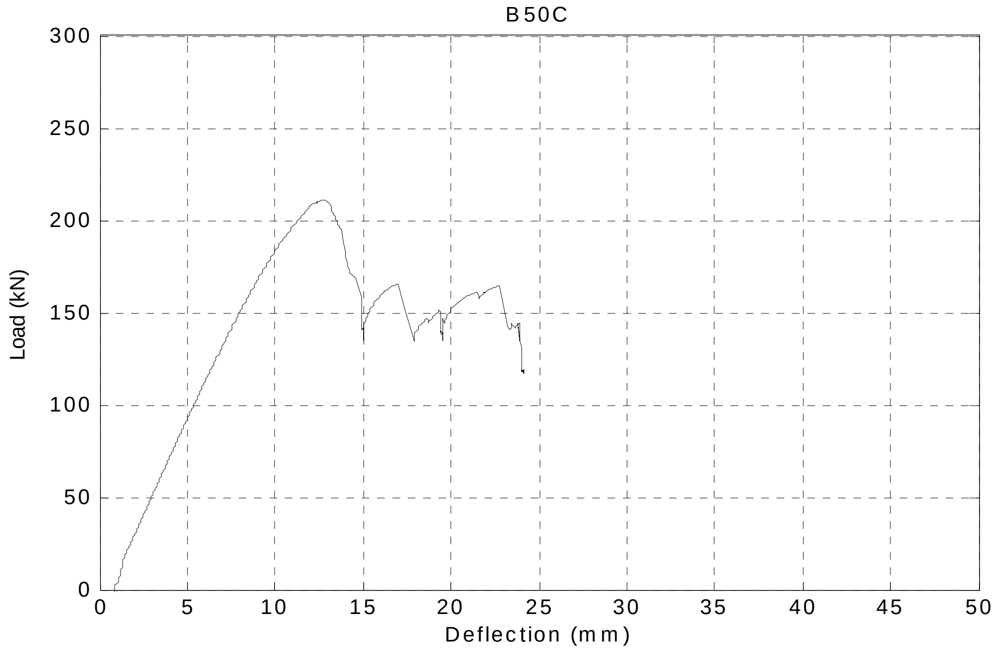

Figure A. 32 Load deflection graph of Group 2 Specimen B50C

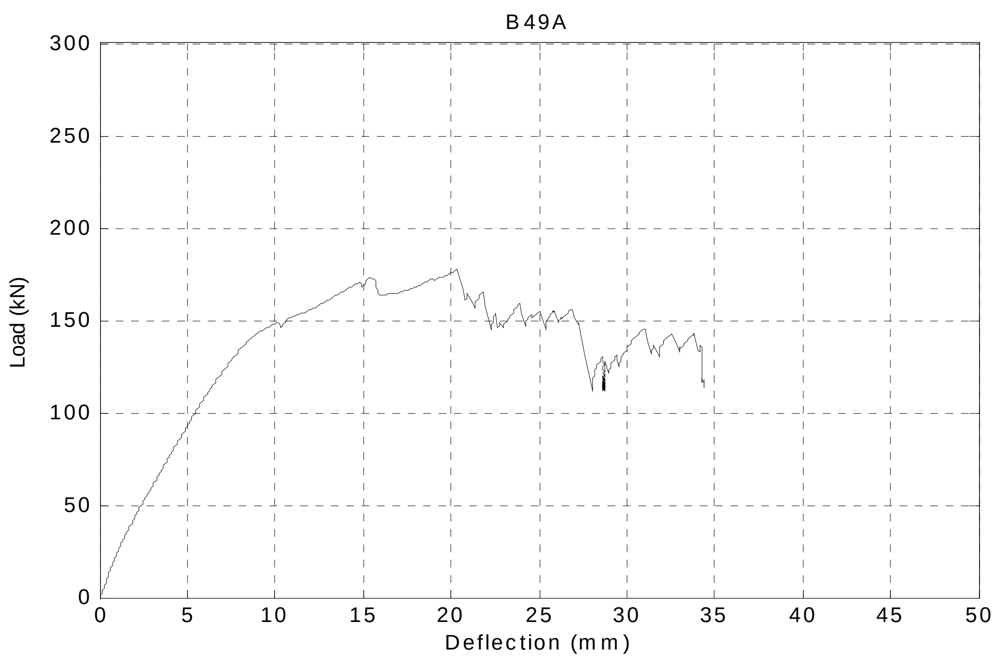

Figure A. 33 Load deflection graph of Group 2 Specimen B49A

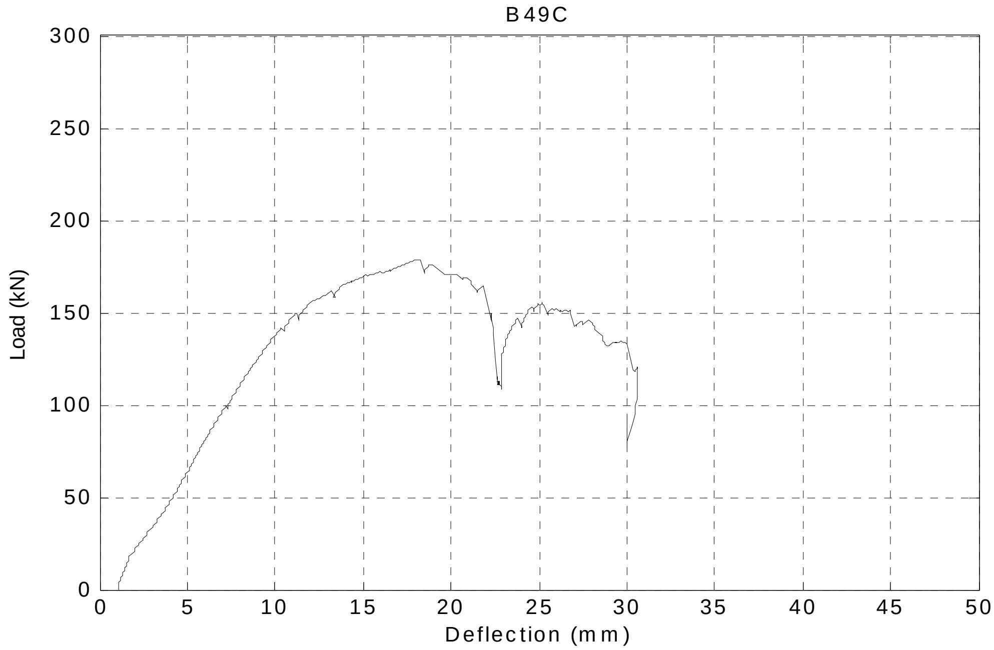

Figure A. 34 Load deflection graph of Group 2 Specimen B49C

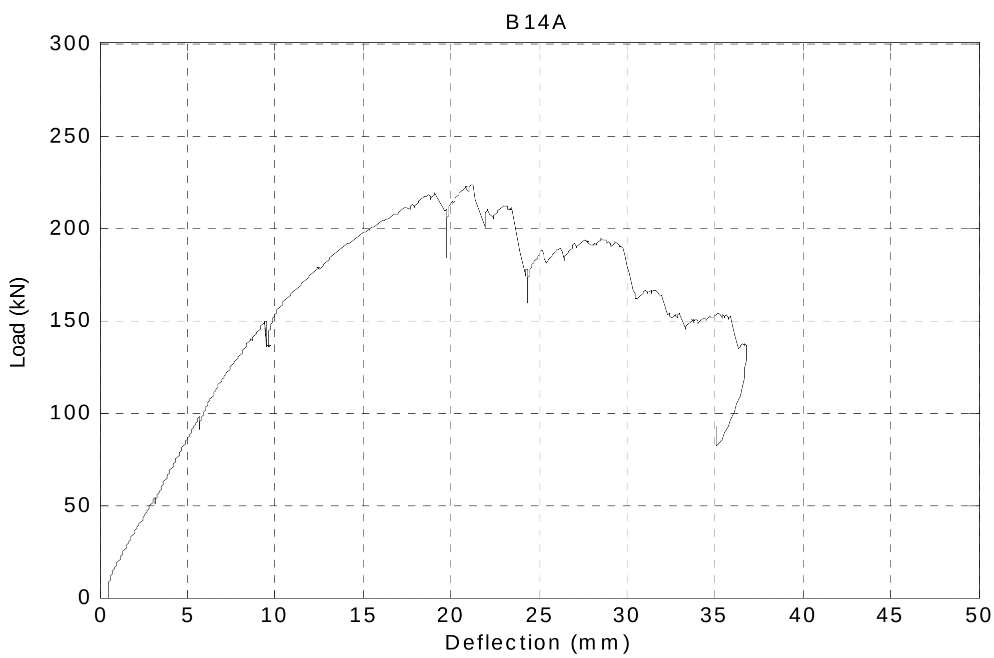

Figure A. 35 Load deflection graph of Group 2 Specimen B14A

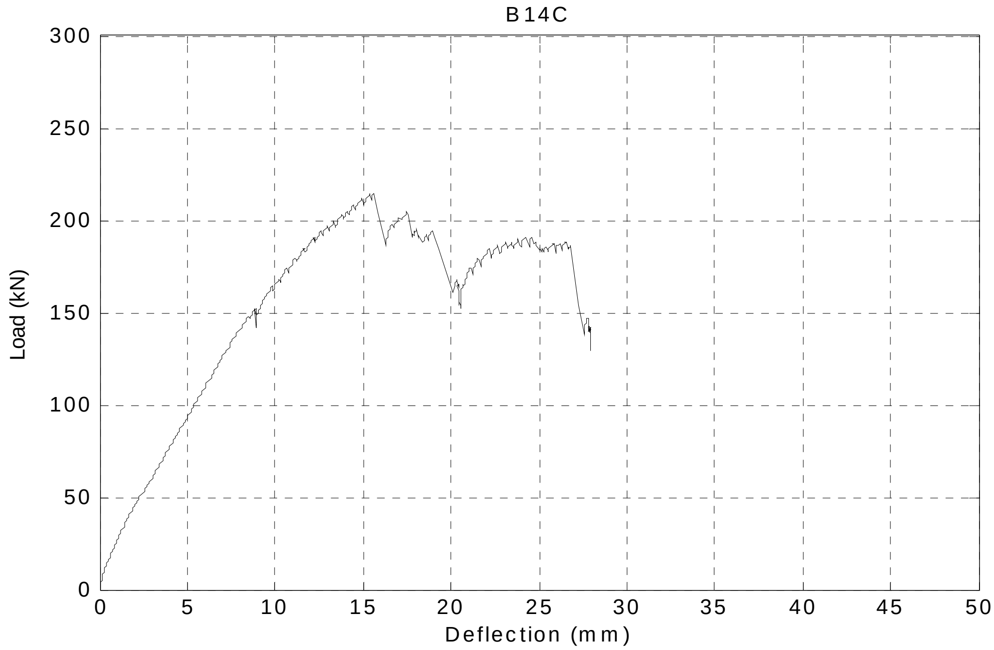

Figure A. 36 Load deflection graph of Group 2 Specimen B14C

Appendix B

Shear strength graph of Group 1 specimens

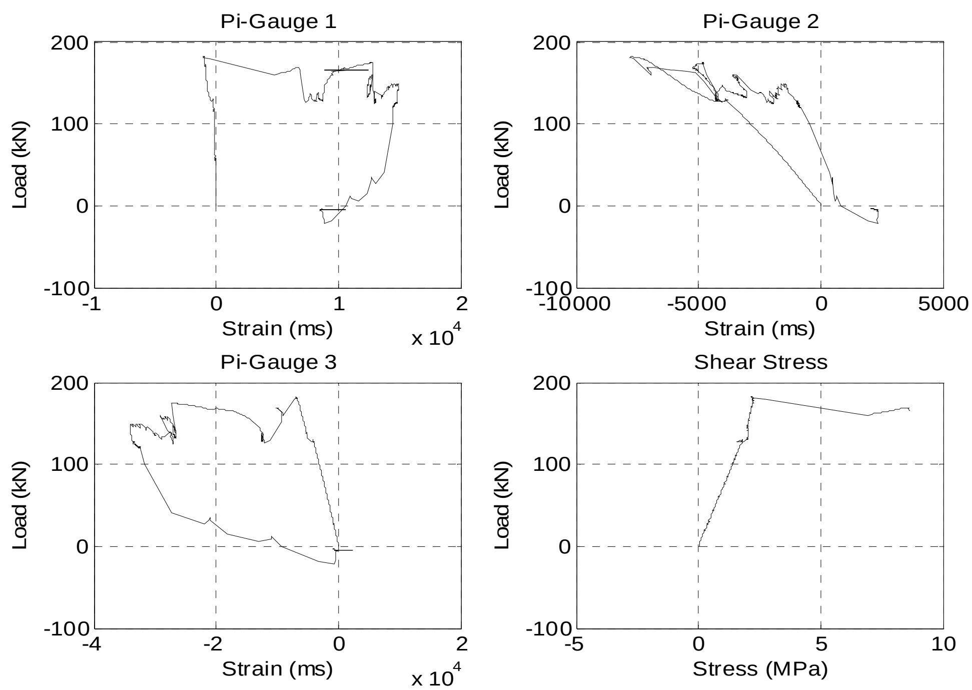

Figure B. 1 Strain profile and shear stress of specimen 2A

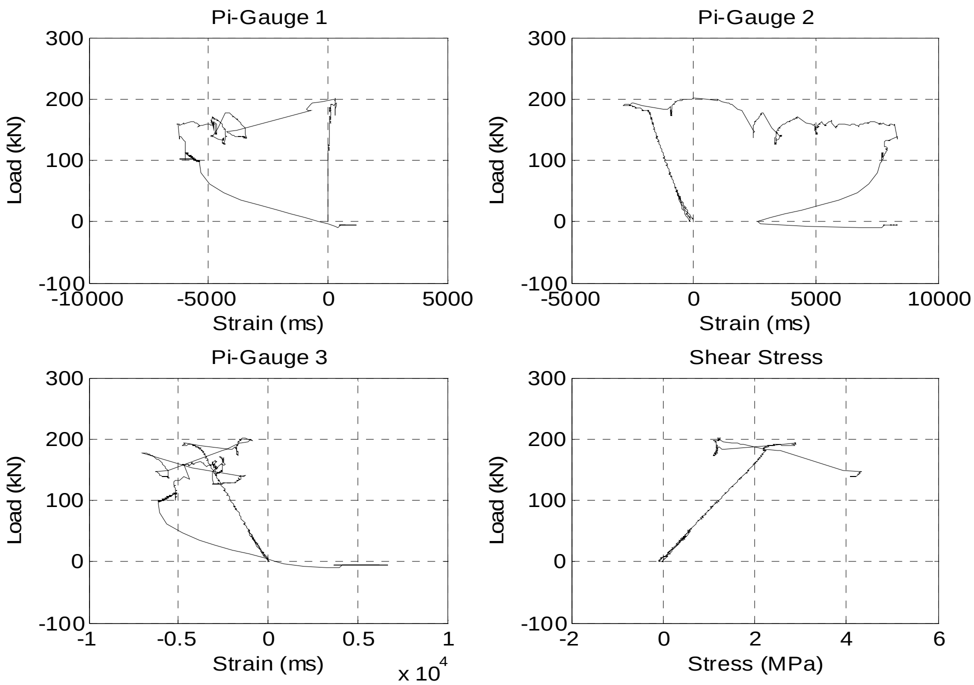

Figure B. 2 Strain profile and shear stress of specimen 2C

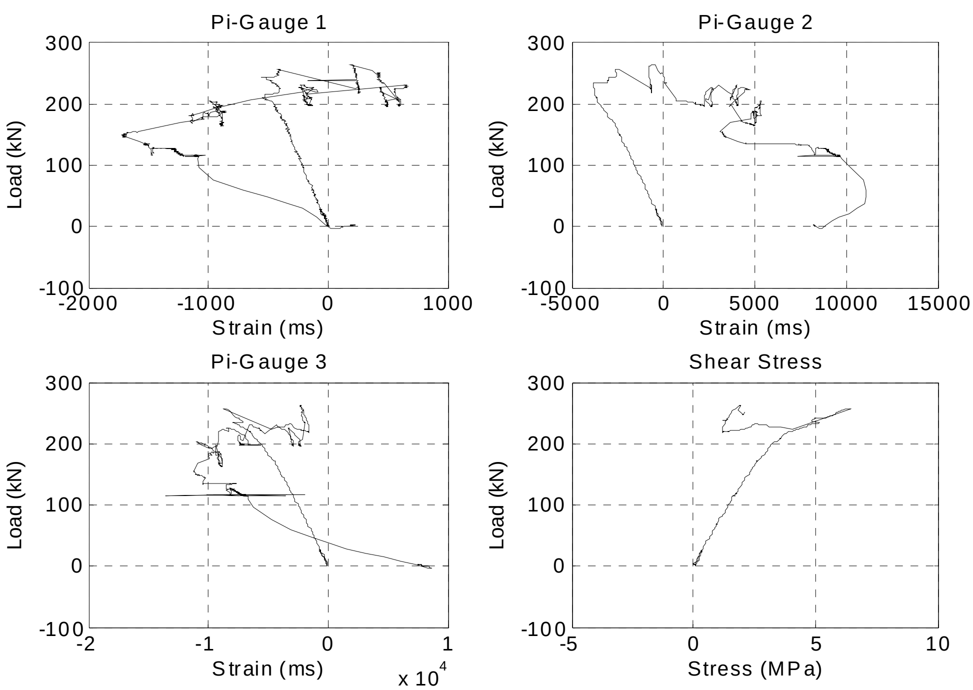

Figure B. 3 Strain profile and shear stress of specimen 4C

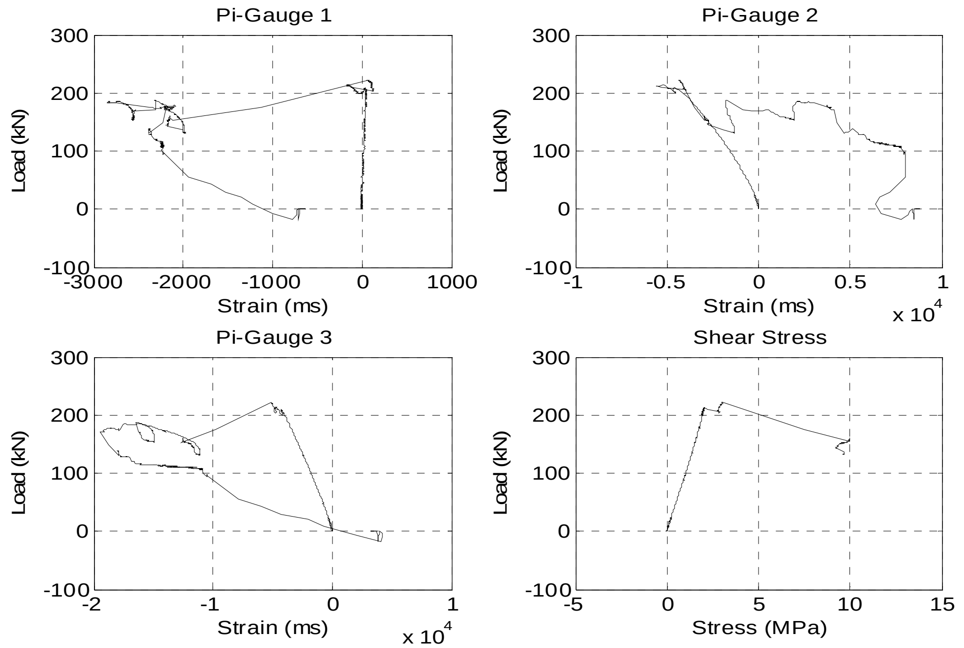

Figure B. 4 Strain profile and shear stress of specimen 13A

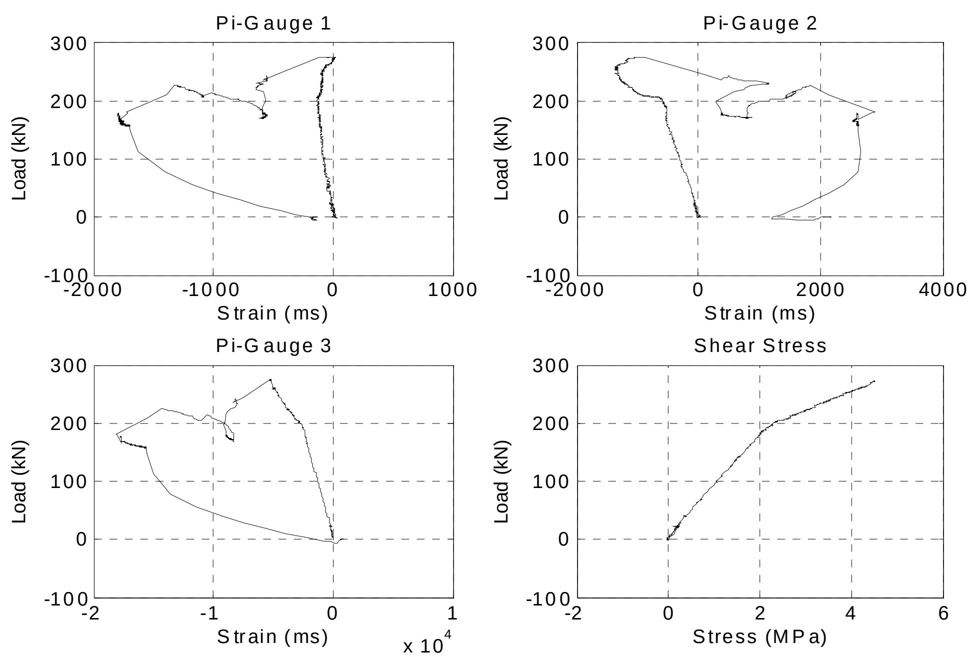

Figure B. 5 Strain profile and shear stress of specimen 13C

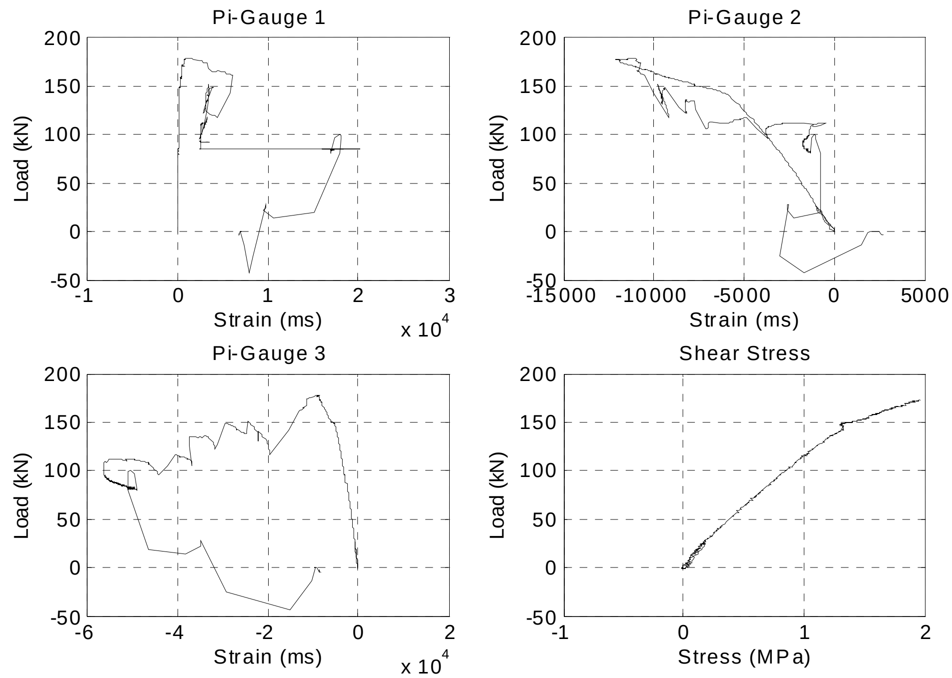

Figure B. 6 Strain profile and shear stress of specimen 28C

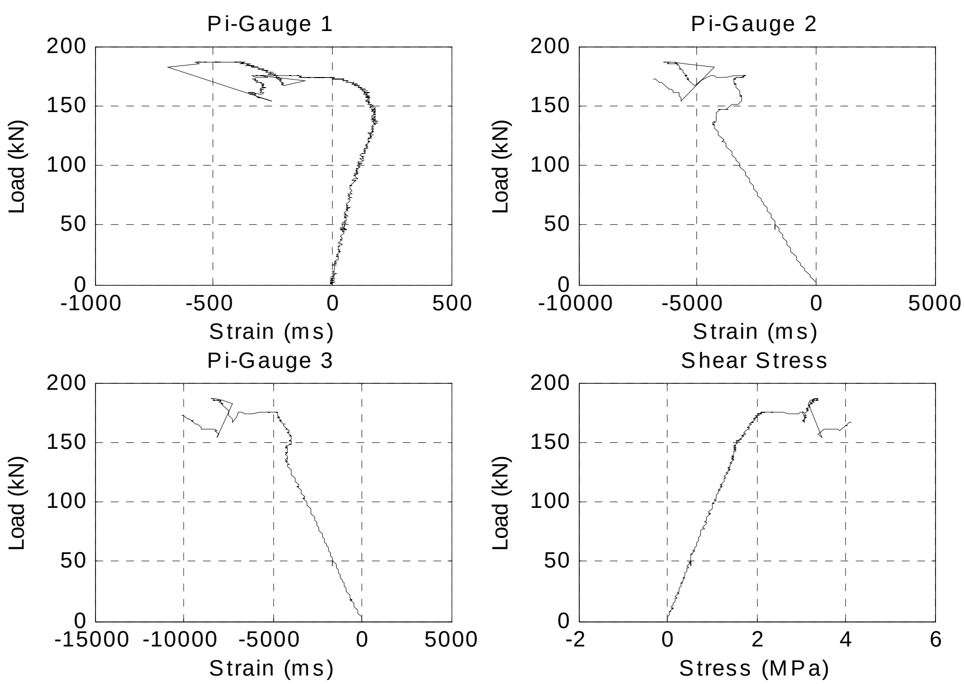

Figure B. 7 Strain profile and shear stress of specimen 23A

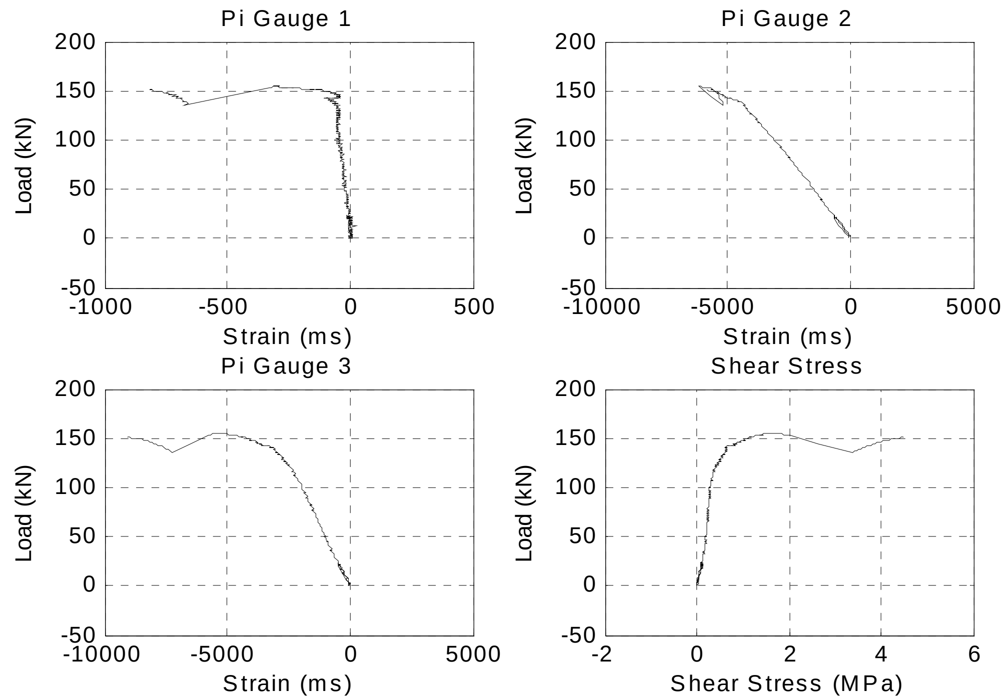

Figure B. 8 Strain profile and shear stress of specimen 21C

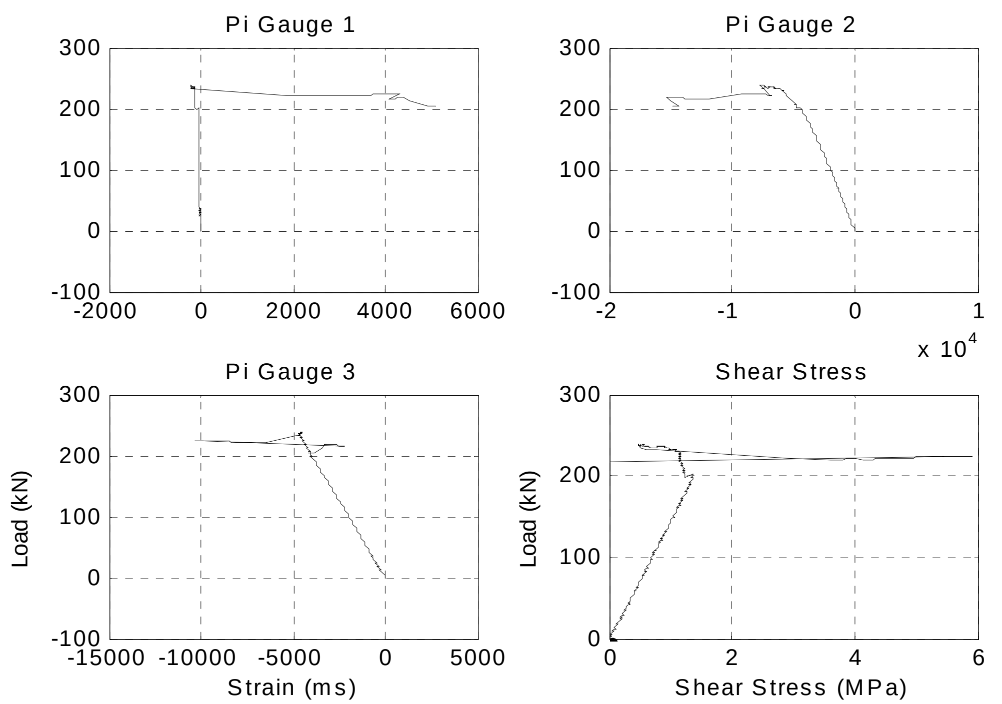

Figure B. 9 Strain profile and shear stress of specimen 17A

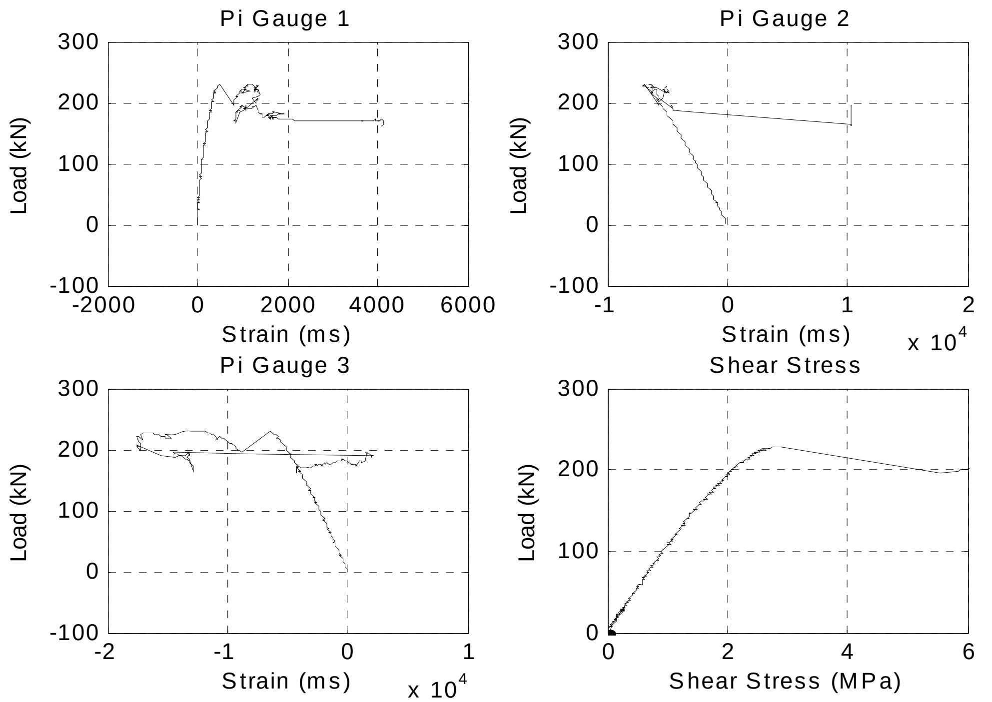

Figure B. 10 Strain profile and shear stress of specimen 17C

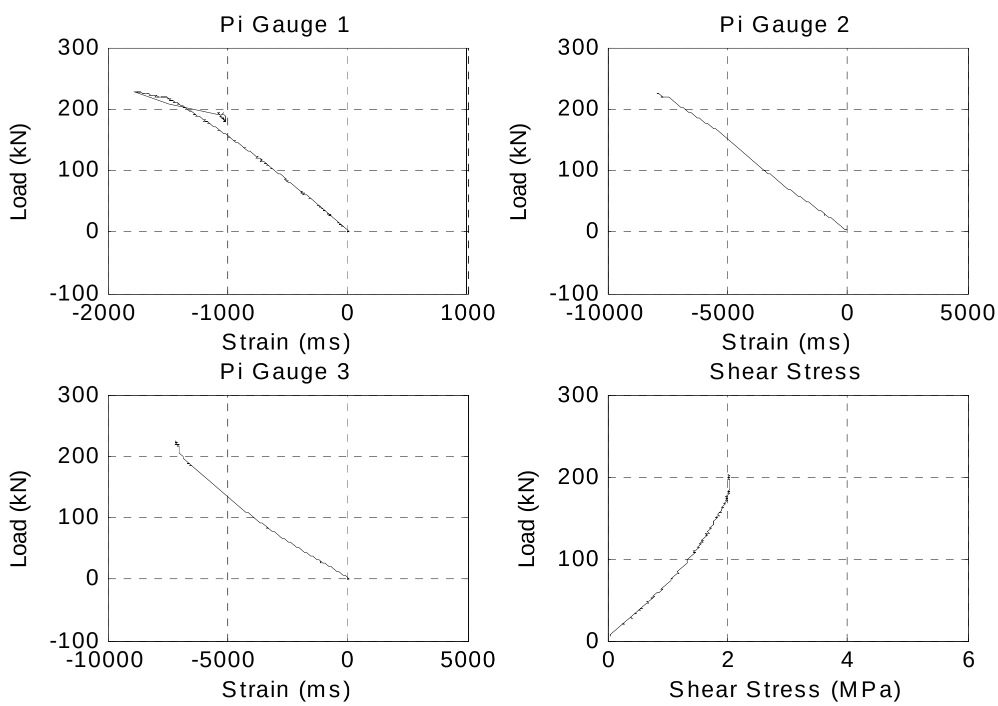

Figure B. 11 Strain profile and shear stress of specimen 16C

Shear strength graph of Group 2 specimens

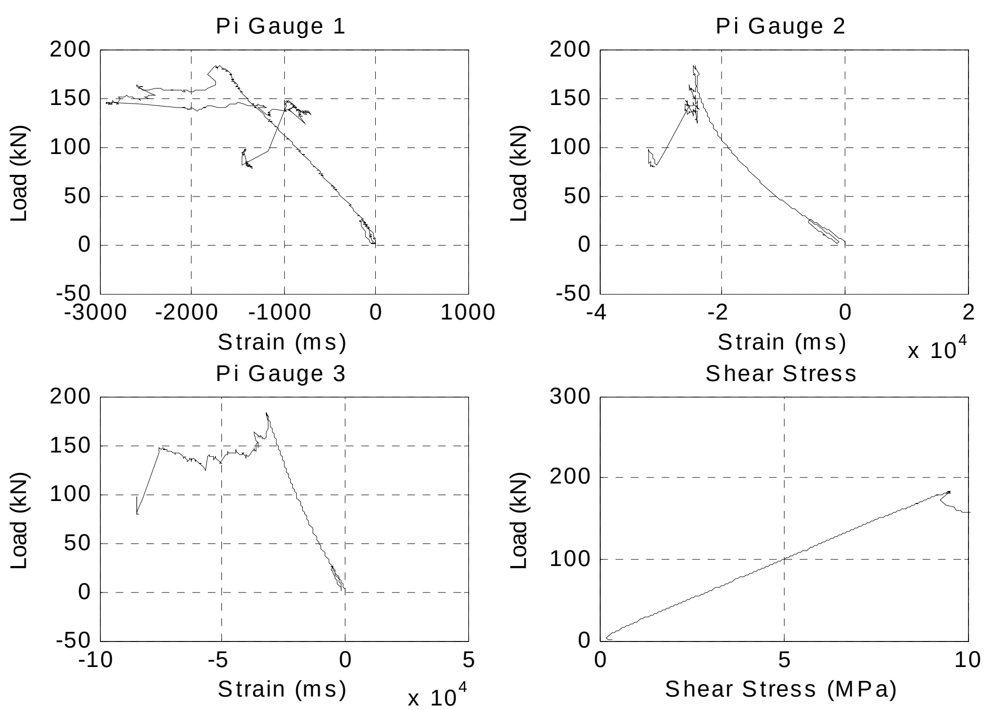

Figure B. 12 Strain profile and shear stress of specimen 5C

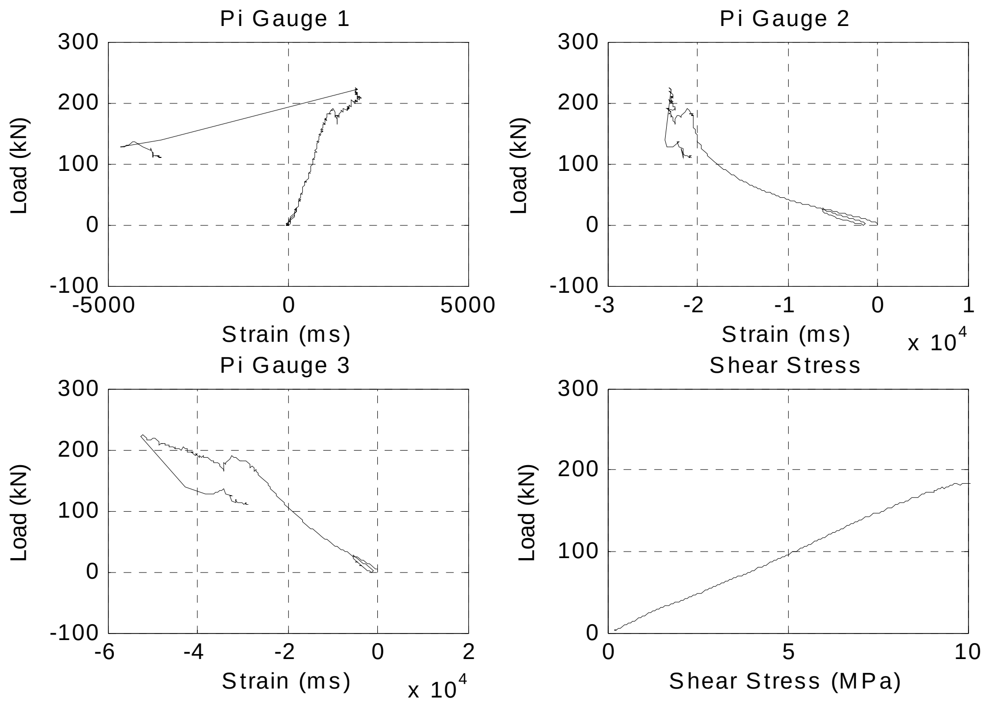

Figure B. 13 Strain profile and shear stress of specimen 10A

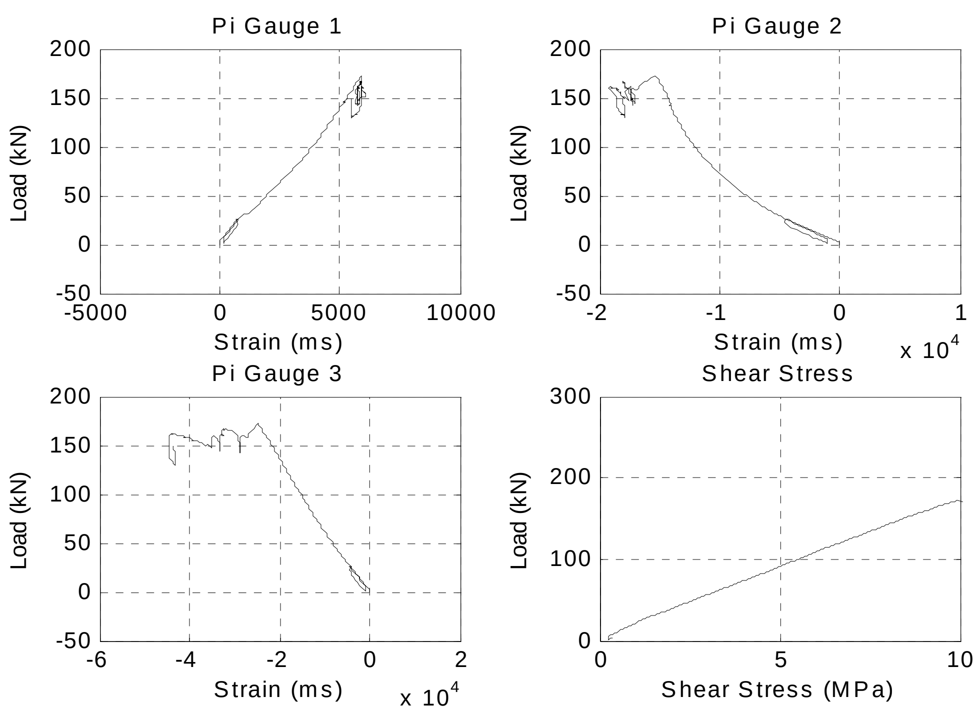

Figure B. 14 Strain profile and shear stress of specimen 11C

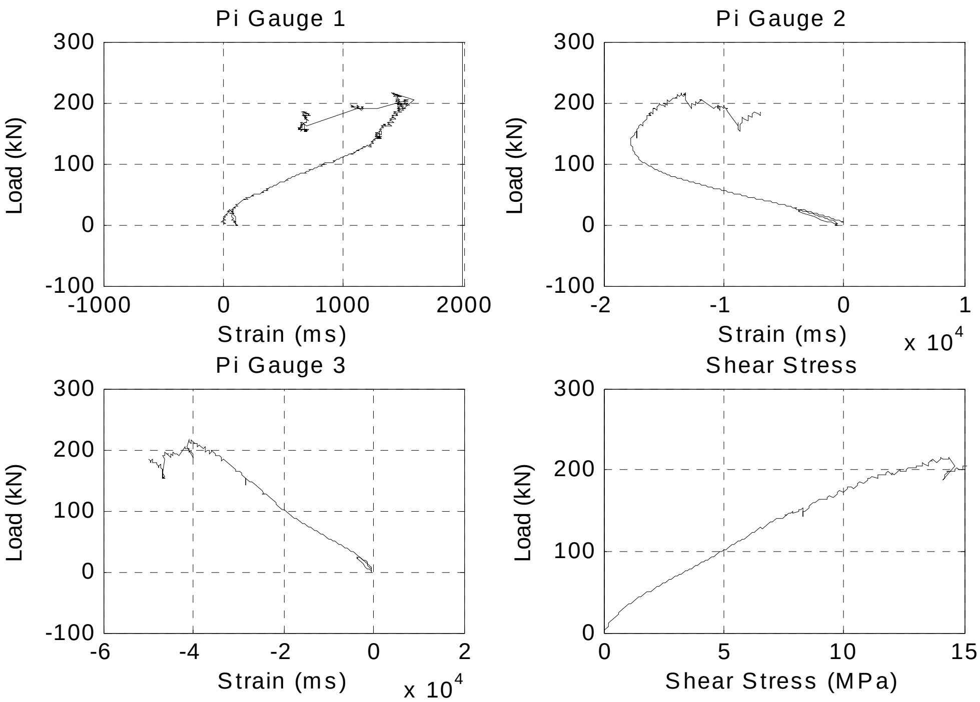

Figure B. 15 Strain profile and shear stress of specimen 14C

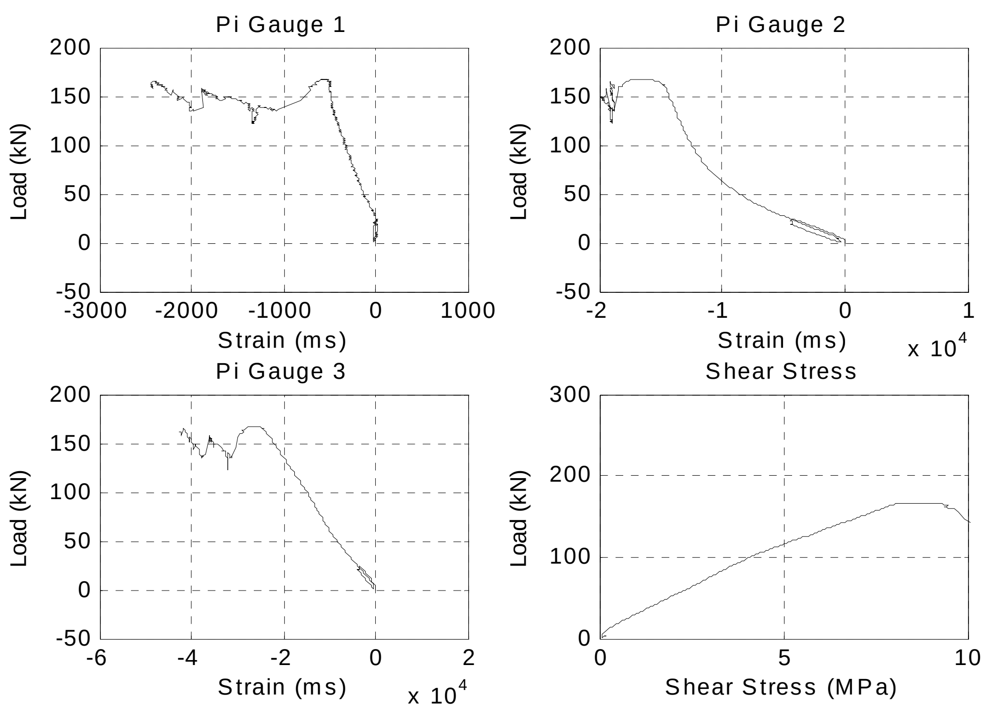

Figure B. 16 Strain profile and shear stress of specimen 15A

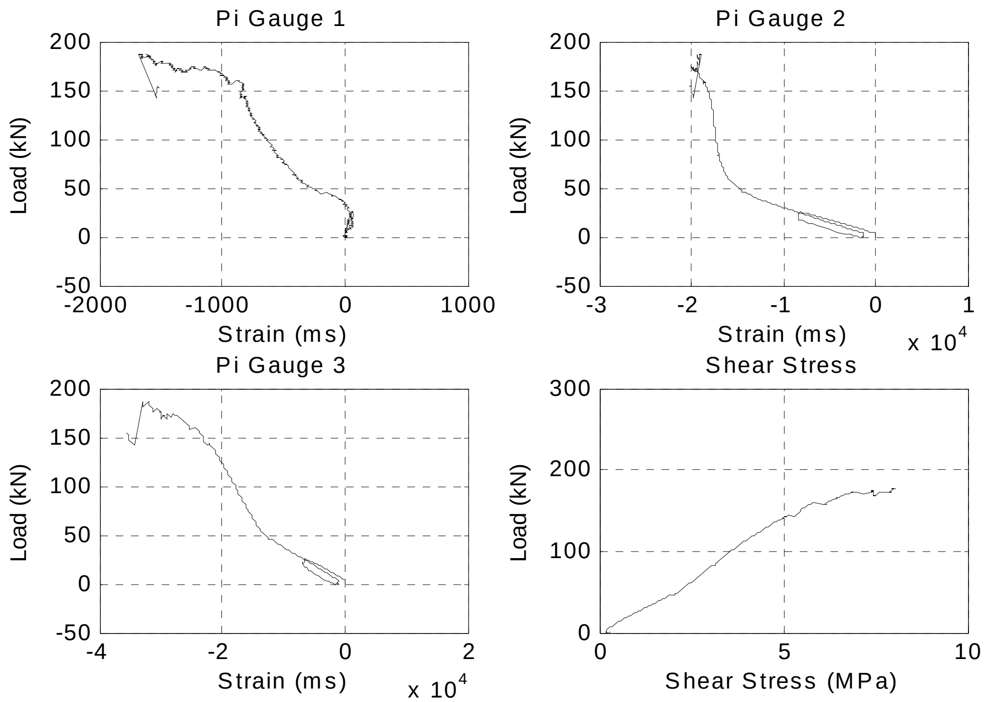

Figure B. 17 Strain profile and shear stress of specimen 41A

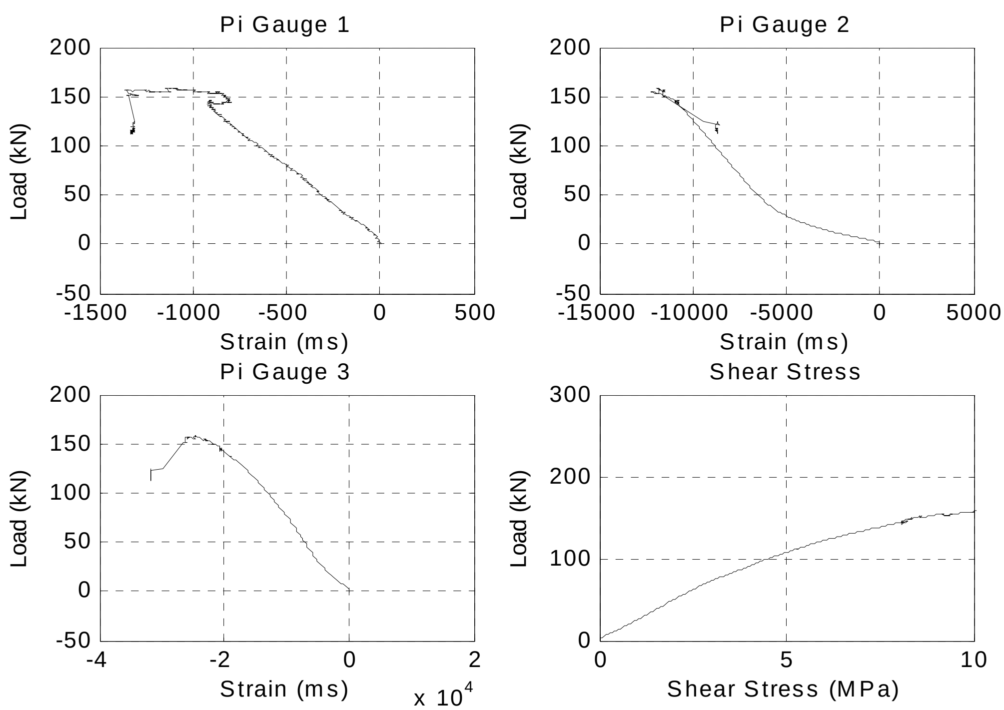

Figure B. 18 Strain profile and shear stress of specimen 41C

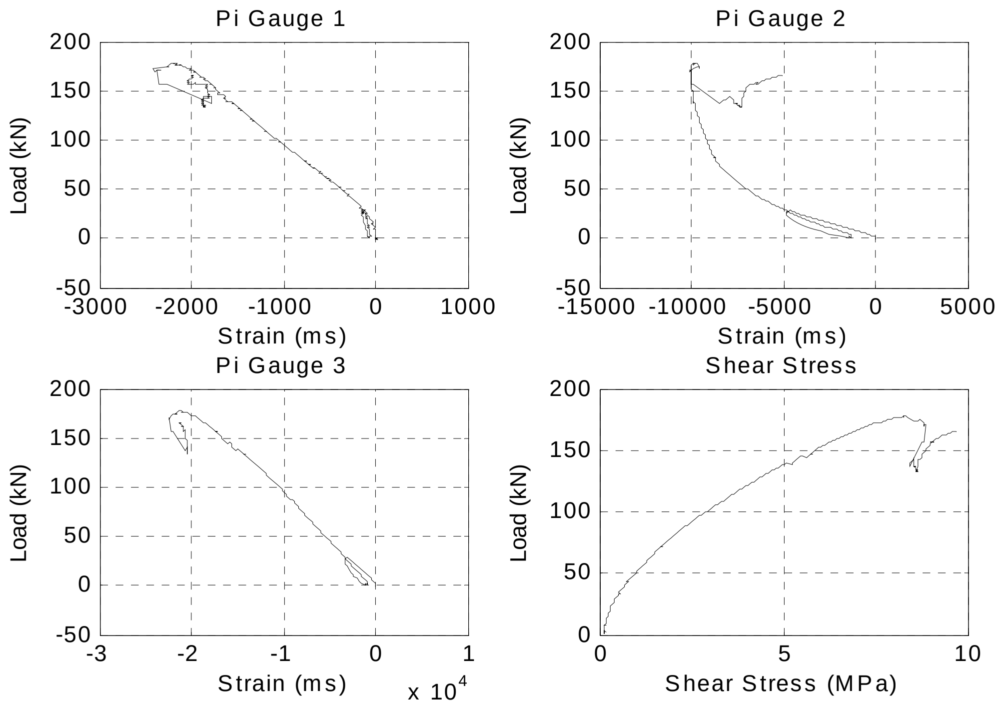

Figure B. 19 Strain profile and shear stress of specimen 44A

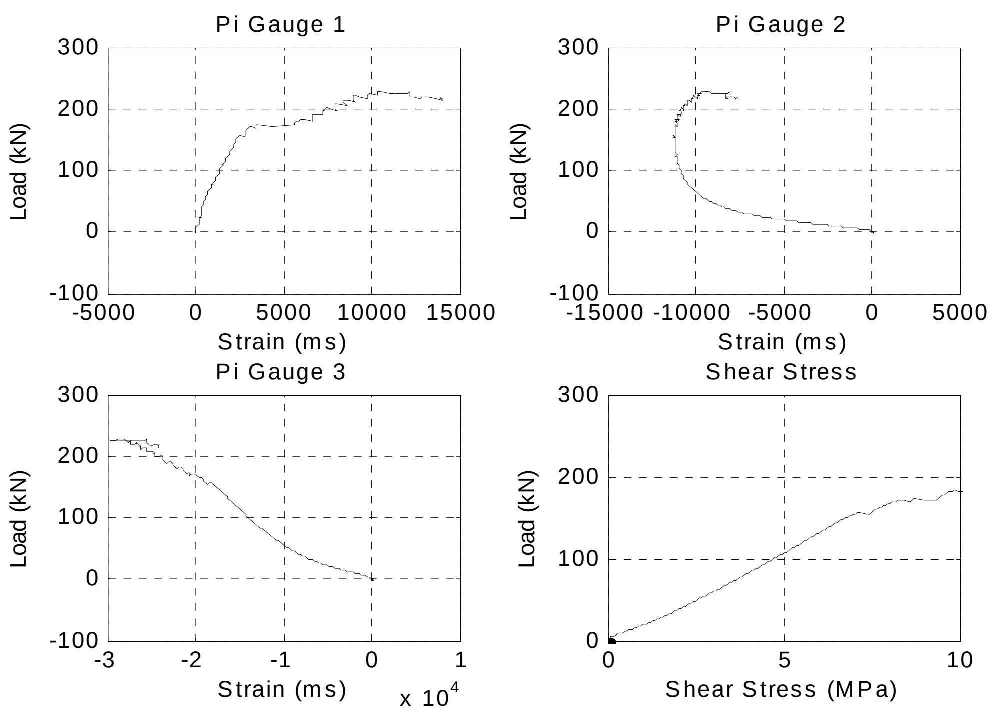

Figure B. 20 Strain profile and shear stress of specimen 44C

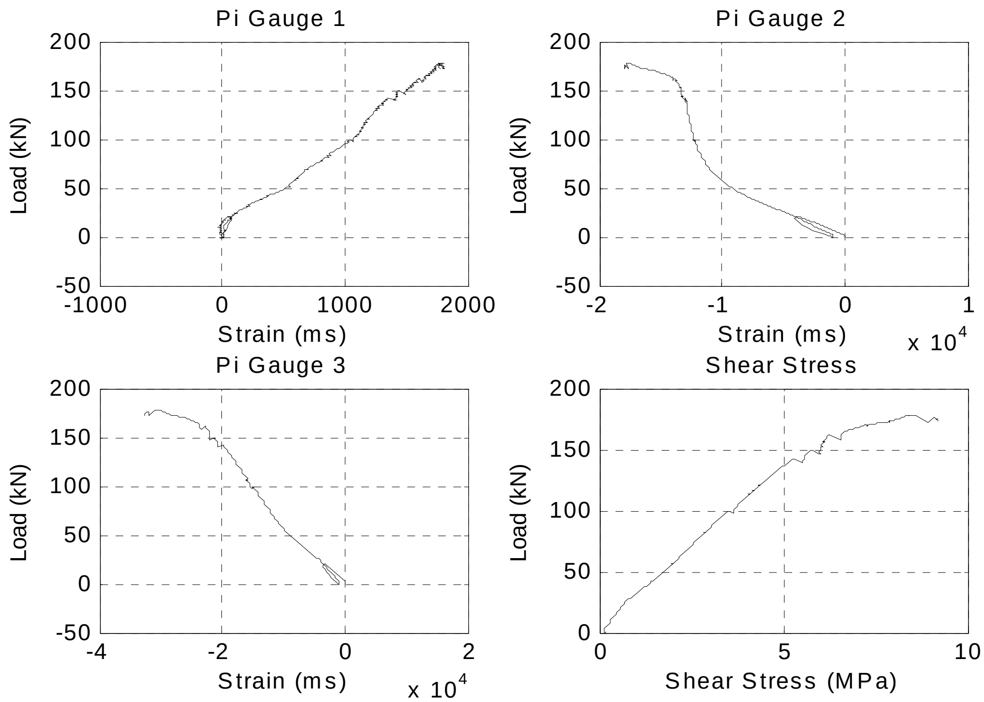

Figure B. 21 Strain profile and shear stress of specimen 49C

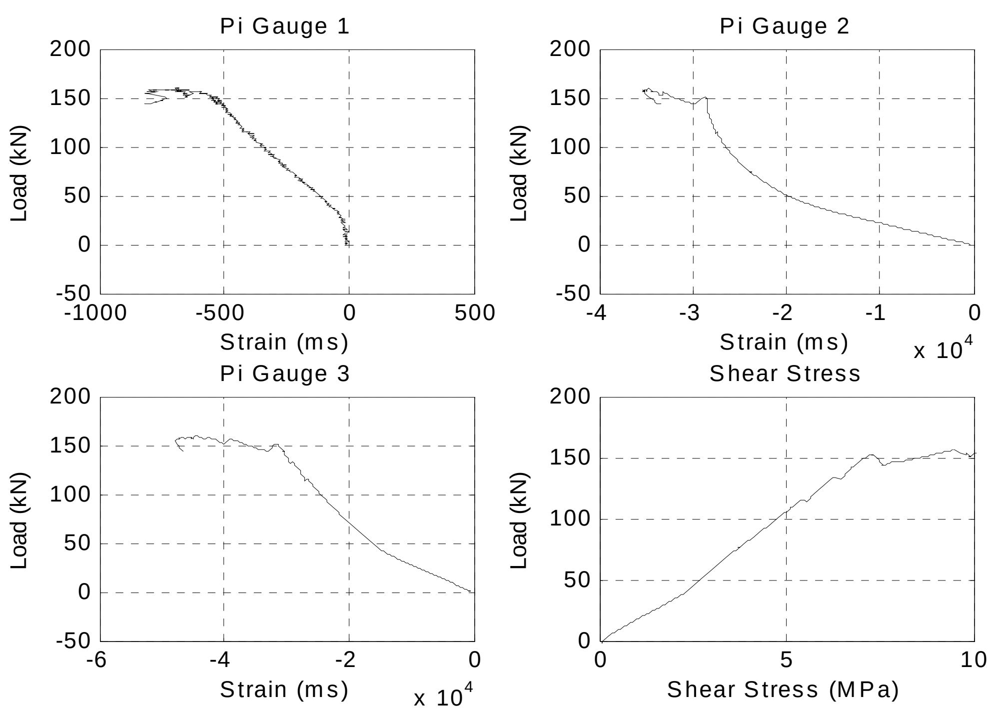

Figure B. 22 Strain profile and shear stress of specimen 50A